

PHOSPHORUS SORPTION AND DESORPTION IN EPHEMERAL GULLY EROSION

by

JAMES BRIGHAM COOVER

B.S., Kansas State University, 2012

A THESIS

submitted in partial fulfillment of the requirements for the degree

MASTER OF SCIENCE

Department of Agronomy

College of Agriculture

KANSAS STATE UNIVERSITY

Manhattan, Kansas

2014

Approved by:

Major Professor

Dr. Nathan O. Nelson

Copyright

JAMES BRIGHAM COOVER

2014

Abstract

Phosphorus (P) is an essential nutrient in crop production, but P inputs to surface waters have resulted in impairments such as eutrophication and algae blooms. Non-point sources such as agricultural fields are a main contributor of P. Kansas, being a high agricultural dependent state, has frequent fresh water body impairments. Multiple erosion and transport processes contribute to P loss. While P loss from sheet and rill erosion has been studied extensively, P loss from ephemeral gully erosion is largely unknown. The objective of this study is to understand the effects ephemeral gullies have on the transport and transformation of P. Three fields in McPherson County with well-defined ephemeral gullies were studied. Soil samples were taken in field locations that are effected by ephemeral gullies at the 0 to 2, 2 to 5, 5 to 15, and 15 to 30 cm depths. Samples were analyzed for total P, anion exchange phosphorus (AEP) (labile P), ammonium-oxalate extractable Fe, Al, and P (Fe_{ox} , Al_{ox} , P_{ox}), Mehlich 3 extractable Fe, Al, Ca, and P (Fe_{M3} , Al_{M3} , Ca_{M3} , P_{M3}), equilibrium phosphorus concentration at zero net sorption (EPC_0), 1:1 soil to water pH, and texture. Soil testing showed that P quantities tend to be much higher in surface soils eroded by sheet and rill erosion and lower in subsoil soil that is eroded by ephemeral gullies. The quantity of sorptive elements such as Fe and Al, were not significantly different throughout the tested area except in areas of changing soil texture. EPC_0 testing showed it was likely that P desorbs from the surface erosion of sheet and rill and is adsorbing onto the subsoil eroded from ephemeral gullies. Sediment eroded by ephemeral gullies has a P buffering capacity greater than the sediment eroded by sheet and rill, and a small quantity of ephemeral gully subsoil will have a large effect on the dissolved P concentration of runoff. Sediment, total P loss and expected dissolved P in runoff was surveyed and modeled for two of the fields. Ephemeral gullies contributed to a majority of sediment and total P loss. The addition of ephemeral gully sediment to the erosional mix of sheet and rill sediment caused the dissolved

P concentration to decrease from 0.0204 to 0.0034 mg L⁻¹ in one field and from 0.0136 to 0.0126 mg L⁻¹ in another. The results of this study show that best management practices (BMPs) such as grass waterways could cause the losses of total P to decrease as much as 2 to 12 times in fields with ephemeral gullies. However, reducing ephemeral gully erosion will likely increase dissolved P concentrations up to 600% more in runoff. Therefore, BMPs need to be combined to fully control P loss from agricultural fields.

Table of Contents

List of Tables	ix
List of Figures	x
List of Abbreviations	xiv
Acknowledgements	xv
Dedication	xvi
Chapter 1: Phosphorus within the environment and effect of ephemeral gully erosion	1
Environmental aspects of excess phosphorus	1
Ephemeral gully formation and definition	2
Current research in phosphorus loss from ephemeral gullies	3
Characteristics of subsoil eroded in ephemeral gullies	4
Soil parameters and environmental soil test.....	5
Thesis Objectives	6
References	8
Chapter 2: Ephemeral gully influence on soil characteristics and phosphorus sorption ..	13
Introduction	13
Materials and Methods	15
Study site and sampling description.....	15
Laboratory methods-soil analysis.....	16
Statistical analysis	21
Results and Discussion	22
Landscape and depth Influence on soil characteristics	22
EPC ₀ within the field and ephemeral gully.....	22
Anion exchange phosphorus within the field and ephemeral gully	24
Total phosphorus within the field and ephemeral gully.....	26
Degree of phosphorus saturation indexes	26
Mehlich 3 and degree of phosphorus saturation	28
Correlation between EPC ₀ to indexes and soil properties	28
Conclusions	30
References	32

Chapter 3: Mixing of sediments with differing depths and phosphorus buffering capacity	51
Introduction	51
Methods and Materials	52
Sampled soils used in mixing study	52
Determining EPC_0 and EPC_0 determined buffering capacity	53
Linear and FMBP model for determining EPC_0 of mixed sediments.....	55
Statistical Analysis.....	57
Results and Discussion	58
Conclusions.....	60
References.....	62
Chapter 4: Phosphorus loss and change in dissolved phosphorus caused by ephemeral gullies	68
Introduction	68
Methods and Materials	69
Field Surveying- soil loss estimation from ephemeral gully	69
WEPP modeling- soil loss estimation for sheet and rill erosion.....	71
Estimations of total phosphorus and labile phosphorus loss	73
Using FMBP model to determine dissolved P in runoff.....	73
Results and Discussion	75
Weedel field sediment and P loss	75
Schmidt field sediment and P loss	76
Conclusions.....	78
References.....	80
Chapter 5: Conclusions and Recommendations	93
Appendix A: Extra explanatory figures for chapter 2.....	94
Appendix B: SAS code	99
Appendix C: WEPP model inputs	102

List of Tables

Table 1.1. Relative contribution of ephemeral gully erosion to total sediment loss measured in research studies from 10 different states.....	12
Table 2.1. Soil properties found in ammonium-oxalate and Mehlich 3 test that influence P sorption in past studies	35
Table 2.2. Testing fields with management and soil type and class	35
Table 2.3. Levels of significance (p-values) for the effects of landscape position, depth, and their interaction for the three fields based on ANOVA	36
Table 2.4 Pearson Correlation Matrix of tested soil characteristics and indexes	37
Table 2.5. Prediction equations for EPC_0 using soil characteristics and indexes	38
Table 3.1. Field, soil depth, texture, DPS, and total P of selected soils	63
Table 3.2. Soil mixtures 1-6 with AEP, original EPC_0 , and buffering determination	63
Table 4.1. Landscape position and depth of soil and phosphorus loss in the Weedel field.....	82
Table 4.2. WEPP predicted water runoff and size of field	83
Table 4.3. Soil landscape and depth with corresponding EPC_0 and contribution percentage to total soil loss for Weedel field	83
Table 4.4. Landscape position and depth of soil and phosphorus loss in the Schmidt field.....	84
Table 4.5. Sediment gained calculations from Schmidt field in second time period	85
Table 4.6. Soil landscape and depth with corresponding EPC_0 and contribution percentage to total soil loss for Schmidt field	85

List of Figures

Figure 1.1. Phosphorus enrichment onto sediment based upon sediment concentration in runoff.....	12
Figure 2.1. McPherson County with locations of the three fields	39
Figure 2.2. Diagram of landscape positions from which soil samples were collected at the Weedel field	40
Figure 2.3. Example 3D model of bank and gully describing sampling points	41
Figure 2.4. Weedel field display of gully and watershed	42
Figure 2.5. Garring field display of gully and watershed	42
Figure 2.6. Schmidt field display of gully and watershed	42
Figure 2.7. Equilibrium phosphorus concentration at zero net sorption (EPC_0) for Weedel field based upon soil depth and field location.....	43
Figure 2.8. Equilibrium phosphorus concentration at zero net sorption (EPC_0) for Garring field based upon soil depth and field location.....	43
Figure 2.9. Equilibrium phosphorus concentration at zero net sorption (EPC_0) for Schmidt field based upon soil depth and field location.....	44
Figure 2.10. The relation between equilibrium phosphorus concentration at zero net sorption (EPC_0) and anion exchange phosphorus (AEP).....	45
Figure 2.11. Anion exchange phosphorus for Weedel field based upon soil depth and field location.....	45
Figure 2.12. Anion exchange phosphorus for Garring field based upon soil depth and field location.....	46
Figure 2.13. Anion exchange phosphorus for Schmidt field based upon soil depth and field location	46

Figure 2.14. Total phosphorus for Weedel field based upon soil depth and landscape position	47
Figure 2.15 Total phosphorus for Garring field based upon soil depth and landscape position	47
Figure 2.16 Total phosphorus for Schmidt field based upon soil depth and landscape position	48
Figure 2.17. Degree of phosphorus saturation index of oxalate extraction (DPS_{ox}) for Weedel field based upon soil depth and field location	48
Figure 2.18. Degree of phosphorus saturation index of oxalate extraction (DPS_{ox}) for Garring field based upon soil depth and field location	49
Figure 2.19. Degree of phosphorus saturation index based on ammonium-oxalate extraction (DPS_{ox}) for Schmidt field based upon soil depth and field location.....	49
Figure 2.20. Al_{ox} , Fe_{ox} , and P_{ox} for Weedel field based upon soil depth and field location	50
Figure 2.21. Al_{ox} , Fe_{ox} , and P_{ox} for Garring field based upon soil depth and field location	50
Figure 2.22. Al_{ox} , Fe_{ox} , and P_{ox} for Schmidt field based upon soil depth and field location	50
Figure 3.1. Mixture 1 (W49 and W19) - EPC_0 change of surface soil (W49) with percentage of added subsoil (W19)	64
Figure 3.2. Mixture 2 (W29 and W9) - EPC_0 change of surface soil (W29) with percentage of added subsoil (W9)	64
Figure 3.3. Mixture 3 (G45 and G56) - EPC_0 change of surface soil (G45) with percentage of added subsoil (G56)	65
Figure 3.4. Mixture 4 (G13 and G36) - EPC_0 change of surface soil (G13) with percentage of added subsoil (G36)	65
Figure 3.5. Mixture 5 (S53 and S8) - EPC_0 change of surface soil (S53) with percentage of added subsoil (S8)	66

Figure 3.6. Mixture 6 (S45 and S1) - EPC ₀ change of surface soil (S45) with percentage of added subsoil (S1)	66
Figure 3.7. Observed EPC ₀ vs. Predicated EPC ₀ in FMBP and linear model	67
Figure 4.1. Weedel field ephemeral gully with survey lines of cross sectional loss	86
Figure 4.2. Schmidt field ephemeral gully with survey lines of cross sectional loss	87
Figure 4.3. River Morph (version 5.1) example of lower gully survey line in Weedel field	88
Figure 4.4. WEPP model display of Weedel field showing field slop, manager inputs, and prediction values	89
Figure 4.5. WEPP model display of Schmidt field showing field slop, manager inputs, and prediction values	90
Figure 4.6. Changes in total P and dissolved P due to reductions in ephemeral gully erosion	91
Figure 4.7. FMBP model results and total P loss for the Schmidt field in the first time period	92
Figure A.1. Phosphorus Sorption Isotherm and fitted Freundlich equation curve.....	94
Figure A.2. Texture analysis for Weedel (top), Garring (middle), and Schmidt (bottom) by depth and landscape	95
Figure A.3. Textural triangle of tested texture of the three fields.....	96
Figure A.4. Degree of Phosphorus Saturation for Mehlich extracted Fe & Al and Ca, Weedel (top), Garring (middle), and Schmidt (lower) by depth and landscape	97
Figure A.5. 1:1 soil to water pH analysis by depth and landscape position for Weedel (top), Garring (middle), and Schmidt (lower)	98
Figure B.1. SAS code for ANOVA table and error bars for chapter 2 figures	99
Figure B.2. SAS code for Langmuir and Freundlich curve parameters	100

Figure B.3. SAS code for Pearson Correlation table	100
Figure B.4. SAS code for EPC ₀ stepwise comparisons	101
Figure B.5. SAS for EPC ₀ in mixed sediments in chapter 3	101
Figure C.1. SAS code for Pearson Correlation table	102
Figure C.2. SAS code for EPC ₀ stepwise comparisons	105

List of Abbreviations

Al _{ox} :	Oxalate Extractable Aluminum
Al _{M3} :	Mehlich 3 extracted Aluminum
AEP:	Anion Exchange Extractable P
Ca _{M3} :	Mehlich 3 extracted Calcium
Dissolved P:	Dissolved Phosphorous
DPS:	Degree of Phosphorous Saturation
DPS _{ox} :	Degree of Phosphorous Saturation determined by Al _{ox} , Fe _{ox} , and P _{ox}
DPS _{M3} :	Degree of Phosphorous Saturation determined by Al _{M3} , Fe _{M3} , and P _{M3}
DPS _{Ca} :	Degree of Phosphorous Saturation determined by Ca _{M3} and P _{M3}
EG:	Ephemeral Gully
EPC ₀ :	Equilibrium at Zero Net Phosphorous Sorption
Fe _{ox} :	Oxalate Extractable Iron
Fe _{M3} :	Mehlich 3 extracted Iron
G:	Garring field
ICP:	Inductively Coupled Plasma Spectroscopy
LP:	Landscape Position
Mg _{M3} :	Mehlich 3 extracted Magnesium
Mg _{ox} :	Oxalate Extractable Magnesium
P:	Phosphorus
P _{M3} :	Mehlich 3 extracted Phosphorus
P _{ox} :	Oxalate Extractable Phosphorus
S:	Schmidt field
W:	Weedel field

Acknowledgements

Of course I would like to first thank my advising Professor, Dr. Nathan Nelson. His constant guidance, time commitment, and dedication was an important part to the completion of this thesis. I would also like to thank my committee members Dr. Ganga Hettiarachchi and Dr. Aleksey Sheshukov for their advice and help along the way. Chapter 4 would have not been possible without the work of Katie Burke (under Dr. Timothy Caine) and Vladimir Karimov and I wish them both the best of luck in finishing their Ph.Ds.

Another group of people I would like to thank are the ones who helped me and supported me along the way, fellow lab students, Nate Dorsey and Ammar Bhandari, and also the undergrads Tyler, Brent, Christian, and Reggeany. Reggeany Barrios was especially helpful and spent a whole summer keeping me on track and organized in many hours of lab work. I am happy to have gotten to know her and I know she will go on to do great things.

Thank you as well to Kathy Lowe and the KSU soil testing lab for processing my samples quickly and helping me with understanding lab processes even when they were busy.

My final thanks go to the organization that funded this project, the National Institute of Food and Agriculture (NIFA).

Dedication

I would like to dedicate this thesis to my beautiful girl and to my family. Kathryn's love and my family's support is what truly made this thesis possible.

Chapter 1: Introduction

Phosphorus within the environment and effects of ephemeral gully erosion

Environmental aspects of excess phosphorus

Phosphorus (P) is a major nutrient that contributes to algae blooms and subsequent eutrophication in water bodies and is commonly considered the main controlling nutrient in fresh water systems (Belmont et al., 2009; Carpenter et al., 1998). Eutrophication in fresh water lakes causes a number of environmental and economic concerns, such as the loss of biodiversity, contaminations in drinking water, loss of lake use, and property value reduction around the lake; the expected annual monetary losses from these problems are likely two billion dollars or more within the U.S. (Dobbs et al., 2008). Algae blooms in fresh water bodies can create highly potent toxins that can be deadly to nearby animals, cause sickness in people recreationally using the lake, and can be difficult to remove by local water municipalities (Hudnell, 2010). Algae blooms are widespread throughout the U.S. and are becoming more common as nutrient loads into water systems are increasing and species of harmful algae are diversifying (Hudnell, 2010; Heisler, 2008). Eutrophication and algae blooms are becoming better discussed in recent years as large cases of the environmental problem are occurring, an example being wide spread and commonly toxic blooms in Lake Erie (Cheung et al., 2012) and the Chesapeake Bay (Zhang et al., 2013). Treatments directly to watersheds to control the algae blooms, by either algaecides or by nutrient flocculation, can have lasting ecological effects and often are only a temporary solution (Hudnell, 2010). Phosphorus can remain in water bodies for a number of years by adsorbing onto lake and stream sediments and be released during large weather events or seasonal changes (Belmont et al., 2009). Given the difficulties of removing or compensating for P once within a water body environment, it is more feasible to control the P loss from sources of the nutrient.

Agricultural fields represent a large portion of P loss for many watersheds and agricultural management can influence the amount and bioavailability of P lost to surface waters (Wallbrink et al., 2002). Much of the P lost from agricultural fields is particulate P, which is P that is adsorbed to soil particles or part of organic matter. A smaller fraction of the P lost from fields is P dissolved in runoff, commonly referred to as dissolved P, solution P, or soluble P. Although dissolved P represents a smaller fraction of the P in runoff, it has high bioavailability (Rodriguez-Blanco et al., 2009).

Changes in agricultural management have been linked back to reduced particulate P loss as well as increases in dissolved P loss (Daloglu et al., 2012; Sharpley et al., 2012; Richards et al., 2007; Richards and Baker, 2002). Management practices that influence ephemeral gully formation may also influence the amount and form of P leaving fields. This may also influence the short and long-term persistence of P in water bodies and the resultant impacts on eutrophication. However, there is a lack of information on the effects of ephemeral gully erosion on P loss. Additional information is needed to determine the amount of P lost due to ephemeral gully erosion and the effects of ephemeral gully erosion on the forms of P in runoff water.

Ephemeral gully formation and definition

The definition of an ephemeral gully (EG) is loosely defined. Generally it is considered any gully that is temporary in nature in a conventional tillage field but will likely later return during a runoff event (SSSA, 2013), or a gully that is too large to be considered rill erosion but still small enough to be driven across by farm equipment. Studies that need to define a clear line of classification between the upper and lower limits of an EG do so with various parameters (Poesen et al., 2003). Ephemeral gully erosion is a form of erosion that is much less studied than

well-known erosion of sheet and rill but yet can represent a major proportion of sediment loss from a field (Poesen et al., 2003). New models are attempting to fully calculate the contributions of EG erosion but are limited because EGs represent a number of difficult to calculate factors. Slope, hydraulic flow, and critical shear stress of eroding layer can determine the formation of EG and these factors are highly location dependent (Daggupati et al., 2013). Gullies often form in places where water concentrates, but can also form in livestock trails, tire tracks, or planting rows (Poesen et al., 2003). While EGs can be considered a natural erosion process, removing the vegetative cover during farming or in over-grazing of animals, increases the rates of gully formation (Valentin et al., 2005). Ephemeral gullies within a watershed can represent a passage of delivery for sediment direct to waterways, along with the eroded sediments they themselves provide in their formation, leading to carrying of nutrients and sedimentation into water bodies. Table 1.1 shows that sediment from an EG can be a major proportion of the sediment loss from a field, despite that EG erosion is rarely included in erosion models (Poesen et al., 2003).

Current research in phosphorus loss from ephemeral gullies

The current research in the quantification of phosphorus loss due to EGs, and how the EG affects the sorption phosphorus onto sediment is largely unavailable. Although research into EG is becoming more common, much of it relates to details of gully formation models and the erosion of sediments. There are however a few studies that relate to P loss from EG fields. Tang et al., (2013) working on a region in Northeast China, found that EGs reduced available P (determined by 0.5 M sodium bicarbonate extraction) by 25%. Zheng et al., (2004) preformed a study after deforestation and found that EGs were the main contributor to soil and nutrient loss. This study found that 86.6% of available P was loss after 7 years of deforestation through all forms of erosion. Zheng at al., (2004) also found that sediment nutrient enrichment changed

depending on rainfall amounts and which erosion process was dominating (Figure 1.1). In lower rainfall and intensity, sheet erosion was dominant, resulting in mostly enriched fine particles. When rainfall intensity increased rill and small gullies reduced enrichment with increased erosion of larger particles. As rainfall intensity continued to increase, large enriched clods and aggregates began to erode, increasing the enrichment. This study shows that as different erosion processes take place with increasing rainfall intensity, sediment contributions and P sorption are also likely to change.

Characteristics of subsoil eroded in ephemeral gullies

Subsoil has a much larger P buffering capacity and tillage is used to mix surface with subsoil to reduce the P stratification that is often seen in fields (Peltovuori, 2002). A pronounced stratification of P can take place within no-till systems where this mixing is not taking place and P fertilizer is continually being applied to the surface (Verbree, 2010). Due to this large P stratification, erosion processes that removes certain depths of soil is likely also the effect the removal of P and P enrichment of eroded sediments. Ephemeral gullies represent a soil loss that is different from that of sheet and rill erosion because much of the sediment contribution is from the subsoil and has soil properties different than that of the surface soil. These properties can affect P sorption and change the P form composition runoff.

The adsorption and desorption of P is controlled by variety of soil parameters including texture (clay content), Al and Fe oxides, Ca content, pH, and P saturation (Hongthanat, 2011; Scalenghe et al., 2007; Zhang et al., 2005). These soil parameters are also interrelated in that high clay usually means higher Al & Fe oxide content. Also the effectiveness of Al and Fe oxide and Ca sorption of P depends on pH; in lower pH, Al and Fe oxide have a large effect in P

sorption (Zhang et al., 2005), while in higher pH (>7.5), Ca also tends to control P sorption (Ige et al., 2007). As it can be seen the sorption of P within soil can be highly complex and is often difficult to determine.

Soil parameters and environmental soil test

The expectation of soil to absorb and desorb P into a solution can be calculated using sorption isotherms to determine the equilibrium phosphorus concentration at zero point sorption (EPC_0). Equilibrium phosphorus concentration at zero point sorption is a soil parameter that helps to determine the point at which a soil will neither adsorb nor desorb P at a certain P solution concentration. Also EPC_0 gives expectations on how the soil P sorption will respond in a changing P environment. EPC_0 is commonly used in environmental P studies where the final sediment ends up in a fresh water body and is useful in determining P adsorption or desorption in sediment mixing events (Kerr, 2010; Hartikainen et al., 2010; Peltovuori, 2002; Agudelo et al., 2011). EPC_0 has been shown to drop quickly with soil depth, where topsoil is more likely to release soluble P (Hongthant et al., 2011). When surface soil and subsoil are mixed, subsoil has a much higher P buffering capability, and only a small proportion of subsoil is needed to adsorb P that is desorbed from surface soils, thereby reducing the EPC_0 of the mixture (Peltovuori, 2002). During EG erosion when surface soil and subsoil are mixed, EPC_0 is a useful parameter in determining the expected resulting dissolved P in runoff.

Degree of phosphorus saturation (DPS) is another soil parameter that is often used. Degree of phosphorus saturation is a unitless proportion telling how much P sorption sites are already occupied by P, and since P sorption is controlled by a variety of soil characteristics, there is also a number of ways to calculate different types of DPS indexes (Hongthanat et al., 2011).

The DPS calculations require a few testable soil properties such as quantities of; Al oxides, Fe oxides, P associated with the Al and Fe oxides, Mehlich 3 Ca, Mehlich 3 P, Mehlich3 Fe, and Mehlich3 Al. These calculations will be better discussed in chapter 2. Degree of phosphorus saturation has also been shown to drop quickly with soil depth (Peltovuroi, 2002) and has been used in a variety of environmental level of threshold studies (Zhang et al., 2005; Hongthanat et al., 2011; Nair et al., 2004). The quantity of labile P within sediment is important for determining the total desorbable P that can be released into an environment. Anion exchange resin P (AEP) uses a semi-permeable membrane that acts as a P sink to the labile P within a soil suspension. The labile P determined by AEP is commonly associated with the fraction of total P that can be considered bioavailable. Anion exchange resin is also used in conjunction with isotherms to determine P sorption/desorption expectations when sediment enters an aquatic environment (Agudelo et al., 2011; McDowell et al., 2003).

Thesis objectives

Ephemeral gully erosion effects on nutrients remains fairly unstudied. How changes in sediment composition in response to EGs affect the sorption and desorption within runoff and sediment is largely unknown. Additional information is needed on EG effects on P sorption as well as EG contribution to P loss from fields. Since P sorption/desorption involves a variety of soil characteristics, these characteristics are important for understanding how an EG will change the composition of eroded sediments and how this will affect the P sorption/desorption within the runoff. This research will analyze soil properties and P fractions by depth, and examine relative differences between EG soils and bulk field soils.

Four interrelated objectives are examined within this study;

1. Detailed analysis of soil characteristics that affect P sorption with respect to soil depth and field location within fields containing ephemeral gullies.
2. Determine if easily measured soil properties (e.g. DPS and pH) can be used to estimate more complex soil parameters related to P sorption (e.g., $EPC_{(0)}$ and P buffering capacity).
3. Develop methods to predict the soluble P concentration when diverse sediments are mixed in suspension.
4. Determine the mass of P loss due to ephemeral gully erosion relative to sheet and rill erosion and expected changes in dissolved P in runoff caused by ephemeral gullies.

References

- Agudelo, S.C., N.O. Nelson, P.L. Barnes, T.D. Keane, and G.M. Pierzynski. 2011. Phosphorus adsorption and desorption potential of stream sediments and field soils in agricultural watersheds. *J. Environ. Qual.* 40:144-152.
- Belmont, M.A., J.R. White, and K.R. Reddy. 2009. Phosphorus sorption and potential phosphorus storage in sediments of lake Istokpoga and the upper chain of lakes, Florida, USA. *J. Environ. Qual.* 38:987-996.
- Carpenter, S., N. Caraco, D. Correll, R. Howarth, A. Sharpley, and V. Smith. 1998. Nonpoint pollution of surface waters with phosphorus and nitrogen. *Ecol. Appl.* 8:559-568.
- Cheung, M.Y., S. Liang, and J. Lee. 2013. Toxin-producing cyanobacteria in freshwater: A review of the problems, impact on drinking water safety, and efforts for protecting public health. *J. Microbiol.* 51:1-10.
- Daloglu, I., K.H. Cho, and D. Scavia. 2012. Evaluating causes of trends in long-term dissolved reactive phosphorus loads to Lake Erie. *Environ. Sci. Technol.* 46:10660-10666.
- Daggupati, P., A. Sheshukov, and K.D. Mankin. 2014. Evaluating ephemeral gullies with a process-based topographic index model. *Catena* 113:177-186.
- Dodds, W.B., W. Eitzmann, J. Pilger, T. Pitts, K. Riley, A. Schloesser, and J. Thornbrugh. 2009. Eutrophication of U.S. freshwaters: Analysis of potential economic damages. *Environ. Sci. Technol.* 43:12-9.

- Folmar, G., R.W. McDowell, and A.N. Sharpley. 2003. Modification of phosphorus export from an eastern USA catchment by fluvial sediment and phosphorus inputs. *Agric. Ecosyst. Environ.* 99:187-199.
- Hartikainen, H., K. Rasa, and P.J.A. Withers. 2010. Phosphorus exchange properties of European soils and sediments derived from them. *Eur. J. Soil Sci.* 61:1033-1042.
- Heisler, J.G., P.M. Burkholder, J.M. Anderson, D.M. Cochlan, W. Dennison, W.C. Dortch, Q. Gobler, C.J. Heil, C.A. Humphries, E. Lewitus, A. Magnien, R. Marshall, H.G. Sellner, K. Stockwell, D.A. Stoecker, and D.K Suddleson. 2008. Eutrophication and harmful algal blooms: A scientific consensus. *Harmful Algae* 8:3-13.
- Hongthanat, N., J.L. Kovar, and M.L. Thompson. 2011. Sorption indices to estimate risk of soil phosphorus loss in the Rathbun Lake watershed, Iowa. *Soil Sci.* 176:237-244.
- Hudnell, H.K. 2010. The state of U.S. freshwater harmful algal blooms assessments, policy and legislation. *Toxicon* 55:1024-34.
- Ige, D.V., O.O. Akinremi, and D.N. Flaten. 2007. Direct and indirect effects of soil properties on phosphorus retention capacity. *Soil Sci. Soc. Am. J.* 71:95-100.
- Kerr, J.G., M. Burford, J. Olley, and J. Udy. 2011. Phosphorus sorption in soils and sediments: Implications for phosphate supply to a subtropical river in Southeast Queensland, Australia. *Biogeochem.* 102:73-85.

Luz Rodriguez-Blanco, M., M. Mercedes Taboada-Castro, M. Teresa Taboada-Castro, and J.

Luis Oropeza-Mota. 2009. Nutrient dynamics during storm events in an agroforestry catchment. *Commun. Soil Sci. Plant Anal.* 40:889-900.

Nair, V., D. Portier, K.M. Graetz, and D.A. Walker. 2004. An environmental threshold for degree of phosphorus saturation in sandy soils. *J. Environ. Qual.* 33:107-13.

Peltovuorui, T. 2002. Phosphorus extractability in surface soil samples as affected by mixing with subsoil. *Agri. and Food Sci. in Finland* 11:371-379.

Poesen, J., J. Nachtergaele, G. Verstraeten, and C. Valentin. 2003. Gully erosion and environmental change: Importance and research needs. *Catena* 91-133.

Richards, R.P., D.B. Baker, J.P. Crumrine, and A.M. Stearns. 2010. Unusually large loads in 2007 from the Maumee and Sandusky rivers, tributaries to Lake Erie. *J. Soil Water Conserv.* 65:450-462.

Richards, R.P., D.B. Baker, and D.J. Eckert. 2002. Trends in agriculture in the LEASEQ watersheds, 1975-1995. *J. Environ. Qual.* 31:17-24.

Scalenghe, R., A.C. Edwards and E. Barberis. 2007. Phosphorus loss in overfertilized soils: The selective P partitioning and redistribution between particle size separates. *Eur. J. Agron.* 27:72-80.

Sharpley, A., P. Richards, S. Herron, and D. Baker. 2012. Case study comparison between litigated and voluntary nutrient management strategies. *J. Soil Water Conserv.* 67:442-450

- Tang W., B.Y. Liu, T. Liu Liu, L. Hong-hu, and H.W. Bao-yuan. 2013. Effects of gully erosion and gully filling on soil degradation in the black soil region of Northeast China. *J. of Mountain Sci.* 10:913-922.
- Valentin, C., J. Poesen, and Y. Li. 2005. Gully erosion: Impacts, factors and control. *Catena* 63:132-153.
- Verbree, D.A., S.W. Duiker, and P.J.A. Kleinman. 2010. Runof losses of sediment and phosphorus from no-till and cultivated soils receiving dairy manure. *J. of Enviro. Qual.* 39:1762-1770.
- Wallbrink, P.J., C.E. Martin, and C.J. Wilson. 2003. Quantifying the contributions of sediment, sediment-P and fertiliser-P from forested, cultivated and pasture areas at the landuse and catchment scale using fallout radionuclides and geochemistry. *Soil & Tillage Research* 69:53-68.
- Zhang, H., J. Schroder, J. Fuhrman, N. Basta, D. Storm, and M. Payton. 2005. Path and multiple regression analyses of phosphorus sorption capacity. *Soil Sci. Soc. Am. J.* 69:96-106.
- Zhang, Q., D.C. Brady, and W.P. Ball. 2013. Long-term seasonal trends of nitrogen, phosphorus, and suspended sediment load from the non-tidal Susquehanna River basin to Chesapeake bay. *Sci. Total Environ.* 452:208-221.
- Zheng, F., X. He, X. Gao, C. Zhang, and K. Tang. 2005. Effects of erosion patterns on nutrient loss following deforestation on the loess plateau of China. *Agric. Ecosyst. Environ.* 108:85-97.

Table 1.1. Relative contribution of ephemeral gully erosion to total sediment loss measured in research studies. *Source:* Poesen et al., 2003.

Location	Estimated annual sheet and rill erosion	Measured ephemeral gully erosion	Ephemeral gully erosion to sheet and rill erosion
	tons ac ⁻¹ yr ⁻¹	tons ac ⁻¹ yr ⁻¹	%
Alabama	15.60	9.30	59
Illinois	7.10	5.20	73
Iowa	9.60	3.00	31
Kansas	21.98	8.00	36
Louisiana	17.80	6.04	34
Michigan	4.67	1.22	26
Mississippi	17.60	7.50	43
New Jersey	6.70	5.20	77
Virginia	13.0	12.80	98
Washington	0.69	1.89	275

Source: USDA-NRCS, 1997. America's Private Land. A Geography of Hope. United States Department of Agriculture—NRCS, Washington, DC, p. 39.

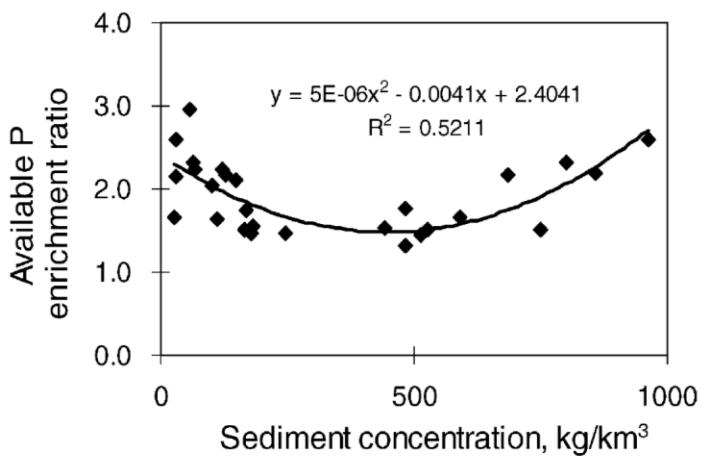


Figure 1.1. Phosphorus enrichment onto sediment based upon sediment concentration in runoff. *Source:* Zheng et al., 2004

Chapter 2: Ephemeral gully influence on soil characteristics and phosphorus sorption

Introduction

Ephemeral gullies (EG) change the dynamics of phosphorus (P) within a field and also with sediment leaving the field. Ephemeral gullies are an erosion process that removes the subsoil because it cuts down into the soil profile. Subsoil can influence P sorption greatly due to its high P buffering capacity and often low P saturation (Peltovuori, 2002; Verbree, 2010). Tillage that continually fills in EGs can also result in even greater amounts of sediment runoff (Gordon et al., 2008). No-till fields can often form pronounced EGs due the widening and lengthening of gullies throughout years of erosional processes. The sediments from a field with EGs comes from a variety of landscape positions; top soil from sheet and rill erosion of the higher ground, sediments within the EG channel and lower ground, and subsoil within the scouring of the EG.

It is likely that the soils in the EG have different soil characteristics than that of the bulk field. Erosional processes in the bulk field have water velocities that are less than in EG erosion, possibility leading to differing particle size erosion. Because of differing particle size preferences in erosion, soil characteristics affect by particle size would also be affected. Another factor that could cause EG soils to have difference soil properties is sedimentation from the upper field. Studies have shown that sedimentation into the lower field from higher elevations is common (Blake et al., 2002). In fields with EGs, sedimentation from the higher topography of the field could change physical and chemical characteristics of the soil, thereby influencing P sorption characteristics and the P concentration, in soils affected by an EG.

The effect of EG on P sorption can be complex, partly due to the changing nature of gullies and the dynamic status of P sorption in soil. There are many chemical and physical processes that influence P adsorption and many forms of P can be found within the soil matrix and solution. Phosphorus within the soil must be analyzed in a variety of ways because each test and soil parameter describes a different component of P sorption. Past research to determine the main soil component that influence P sorption has shown inconsistent and sometimes contradictory results (Table 2.1).

Other soil factors can indirectly influence which soil characteristics are likely to be the main factors controlling P sorption. Generally pH is considered an important indirect influence, as soil that is high in pH might result in Ca controlling P sorption along with Fe or Al oxides (Harrell, 2006). A sorption test such as equilibrium phosphorus concentration at zero net sorption (EPC_0) and degree of phosphorus saturation (DPS) are useful in describing the P buffering of a soil and if P will adsorb or desorb once the sediment is in runoff or a water body. If EPC_0 drops with soil depth, the erosion of deeper soil fractions would be more likely to sorb P that had been desorbed from soils with higher EPC_0 . Degree of phosphorus saturation is also an indicator of P sorption and a lower DPS will more readily adsorb P once in solution.

Concern must be taken in the implantation of certain best management practices (BMPs) that eliminate EGs because it could have an effect on dissolved P in runoff. In Sharpley et al., (1996) a study was done comparing two field watersheds with EGs. One of the watershed's EG had been treated with grass waterways, after the grass has been established the sediment bound P decreased but the dissolved reactive P increased in runoff. In the study this was attributed to an application of fertilizer, but it is possible that, in addition, reducing the highly sorptive subsoil

was also increasing the dissolved P. More research needs to be done to fully describe and analyze the effects of certain BMPs on the outcome of dissolved P in runoff.

Because soil properties and P status of EGs are likely different and EG erosion has different soil depth contributions than that of sheet and rill, it is important to analyze soil characteristics of EGs and the rest of the field separately. The objectives of this study are to:

1. Determine the effect of ephemeral gully formation on the soil P content and P sorption and desorption.
2. Develop simplified methods to estimate P desorption potential of soils.

Materials and Methods

Study site description

This study was conducted in three fields in McPherson County, KS that had visible and well developed gullies; Weedel (W), Garring (G), and Schmidt (S) (Figure 2.1). These fields were selected to represent a range of cropping, EG watershed size, and soil characteristics typical for the region (Table 2.2).

Three replicate composite soil samples were collected from 5 separate landscape positions (bulk field, upper bank, lower bank, upper gully, lower gully) within each field (Figure 2.2; Figure 2.3). Sampling landscape position locations for each field are shown in figures 2.4 to 2.6. The samples were divided into 0 to 2, 2 to 5, 5 to 15, and 15 to 30 cm depths. Each location and depth was a composite of at least 15 sample cores with 0 to 2 cm being at least 20 cores. Samples were taken on July 8th, 2013 after the wheat harvest for the G and S fields and on March

18th, 2013 before sorghum planting in the W field. Once the samples were collected, they were stored on ice in the field then placed in 4 °C cooler immediately upon returning from the field. Within a week, the samples were dried at 50 °C for 2 days, ground, then passed through a 2mm sieve.

The EG characteristics of the W field were pronounced; it contained large gullies that were easily discernible from the surrounding field. In the tested gully, the upper and lower portion was still being fertilized and planted through. Because the G field was continuously tilled, the exact position of the gully banks relative to the gully channel was hard to discern. Therefore, the EG was considered to be in the lowest point of the landscape where water would collect. The entire G field was cultivated and fertilized. The S field had a large active EG but looked as if deposition was occurring in the upper and lower EG segments. The EG within the S field was also planted through.

Laboratory methods - soil analysis

Ammonium-oxalate extraction

Poorly crystalline, oxalate extractable Al (Al_{ox}) and Fe (Fe_{ox}) along with associated P (P_{ox}) was determined by 0.2M ammonium oxalate/oxalic acid extraction. A 0.75-g soil sample was added to a centrifuge tube with 30 mL of extracting solution and shaken horizontally in a reciprocating shaker for 2 hours in the dark. After shaking, tubes were centrifuged at 10,000 rpm for 10 min. Supernatant was filtered through a Whatman #42 filter paper into a 15-ml sample vial. Samples were analyzed by inductively coupled plasma atomic emission spectrometry (ICP-AES), for Al (Al_{ox}), Fe (Fe_{ox}), and P (P_{ox}). Degree of P saturation by oxalate extraction (DPS_{ox}) was calculated with the equation 2.1, where P_{ox} , Fe_{ox} , and Al_{ox} are all expressed in $mmol\ kg^{-1}$ soil (Hongthanat et al., 2011; Zhang et al., 2005)

$$DPS_{ox} = \frac{P_{ox}}{Fe_{ox} + Al_{ox}} \quad \text{Equation 2.1.}$$

Mehlich 3 extraction

Mehlich 3 (M3) extraction solution was made in accordance with Sims (2000). A 2.5-g soil sample was mixed with 25 ml of M3 solution in a 125-ml Erlenmeyer flask and shaken for 5 min at 200 rpm on an orbital shaker. After shaking, the mixture stood for 5 min to allow sediment to settle. Supernatant was filter through a Whatman #42 filter and collected in a 15-ml vial. Samples were analyzed by inductively coupled plasma atomic emission spectrometry (ICP-AES) for Al (Al_{M3}), Fe (Fe_{M3}), and Ca (Ca_{M3}), and colorimetrically for P (P_{M3}). Two degree of P saturation ratios were calculated; DPS_{M3} (mmol kg^{-1}) and DPS_{Ca} (mmol kg^{-1}), using the equations 2.2 and 2.3 (Hongthanat et al., 2011; Zhang et al., 2005).

$$DPS_{M3} = \frac{P_{M3}}{Fe_{M3} + Al_{M3}} \quad \text{Equation 2.2.}$$

$$DPS_{Ca} = \frac{P_{M3}}{Ca_{M3}} \quad \text{Equation 2.3.}$$

Anion exchange extractable P

Anion exchange extractable P (AEP) is the use of anion exchange membrane strips that act as an infinite P sink to induce continuous P desorption during the extraction period. The method used was performed in accordance with Saggar et al., (1990). Resin strips were first cut into 2x8 cm strips of exchange membrane (BDH Laboratory Supply, product # 55164 2S) and were “charged” by shaking with 0.5 M NaHCO_3 adjusted to pH 8.5 for 30 min, repeated twice, and then rinsed 4 times with distilled water. Two grams of soil and 30 ml distilled water were added to centrifuge tubes. Resin membranes of a 2x8 cm size were then inserted into the centrifuge tubes (one per tube) and were shaken for 24 hours with a reciprocating shaker. After

shaking, the resin membranes were removed and individually rinsed with distilled water. The membrane strips were then eluted by shaking with 30 ml 0.5 M NaCl for one hour. The resulting NaCl solution was analyzed for molybdate reactive P with an automated flow-injection analyzer (Lachat Quick Chem method 10-115-01-1-A, Lachat Instruments, 2000).

Total phosphorus

Total phosphorus was determined with a salicylic-sulfuric acid digestion in accordance to Bremner and Mulvaney, (1982). An acid solution was created with 74 g salicylic acid dissolved into 2.5 L of sulfuric acid. One gram of soil was added to 100-ml digestion tubes and 10 ml of acid solution was added. Samples stood for two hours, and then 0.7 g of sodium thiosulfate was added and mixed on a vortex mixer. Tubes were then allowed to stand overnight. Tubes were placed onto a digestion block at 200 °C for 1 hour then 380 °C for 1 hour. After first digestion, a catalyst tablet of 1.5 g K₂SO₄ and 0.125 g CuSO₄ was added to each tube. Tubes were returned to heating block and digested for 3.5 hours more at 380 °C with the use of a reflux lid. After digestion, tubes were filled to 100 ml with distilled water and hand mixed end over end. Sediment solution was allowed to settle; supernatant was filtered with a Whatman #42 filter and collected in sample vials. Samples were analyzed with inductively coupled plasma atomic emission spectrometry (ICP-AES).

Texture

Particle size analysis was determined using the hydrometer method (Bouyoucos, 1962). One hundred milliliters of sodium hexametaphosphate was added to a 500-ml Erlenmeyer flask with 250 ml distilled water and 50 g of soil. After mixing flask by hand, mixture was allowed to sit for 15 min. Mixture was then blended for 5 min and poured into a 1000-ml graduated

cylinder. Distilled water was added to 1000 ml volume. Capped cylinders were turned end over end and then left to settle. Readings using a hydrometer were taken after 40 sec and again after 5 hours. The 40-sec reading was repeated three times by remixing the capped cylinders (n=3).

Temperature and blank solution cylinders were used for calibration.

pH- 1:1 soil to water solution

Soil pH was determined with a 1:1 soil to water solution. A 5-g soil sample was added to a 15-ml conical tube with 5 ml of distilled deionized water. Solution was shaken and allowed to rest for 30 min, shaken again and let to rest for another 30 min. After second resting period, pH was measured using an Accumet pH meter (08409) while being shaken on a vortex shaker.

Equilibrium phosphorus concentration at zero net sorption (EPC_0)

A phosphorus sorption isotherm was determined by mixing 1 g of soil with 25 ml of solution containing a background electrolyte and increasing concentrations of P (KH_2PO_4) (0.00, 0.05, 0.1, 0.2, 0.5, 2, 10 mg P L⁻¹). The background electrolyte was 0.006-M $CaCl_2$ to simulate the ionic strength of stream water. The soil solutions were mixed on an end to end mixer for 24 hours then centrifuged at 10,000 rpm for 10 min. The supernatant was filtered through a 0.45- μ m nylon syringe filter and stored in a 15-ml vial at 4 °C. The samples were analyzed for molybdate reactive P with an automated flow-injection analyzer (Lachat Quick Chem method 10-115-01-1-A, Lachat Instruments, 2000).

The Freundlich equation (Equation 2.4) was fit to phosphorus sorption isotherm data with non-linear regression using PROC NLIN (SAS v. 9.1) (SAS code- Appendix B: Figure B.1).

$$Q = K_f C^b \quad \text{Equation 2.4.}$$

Where Q is the labile P determined by AEP that has been sorbed on the soil plus the added quantity of dissolved P sorbed from solution (mg kg^{-1}) and C is the P concentration in solution (mg L^{-1}). With the fitting parameter and coefficient, b and K_f , EPC_0 was determined using the equation 2.5.

$$EPC_0 = 10^{\frac{\log(\frac{Q}{K_f})}{b}} \quad \text{Equation 2.5.}$$

Where Q is the adsorbed P concentration as estimated by AEP (mg kg^{-1}), K_f is the Freundlich adsorption coefficient, EPC_0 is the final equilibrium P concentration in solution (mg L^{-1}) and b is a fitting parameter.

An example of the P isotherm data fit to the Freundlich equation is included in Appendix A: Figure A.1, and shows that the Freundlich equation fits the P sorption isotherm well. The Langmuir equation did not fit as well as the Freundlich, although it is commonly used to predict the sorption of elements. In the P sorption isotherm we used for this study, we added AEP onto the P that was removed from the dissolved P in solution when it was mixed with sediment to find the total amount of P sorbed (Q in Equation 2.4). After we added the AEP in Q, the P isotherm data fit better with the Freundlich rather than the Langmuir. An equation for the buffering capacity, or slope of the adsorption isotherm, can be determined by taking the first derivative of the Freundlich equation (Equation 2.6).

$$\beta = K_f * b * C^{(b-1)} \quad \text{Equation 2.6.}$$

where β is the buffering capacity (L kg^{-1}) and other parameters are as previously defined. The buffering capacity at EPC_0 was determined using equation 2.6, where EPC_0 is substituted for C.

Statistical analysis

The upper and lower bank samples and the upper and lower gully samples were combined as bank and gully landscape positions respectively for statistical analysis. This was done because analysis of variance (ANOVA) with upper and lower EGs as separate landscape positions showed few and inconsistent effects of gully position (upper vs. lower). Therefore, there were three landscape positions (LPs) used for statistical analysis, representing combined upper and lower bank, combined upper and lower gully, and bulk field. Analysis of variance was conducted with PROC MIXED (SAS version 9.2), where landscape position and depth were fixed effects (SAS code- Appendix B: Figure B.2). Error bars for graphs were computed as the 95% confidence interval for means.

A correlation matrix (Table 2.4) determining of relationships of soil characteristics and soil indexes to each other was created using (PROC CORR) SAS version 9.2 (SAS code- Appendix B: Figure B.3). An added term of $\frac{1}{\log(EPC_0)}$ was added to the matrix. This was done to linearize the EPC_0 data to better fit the data of the other soil characteristics. Because EPC_0 was determined using equation 2.5, EPC_0 of different soils could differ by several orders of magnitude, skewing relationships.

Regressions were created to approximate EPC_0 using other defined soil characteristics such as Al_{ox} , Fe_{ox} , P content, and indexes (Equations 2.1-2.3). Stepwise regressions were done using PROC REG (SAS version 9.2), at the 95% probability level (SAS code- Appendix B: Figure B.4). Strengths of relationships were tested with R^2 and Nash-Sutcliff efficiency (NSE). The NSE measures the consistency of the predicted values vs. the observed data or the fit of the data to the observed 1:1 line to the best fit line of the predicated values (Parajuli et al., 2009). The range of the NSE goes from negative infinity (poor fitting) to positive one (perfect fit).

Equation 2.7 describes the NSE with O_i being the observed value for sample i and P_i being the predicted value for sample i .

$$NSE = 1 - \frac{\sum_{i=1}^n (O_i - P_i)^2}{\sum_{i=1}^n (O_i - \bar{O})^2} \quad \text{Equation 2.7.}$$

The data points for the correlation matrix and the stepwise regression were done using all soil samples from each of the three fields for a total of 180 soil samples (3 fields x 5 landscape positions x 4 depths x 3 replications). The ANOVA analysis was performed by field using the landscape positions, depths, and replications (60 samples per field).

Results and Discussion

Landscape and depth influence on soil characteristics

Landscape position and soil depth influenced many of the soil characteristics (Table 2.3). The landscape position effect was significant for nearly every characteristic, meaning that there are differences between the gully bank, within the gully, and in the bulk field. The depth effect also shows the differences in characteristics are common with depth. The landscape by depth effect however was not significant in the G field. This is likely due to tillage homogenizing the soil so that while characteristics change with depth, those changes are the same within the landscape.

EPC₀ within the field and ephemeral gully

The results showed that there is a decrease in EPC₀ from the 0 to 2 cm depth to the proceeding 2 to 5 cm depth in nearly every field location from the three fields (Figure 2.7 for W,

2.8 for G, and 2.9 for S). However in most locations there was no statistical difference between the 5 to 15 and 15 to 30 cm soil depth fractions and the minimal detectable limits, or the EPC_0 dropped to a minimal detectable limit after 5 cm of depth. The general trend for the decrease in EPC_0 with depth has been shown in other studies (Peltovuori, 2012; Hongthanat et al., 2011).

The W field had a very high EPC_0 in the 0 to 2 cm of the bulk field in comparison to the next depth fraction (Figure 2.7). This is likely due to the years of surface-broadcast fertilization combined with no-till management, leading to P saturation of the surface. This however was not seen in the S or G field (Figure 2.8, and Figure 2.9) where, within the bulk field, there was no significant difference at any tested depth. Both the W and S field are no-till fields, however the S field has been in no-till for a shorter period of time (Table 2.2), stronger P stratification could occur over time. The S field had no significance by depth and landscape according to table 2.3; however the p-value for the depth by landscape position interaction was 0.07.

With the three fields, the relation between the bulk field to the EG soils in regards to the EPC_0 were inconsistent. The W field had a higher EPC_0 at the 0 to 2 cm depth in the bulk field than the bank soils while the G and S field had a lower EPC_0 at the 0 to 2 cm depth in the bulk field. Since fertilization is even across the field, the likely possibility for this is that the sedimentation of enriched sediment is occurring in the G field. The W field is experiencing erosion of the upper bank soils due to sloughing of the bank soil into the gully or strong erosion due to water overflowing the gully. The S fields change in EPC_0 of the bank soils is more due to changes in texture (Appendix A: Figure A.2 and Figure A.3) and P sorption capacity rather than increases in P quantity; this is farther discussed in the total P and DPS_{ox} sections.

Another feature of this study is the 0 to 2 cm fraction within the gully channel had a greater EPC_0 than the next fraction for each of the three fields and a higher EPC_0 than its depth within the soil relation to the bank (the gully channel being lower than the bank). This indicates that enriched sediments may have been deposited within the gully channels as water speed decreased until sediment fallout occurred (Poesen et al., 2003). This increase in P and enriched sediments being deposited at the end of erosional event is evident in the other soil test such as AEP, total P, and DPS_{ox} . Also note that at times the sedimentation within in channel had some effect on EPC_0 in the 2 to 5 cm fraction as well when some of the deposited soil was deep enough to be collected in the 2 to 5 cm fraction.

The EPC_0 results show that the addition of subsoil (below 5 cm) would create a lower dissolved P concentration during an erosion event compared to sediments just eroded from the 0 to 2 cm depth fraction. Therefore, if sediments from the subsoil and surface soil were mixed in solution, the subsoil would be more likely to adsorb P from solution while surface soils would desorb P. The sheet and rill erosion of the studied fields rarely exceeded the 0 to 2 cm fraction (due to the field's low slope and supported by visual observation) while the EGs eroded the deeper soil fractions. Mixing sediments eroded from the EG formation with runoff and sediments from sheet erosion would likely decrease the dissolved P concentration in the runoff.

Anion exchange phosphorus within the field and ephemeral gully

Anion exchange phosphorus (AEP) represents the total amount of readily desorbable P and is closely correlated to EPC_0 (Figure 2.10). The strength of the relation between AEP and EPC_0 is changed by certain soil characteristics. Figure 2.10 shows that the samples with more sand held a different relation of AEP to EPC_0 than samples with more clay. The increased sand and less clay in the S field compared to the W and G field is decreasing AEP while still

increasing EPC_0 , although the total P of the S field is less (total P discussed in next section). This is an indication that P sorption differences between the two characteristics are altered by texture, likely indirectly due to clay's relation to Al_{ox} (Table 2.4).

Within the W and G field, EPC_0 and AEP follow some similar trends of reduction in depth and location while the S field shows some differences (Figure 2.11 for W, Figure 2.12 for G, and Figure 2.13 for S). The AEP of the W and S field has a higher bulk field 0 to 2 fraction than within gully and bank soils while the G bulk field 0 to 2 is lower. However in the S field, the EPC_0 of the bank soil was higher than the bulk field while the AEP of the bank soil was lower than the bulk field (Figure 2.9 for EPC_0 and Figure 2.13 for AEP). This could be due to the presence of higher sand in the bank soils compared to the bulk field that is changing the relation of EPC_0 to AEP. According to the correlation matrix (Table 2.4), EPC_0 is more related to sand percentage than AEP. Soil characteristics can have a large effect on P buffering and that soil tests are affected directly; the influence of sand in the S field is consistent with texture analysis (Appendix A: Figure A.2 and Figure A.3). Table 2.3 shows that the depth by landscape position for the G field is not significant, likely due to conventional tillage.

Because the W and S fields have higher bulk field AEP than EG soils the erosion of the bulk field from sheet and rill erosion would likely deliver more AEP in runoff, given that erosional amounts and enrichment ratios were similar. With the G field the EG gully soils are more likely to supply quantities of labile P. This shows that when testing a field for contributions of P into a watershed, concern must be taken for the landscape position and depth from which the contributing soil is eroded.

Total phosphorus within the field and ephemeral gully

The three fields showed differing results for total P (Figure 2.14 for W, Figure 2.15 for G, and Figure 2.16 for S). The W field had decreasing total P with depth in both the bulk field and EG soils, similar to AEP and EPC_0 though not as quick of a decrease. The G field showed little total P change between depths or by landscape, though significantly different (Table 2.3). The S field had a decreasing total P in the bulk field but had little difference in the gully soils, again likely due to the sandy texture.

Total P was largely shown to be misleading as useful parameter for expectations of P loss from a field. For instance in the W field the total P never dropped below 100 mg kg^{-1} while the EPC_0 indicates continued strong P sorption at P levels well above that point. The Pearson correlation table (Table 2.4) shows that while total P and EPC_0 are correlated, the correlation is nearly not significant. Another example is in the Schmidt field where total P in the EG soils show little difference in depth, the EPC_0 and AEP of the same soil fractions decreases quickly, showing that total P can mislead on what amount is actually desorbable in solution and bioavailable. Studies have shown that most of total P is not desorbable as labile P. In a study done by Uusitalo et al., (2001) demonstrated that 92% of total P was sediment bound and only 7% of sediment bound was P was desorbable by AER. Our results showed that about 7% of total P is desorbable as labile AEP. Total P is useful however when the P buffering of soil is needed to be ignored and strict total quantities of P loss need to be evaluated.

Degree of phosphorus saturation indexes

Degree of phosphorus saturation (DPS) indexes and are described as the current level of P which has been adsorbed over the total maximum sorption based upon soil chemical properties

that influence adsorption. The results for the DPS_{ox} index using the results from the Al and Fe oxide extraction along with the associated P for the three fields are described in figures 2.17 for W, 2.18 for G, and 2.19 for S. It is also important to note that P saturation does not need to reach maximum levels (a DPS of 100%) before P is desorbed. Common environmental thresholds between 20-25% have been set for DPS_{ox} for certain European countries (Zhang et al. 2005; Hartikainen et al. 2010).

The three fields show a decreasing trend in the DPS_{ox} with depth. For the three fields, the gully bank and within the gully show similar DPS_{ox} status even though sampling within the gully starts at a point that is lower in the soil profile than the bank. Within the W field, DPS_{ox} drops quickly with depth so that the 2 to 5 cm fraction is significantly lower than the 0 to 2 cm fraction and the 5 to 15 cm fraction is lower than the 2 to 5 cm fraction in each of the three field locations. The G field DPS_{ox} also decreased with depth but the rate of decline was less than what was observed in the other two fields.

Within the W and G field the change of DPS_{ox} with depth is shown to be the result of the decrease in P_{ox} with depth rather than the change of Al_{ox} and Fe_{ox} (Figure 2.20 and Figure 2.21 respectively). These two fields have higher clay content a heavy clay soil texture that was consistent down to 30 cm (Appendix A: Figure A.2 and Figure A.3), and the clay soil fraction is major proportion responsible for the amounts of poorly crystallized Fe and Al that measured with ammonium-oxalate extraction. The S field also had a decrease in DPS_{ox} (Figure 2.22) however the reason for this in the EG soils was because of the increase in Fe_{ox} and Al_{ox} that corresponded with an increase in clay with depth rather than the decrease in P_{ox} . This textural change was consistent with NRCS Web Soil Survey, (2013) soil maps indicating a soil map unit change at the head cut of the EG. The lack of P stratification in the EG soils that would be expected was

also evident in total P of the S field (Figure 2.16). This shows that indexes that are affected by P sorption can be due to changes in soil characteristics that affect sorption capacity and is not always tied to changes in P quantity.

Mehlich 3 and degree of phosphorus saturation

The results for the Mehlich 3 test (Fe_{M3} , Al_{M3} , P_{M3}) were similar to the oxalate extractions (Fe_{ox} , Al_{ox} , P_{ox}) in the Fe, and Al was largely uniform through the soil depth with each field location while P decreased with soil depth, this lead to trends in DPS_{M3} that were similar to those observed for DPS_{ox} (Appendix A: Figure A.4).

A Mehlich 3 test was also done for Ca (Ca_{M3}) to determine DPS_{Ca} (Appendix A: Figure A.4). In calcareous soils it has been shown that Ca can be the main controller to the sorption of P (Xue et al. 2014). Although these soils are not known to be calcareous, Ca could still be a factor to P sorption. Soil pH data are shown in Appendix A: Figure A.5. The DPS_{Ca} also followed the same trend as the other two DPS indexes where it decreased with soil depth at each field location. This was also mainly due to the stratification of P.

Correlation between EPC_0 to indexes and soil properties

Equilibrium phosphorus concentration at zero net sorption (EPC_0) is a highly useful soil test in estimating the balance between P sorption and desorption once soil is in solution or a water body. Because this test is time consuming, it would be advantageous to estimate EPC_0 with the use of soil properties that are simpler to determine. Most other studies use static soil characteristics, such as sorption maximum (S_{max}) or phosphorus retention index (PRI), for the determination of soil factors that are responsible for P sorption (Ige et al., 2007; Hongthanat 2011; Hartikainen 2010; Zhang et al., 2005; Bruland and Richardson 2004; Harrell 2006) and

less commonly with indexes and isotherms that take into account the presence of P already in the soil and how they relate to each other.

The table 2.4 showed that anion exchange phosphorus (AEP) as well as the three degree of phosphorus saturation indexes (DPS_{ox} , DPS_{M3} , DPS_{Ca}) are highly correlated with EPC_0 . Within the ammonium-oxalate extraction, Fe_{ox} , Al_{ox} , and P_{ox} , are each independently significantly correlated with EPC_0 , however the combination of the oxalate soil characteristics into the DPS_{ox} soil index provides an even higher correlation to EPC_0 . The Mehlich 3 extractions were similar in the P components (P_{M3}) of DPS_{M3} and DPS_{Ca} and were independently significantly correlated; however the derived DPS indexes with Fe_{M3} , Al_{M3} , and Ca_{M3} included had a higher level of correlation. Soil texture components of sand and clay were also correlated with EPC_0 , though likely through indirect soil factors of clay's relation to Al and Fe as also described by Zhang et al., (2005) and Ige et al., (2007). The correlation table 2.4 also shows this relation as clay is positively correlated with Al_{ox} and Al_{M3} although not with Fe_{ox} and Fe_{M3} . In this study Ca_{M3} content was also related to clay. Sand was positively correlated with EPC_0 and negatively correlated with Al_{ox} , Al_{M3} and Ca_{M3} , likely due to that fact that if there was greater percentage of clay there was a smaller percentage of sand.

A stepwise regression determined with SAS version 9.2 was used to find the ability of indexes and certain soil characteristics to determine the predictability of EPC_0 . As certain terms were found to be predictive of EPC_0 , marginally predictive terms were removed to simplify the model. Many terms are statistically significant in their predictability of EPC_0 but don't add much to the ability of the model to predict. As listed in table 2.5, it was determined that AEP and the DPS indexes were useful in predicting EPC_0 however the combining of both AEP and the index significantly improved the model fit. This research showed that the DPS formed by the

Mehlich 3 extraction was the most useful in determining EPC_0 . Al_{ox} and Al_{M3} were more useful in determining EPC_0 than Fe_{ox} and Fe_{M3} . It is likely that in this soil the Al fraction of the soil was more responsive to the sorption of P than the Fe fraction. However Al largely exceeded Fe quantities in $mmol\ kg^{-1}$ (Figures 2.21. for W, Figure 2.22 for G, and Figure 2.23 for S).

Adding more variables to the regression equation could improve the goodness of fit of the equation however adding variables that are collinearly related could reduce the accuracy of the equation and add unnecessary expenses to the prediction of the model (Ige et al., 2005). Using AEP, DPS_{M3} , and Al_{ox} gave the best fit of the model but there is likely collinearity between DPS_{M3} and Al_{ox} . Using all the soil components and indexes in a stepwise regression did not improve the R^2 past 0.95. The separation of the three fields into separate regression models also improved the goodness of fit as fields with similar soil characteristics reduced the variability in the data thereby improving the model; however the research was to find models that are usable across various soil ranges and types.

Conclusions

Phosphorus concentrations are generally stratified within the soil and affect many of the soil P sorption characteristics and indexes, such as EPC_0 , AEP, and DPS. The decrease in EPC_0 , AEP, and DPS with depth is mainly due to the increase in P buffering due to P saturation of the surface soil. Texture and P sorptive elements like semi-crystalline Al and Fe remained fairly constant in the W and G fields. The S field texture changed and the P sorptive elements increased with depth in the EG soil, also P stratification was evident.

The results from the no-till W field show strong P stratification in the both the bulk field and EG soils. Phosphorus concentrations are greater in the bulk field, especially in the 0 to 2 cm fraction that sediment for the sheet and rill erosion is expected from. The expected erosional

depths of the bank and gully soils were shown to be highly sorptive with low EPC_0 's, indicating the erosion of subsoil would sorb P in normal runoff conditions.

The conventional tilled G field showed minor amounts of P stratification and less P in the bulk field than in the EG soils. It is likely that sedimentation from the upper field is enriching the soils of the EG before they are lost in an erosional event. The subsoil sorption of P desorbed from the sheet and rill erosion would only be possible if deep EG would form.

The S field was unique due to its change in soil texture. The EG soils were sandy in the surface increased in clay with depth. The increased clay affected the soil characteristics that sorb P and changed the indexes that predict P sorption. There was also likely enriched sediment depositing from the upper field as well. These factors reduce the ability of the surface soil in the EG to sorb P and deeper subsoil erosion would be needed to adsorb P from the sheet and rill erosion.

The three fields show that subsoil is highly P sorptive and during large erosional events that remove EG soil, it is likely that EG subsoil is reducing the dissolved P in solution that has been desorbed from the bulk field. It is concluded that for full evaluation of P loss from fields with EGs, the EG soils need to be looked at separately and in conjunction with the bulk field.

The prediction of ECP_0 with other soil parameters is accurate and can achieve a R^2 up to 0.92 with AEP and DPS_{M3} meaning that the model is able to predict EPC_0 with 92% of variability accounted for. Within this research the Al_{ox} fraction of the soil was more responsive to the sorption of P than the Fe_{ox} fraction with respects to prediction EPC_0 . The models for predicting EPC_0 are accurate enough to be used prediction of sorption/desorption expectations of soil or runoff sediment.

References

- Bouyoucos, G. 1962. Hydrometer method improved for making particle size analyses of soils. *Agron. J.* 54:464-&.
- Bremner, J.M., and C.S. Mulvaney. 1982. Salicylic acid thiosulfate modification of the Kjeldhal method to include nitrate and nitrite. p. 621. *In* Miller, R.H. Miller, and Keeney, D.R., (eds.) *Methods of Soil Analysis. Part 2.* Am. Soc. Agron. Inc. Madison, WI
- Bruland, G.L., and C.J. Richardson. 2004. A spatially explicit investigation of phosphorus sorption and related soil properties in two riparian wetlands. *J. Environ. Qual.* 33:785-94.
- Gordon, L.M., S.J. Bennett, C.V. Alonso, and R.L. Binger. 2008. Modeling long-term soil losses on agricultural fields due to ephemeral gully erosion. *J. of Soil and Water Cons.* 63:173-181.
- Harrell, D.L., and J.J. Wang. 2006. Fractionation and sorption of inorganic phosphorus in Louisiana calcareous soils. *Soil Sci.* 171:39-51.
- Hartikainen, H., K. Rasa, and P.J.A. Withers. 2010. Phosphorus exchange properties of European soils and sediments derived from them. *Eur. J. Soil Sci.* 61:1033-1042.
- Hongthanat, N., J.L. Kovar, and M.L. Thompson. 2011. Sorption indices to estimate risk of soil phosphorus loss in the Rathburn Lake watershed, Iowa. *Soil Sci.* 176:237-244.
- Ige, D.V., O.O. Akinremi, and D.N. Flaten. 2007. Direct and indirect effects of soil properties on phosphorus retention capacity. *Soil Sci. Soc. of America J.* 71:95-100.

NRCS. 2013. Soil Survey Staff, NRCS, U.S. Department of Agriculture. Web Soil Survey.

Available online at <http://websoilsurvey.nrcs.usda.gov/>. Accessed [10/5/2013].

Parajuli, P. B., Nelson N. O., Frees, L. D., and Mankin, K. R. 2009. Comparison of AnnAGNPS and SWAT model simulation results in USDA-CEAP agricultural watersheds in south-central Kansas. *Hydro. Pro.* 23: 748–763.

Peltovuorui, T. 2002. Phosphorus extractability in surface soil samples as affected by mixing with subsoil. *Agri. and Food Sci. in Finland* 11:371-379.

Saggar, S., M. Hedley, and R. White. 1990. A simplified resin membrane technique for extracting phosphorus from soils. *Fertil. Res.* 24:173-180.

Sharpley, A.N., Smith, S.J., Zollweg, J.A., and G.A. Coleman. 1996. Gully treatment and water quality in the Southern Plains. *J. of Soil and Water Cons.* 51: 498

Verbree, D.A., S.W. Duiker, and P.J.A. Kleinman. 2010. Runoff losses of sediment and phosphorus from no-till and cultivated soils receiving dairy manure. *J. of Enviro. Qual.* 39:1762-1770.

Whiting, P., E. Bonniwell, and G. Matisoff. 2001. Depth and areal extent of sheet and rill erosion based on radionuclides in soils and suspended sediment. *Geology* 29:1131-1134.

Xue, Q.L., Z. Lingli, Q. Yuanqing, D. Lingyu, L. Peibin, S. Xiaoxia, L. Chengliang, and Xianyong. 2014. Deriving sorption indices for the prediction of potential phosphorus loss from calcareous soils. *Environ. Sci. Pollut. Res. Int.* 21:1564-1571.

Zhang, H., J. Schroder, J. Fuhrman, N. Basta, D. Storm, and M. Payton. 2005. Path and multiple regression analyses of phosphorus sorption capacity. *Soil Sci. Soc. Am. J.* 69:96-106.

Table 2.1. Main results from studies that investigated relationships between P sorption and select soil chemical properties.

Author	Soil chemical properties investigated †	Properties significantly related to P sorption †
Ige et al., 2007	Ca _{M3} ; Mg _{M3} ; Al _{M3} ; Fe _{M3} ; Al _{Ox} ; Fe _{Ox} ;	Mg _{M3} ; Ca _{M3} ; Al _{Ox}
Hongthanat 2011	Al _{M3} ; Fe _{M3} ; Al _{Ox} ; Fe _{Ox} ; Mg _{Ox}	Fe _{M3} ; Fe _{Ox}
Hartikainen 2010	Al _{Ox} ; Fe _{Ox} ; Mg _{Ox}	Al _{Ox}
Zhang et al., 2005	Al _{Ox} ; Fe _{Ox} ; Mg _{M3} ; Al _{M3} ; Fe _{M3} ; Ca _{M3}	Al _{Ox} ; Fe _{Ox}

† Ca_{M3}, Mg_{M3}, Al_{M3}, and Fe_{M3} are Mehlich 3 extractable Ca, Mg, Al, and Fe, respective, and Al_{Ox}, Fe_{Ox}, and Mg_{Ox} are ammonium-oxalate extractable Al, Fe, and Mg, respective

Table 2.2. Management practices and soil map units in the fields under investigation.

Name	Management	Crop	Soil Texture †	Soil Map Units ‡	EG watershed size
Weedel	No-till for 12 years	Sorghum	Slity Clay Loam	Crete Silt Loam 0-3% slope	1.2 ha
Garring	Conventional Till	Wheat	Clay Loam	Longford Silty Clay Loam 3-7% Slope	5.2 ha
Schmidt	No-till for 5 or 6 years	Wheat	Sandy Loam Clay Loam	Crete Silt Loam and Farnum Loam 1-3%	7.6 ha

† Soil textural class as determined by analysis (see Appendix B for further details).

‡ Determined from NRCS Web Soil Survey (NRCS)

Table 2.3. Levels of significance (*p*-values) for the effects of landscape position (LP), depth, and their interaction for the three fields based on ANOVA.

Field	Effect	Analytical Parameters †													
		AEP	TP	EPC ₀	Fe _{ox}	Al _{ox}	P _{ox}	DPS _{ox}	P _{M3}	Fe _{M3}	Al _{M3}	Ca _{M3}	DPS _{M3}	DPS _{Ca}	Clay
Weedel	LP	***	***	***	***	***	***	***	***	***	***	***	***	***	***
	Depth	***	***	***	***	***	***	***	***	***	***	***	***	***	***
	LP*Depth	***	***	***	***	***	***	***	***	***	***	***	***	***	***
Garring	LP	***	***	***	***	***	***	***	***	***	***	***	***	***	**
	Depth	*	***	NS	***	***	***	***	***	***	***	***	***	***	***
	LP*Depth	***	***	***	***	***	***	***	***	***	***	***	***	***	NS
Schmidt	LP	***	***	***	***	**	***	***	***	***	***	***	***	***	***
	Depth	***	NS	***	NS	**	***	***	***	***	***	***	***	***	***
	LP*Depth	***	***	***	***	***	***	***	***	***	***	***	***	***	*

* Significance at 0.05 probability

** Significance at 0.01 probability

*** Significance at 0.001 probability

†AEP is Anion Exchange Phosphorus, TP is Total Phosphorus TP; EPC₀ is Equilibrium Phosphorus Concentration at Zero Net Sorption, Fe_{ox} is Oxalate Extractable Fe, Al_{ox} is Oxalate Extractable Al, P_{ox} is associated P in Oxalate Extraction, DPS_{ox} is Degree of Phosphorus Concentration for oxalate extraction, P_{M3} is Mehlich 3 P, Fe_{M3} is Mehlich 3 Fe, Al_{M3} is Mehlich 3 Al, Ca_{M3} is Mehlich 3 Ca, DPS_{M3} is Degree of Phosphorus Concentration for Mehlich 3 Fe and Al, DPS_{Ca} is Degree of Phosphorus Concentration for Mehlich 3 Ca, and Clay is % of total soil texture classes

Table 2.4 Pearson Correlation Matrix of tested soil characteristics and indexes

	1/Log(EPC ₀)†	EPC ₀	AEP	Fe _{ox} ‡	P _{ox} ‡	Al _{ox} ‡	DPS _{ox} #	TP	P _{M3} ¶	Fe _{M3} ¶	Al _{M3} ¶	Ca _{M3} ¶	DPS _{M3} #	DPS _{Ca} #	Sand	Silt	Clay
EPC ₀	-0.92	1.00															
AEP	-0.85 *	0.73 *	1.00														
Fe _{ox} ‡	-0.03	-0.10	0.21	1.00													
P _{ox} ‡	-0.62 *	0.43 *	0.79 *	0.61 *	1.00												
Al _{ox} ‡	0.35 *	-0.30 *	0.07	0.20	0.13	1.00											
DPS _{ox} #	-0.85 *	0.70 *	0.66 *	0.17	0.71 *	-0.51 *	1.00										
TP	-0.47 *	0.34 *	0.76 *	0.50 *	0.80 *	0.47 *	0.36 *	1.00									
P _{M3} ‡	-0.85 *	0.72 *	0.96 *	0.23	0.83 *	0.01	0.73 *	0.73 *	1.00								
Fe _{M3} ‡	-0.30 *	0.13	0.53 *	0.81 *	0.79 *	0.29 *	0.36 *	0.73 *	0.58 *	1.00							
Al _{M3} ‡	0.08	-0.13	0.33 *	0.30 *	0.37 *	0.89 *	-0.26 *	0.67 *	0.28 *	0.53 *	1.00						
Ca _{M3} ‡	0.53 *	-0.29 *	-0.59 *	-0.49 *	-0.71 *	0.07	-0.57 *	-0.55 *	-0.60 *	-0.67 *	-0.32 *	1.00					
DPS _{M3} #	-0.87 *	0.81 *	0.62 *	-0.09	0.45 *	-0.56 *	0.88 *	0.20	0.70 *	0.15	-0.37 *	-0.36 *	1.00				
DPS _{Ca} #	-0.70 *	0.54 *	0.89 *	0.36 *	0.88 *	0.12	0.65 *	0.76 *	0.92 *	0.71 *	0.41 *	-0.70 *	0.51 *	1.00			
Sand	-0.32 *	0.21 *	-0.05	-0.02	0.05	-0.88 *	0.57 *	-0.39 *	0.03	-0.15	-0.78 *	-0.26 *	0.52 *	-0.01	1.00		
Silt	0.15	-0.09	0.23	0.12	0.15	0.86 *	-0.39 *	0.55 *	0.16	0.33 *	0.85 *	0.03	-0.38 *	0.21	-0.95 *	1.00	
Clay	0.54 *	-0.37 *	-0.26 *	-0.16	-0.37 *	0.75 *	-0.77 *	0.05	-0.34 *	-0.18	0.51 *	0.58 *	-0.66 *	-0.32 *	0.88 *	0.70 *	1.00
pH	0.30 *	-0.13	-0.60 *	-0.50 *	-0.70 *	-0.53 *	-0.22	-0.81 *	-0.57 *	-0.72 *	-0.81 *	0.73 *	-0.01	-0.69 *	0.34 *	-0.51 *	0.02

* Significant correlation at 5% probability level

† Correlation between EPC₀ and associated soil variable was determined with 1 over log transformation of EPC₀

‡ Fe_{ox}, P_{ox}, and Al_{ox} are ammonium oxalate extractable Fe, P and Al respectively

DPS_{ox}, DPS_{M3}, and DPS_{Ca} are Degree of Phosphorus Saturation from oxalate extraction, Melich 3 Fe and Al, and Melich 3 Ca respectively

¶ P_{M3}, Fe_{M3}, Al_{M3} and Ca_{M3} are Melich 3 extractable P, Fe, Al, and Ca respectively

EPC₀ is Equilibrium Phosphorus Concentration at Zero Net Sorption, AEP is Anion Exchange Phosphorus, TP is Total Phosphorus, pH is 1:1 soil to water ratio pH, and Sand, Silt, and Clay are textural percentages

Table 2.5. Prediction equations for EPC₀ using soil characteristics and indexes

Model Variables ¶	Model Equation $1/(\text{Log}(\text{EPC}_0)) = \beta_0 + \beta_1 * X + [\beta_2 * Y]$	Standard Error; respective †	Model R ²	NSE ‡
AEP	=-0.225 + -0.0152(AER)	0.0146, 0.0007	0.73	0.52
DPS _{ox}	=-0.0385 + -0.0595(DPS _{ox})	0.0224, 0.0028	0.72	0.51
DPS _{M3}	=-0.238 + -0.0787(DPS _{M3})	0.0132, 0.0033	0.76	0.50
DPS _{Ca}	=-0.302 + -0.0969(DPS _{Ca})	0.0184, 0.0075	0.48	0.14
DPS _{ox} + AEP	=-0.064 + -0.0354(DPS _{ox}) + -0.0093(AEP)	0.0151, 0.0025, 0.0006	0.87	0.72
DPS _{M3} + AEP	=-0.1762 + -0.0502(DPS _{M3}) + -0.0091(AEP)	0.0084, 0.0025, 0.0005	0.92	0.85
DPS _{Ca} + AEP	= -0.2207 + 0.0408(DPS _{Ca}) + -0.0198(AEP)	0.0142, 0.0114, 0.0015	0.75	0.57
AEP + Al _{ox}	=-0.5518 + -0.0157(AEP) + 0.0083(Al _{ox})	0.0219, 0.0004, 0.0005	0.89	0.79
AEP + Fe _{ox}	= -0.3190 + -0.0158(AEP)+ 0.0056(Fe _{ox})	0.0267, 0.0007, 0.0013	0.75	0.59
AEP + Al _{ox} + DPS _{M3}	=-0.3302+ -0.0111(AEP) + 0.0035(Al _{ox}) + -0.0350(DPS _{M3})	0.0283, 0.0006, 0.0006, 0.0035	0.93	0.85

† conducted at an alpha level of 0.05

‡ Nash-Sutcliff efficiency

¶ AEP is Anion Exchange Phosphorus, DPS_{ox} is Degree of Phosphorus Saturation by oxalate extraction, DPS_{M3} is Degree of Phosphorus Saturation by Mehlich 3 extraction, Al_{ox} is Al by oxalate extraction, and Fe_{ox} is Fe by oxalate extraction.

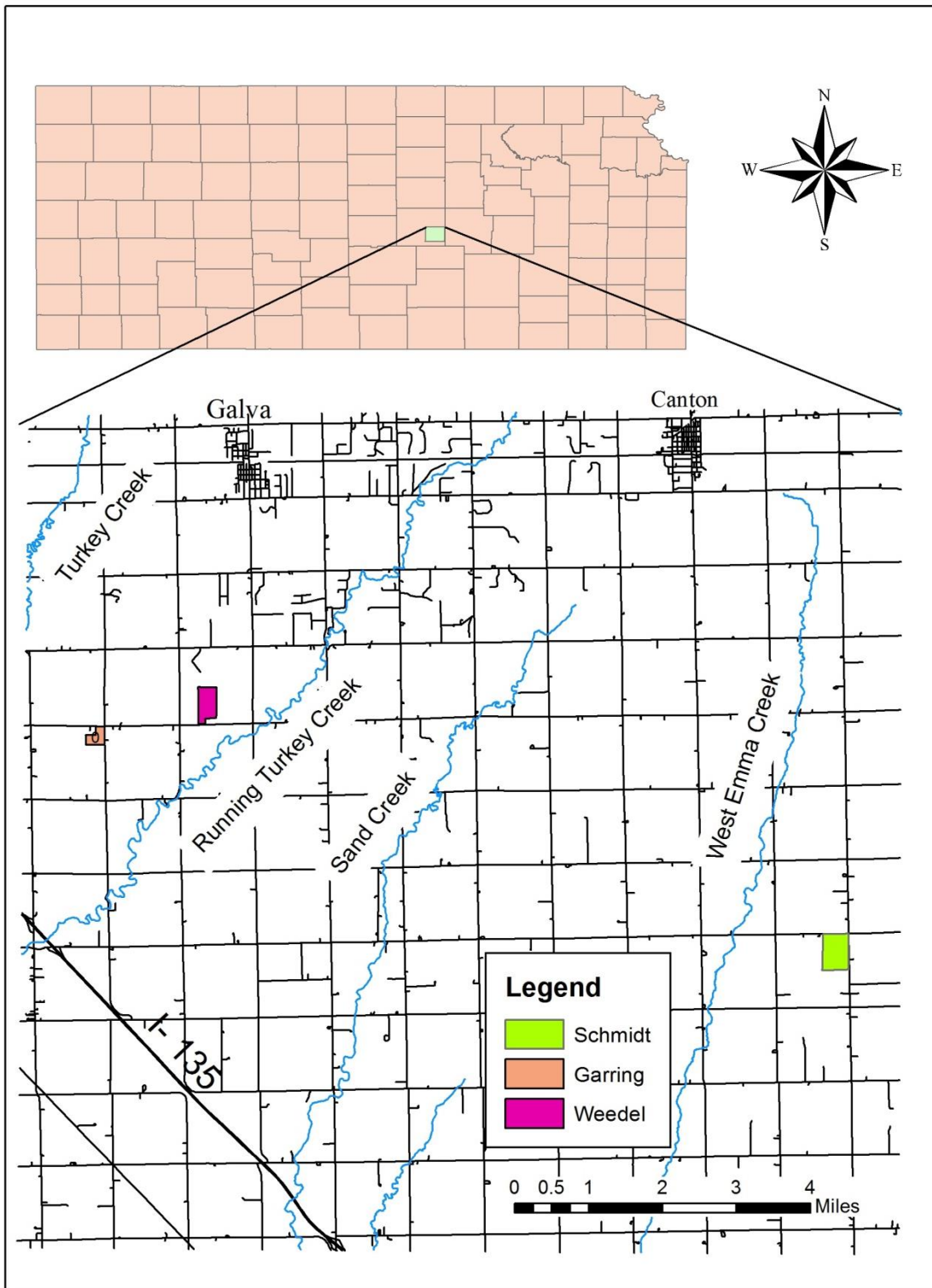


Figure 2.1. McPherson County with locations of the three fields

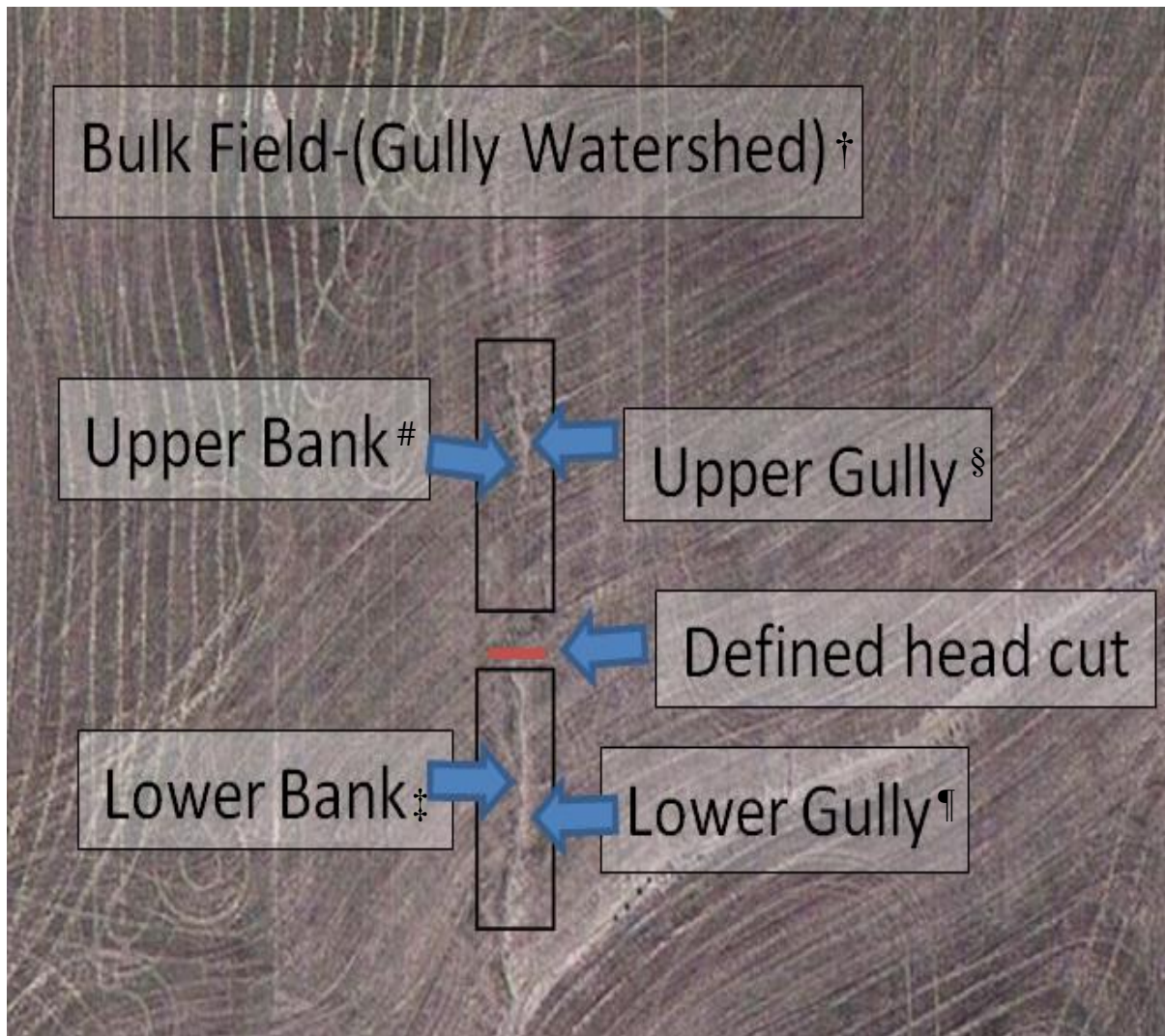


Figure 2.2. Diagram of landscape positions from which soil samples were collected at the Weedel field

† Bulk field had samples taken throughout the field over the gully watershed within the field

‡ Lower Bank samples were taken one foot from edge of well-defined gully and along both sides of gully

¶ Lower Gully samples were taken within the well-defined gully incision, from bottom of gully

Upper Bank samples were taken above the defined head cut, one foot from edge of expected gully formation

§ Upper Gully samples were taken above the defined head cut, within and on the bottom of the expected gully formation

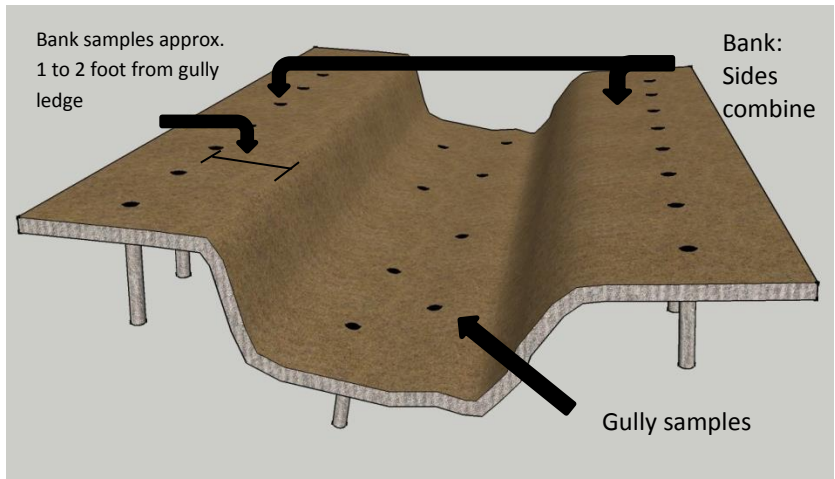


Figure 2.3. Example 3D model of bank and gully describing sampling points

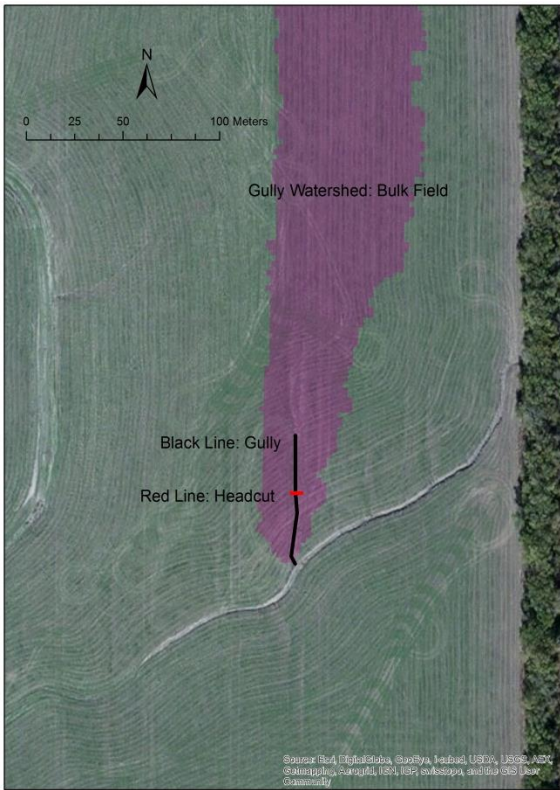


Figure 2.4. Weedel field display of gully and watershed

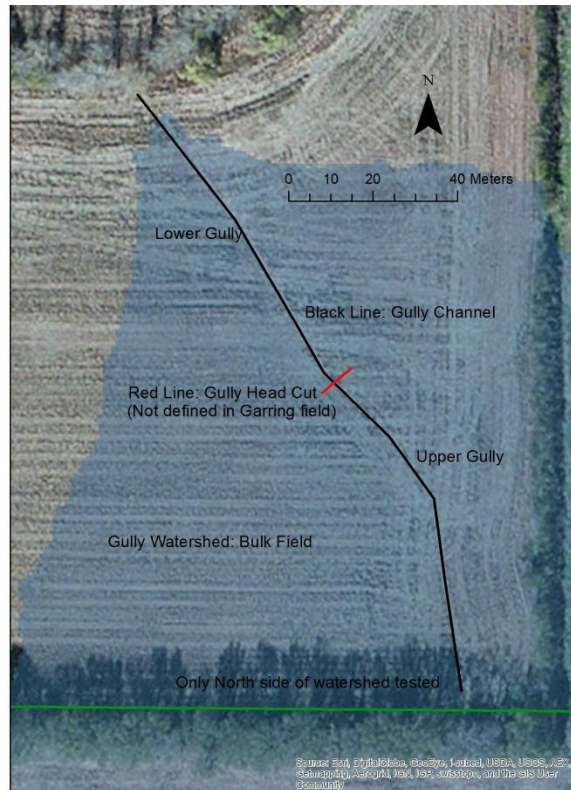


Figure 2.5. Garring field display of gully and watershed

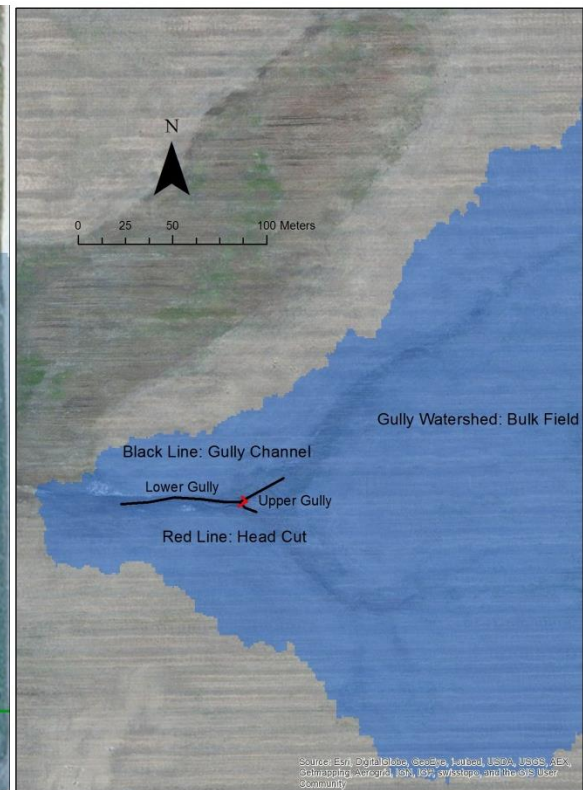


Figure 2.6. Schmidt field display of gully and watershed

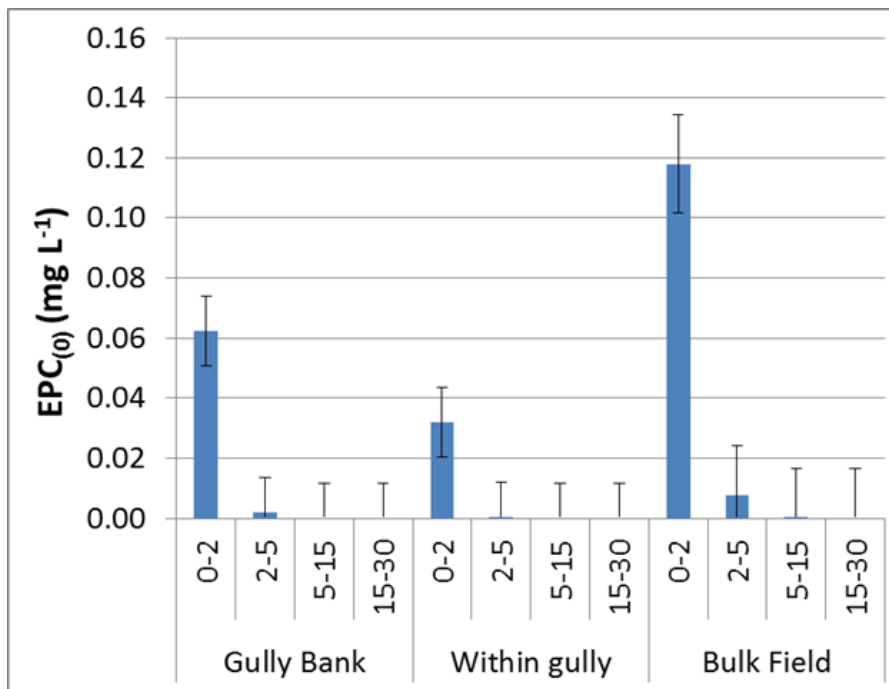


Figure 2.7. Equilibrium phosphorus concentration at zero net sorption (EPC_0) for Weedel field based upon soil depth and field location

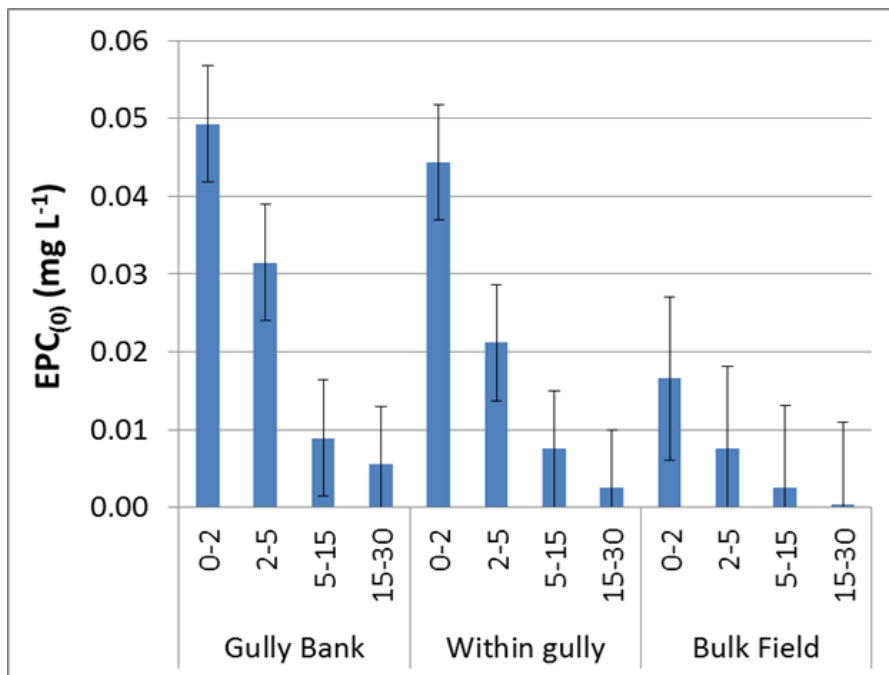


Figure 2.8. Equilibrium phosphorus concentration at zero net sorption (EPC_0) for Garring field based upon soil depth and field location

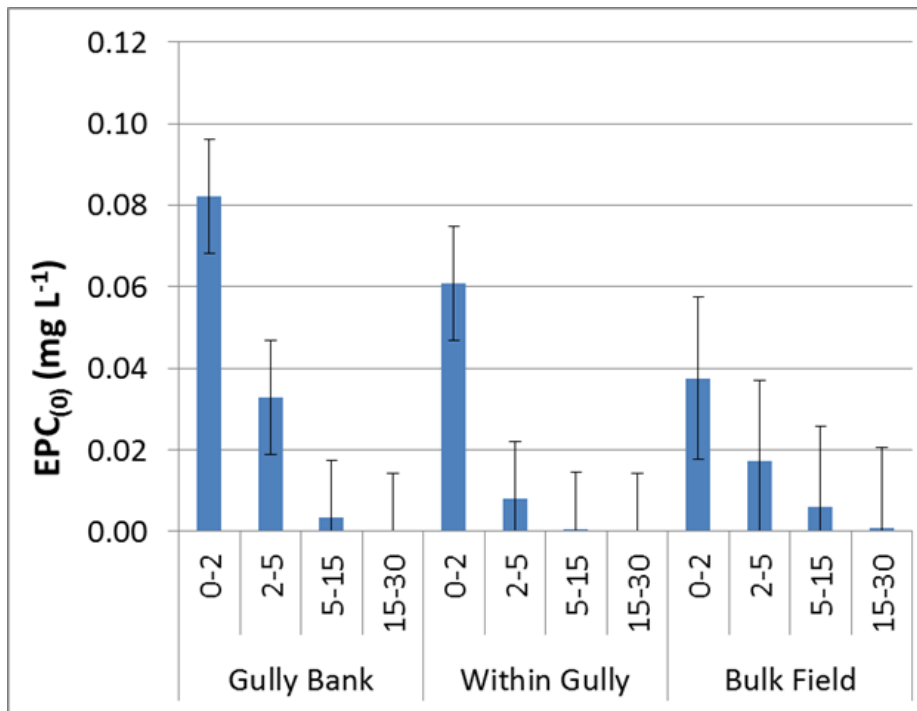


Figure 2.9. Equilibrium phosphorus concentration at zero net sorption (EPC₀) for Schmidt field based upon soil depth and field location

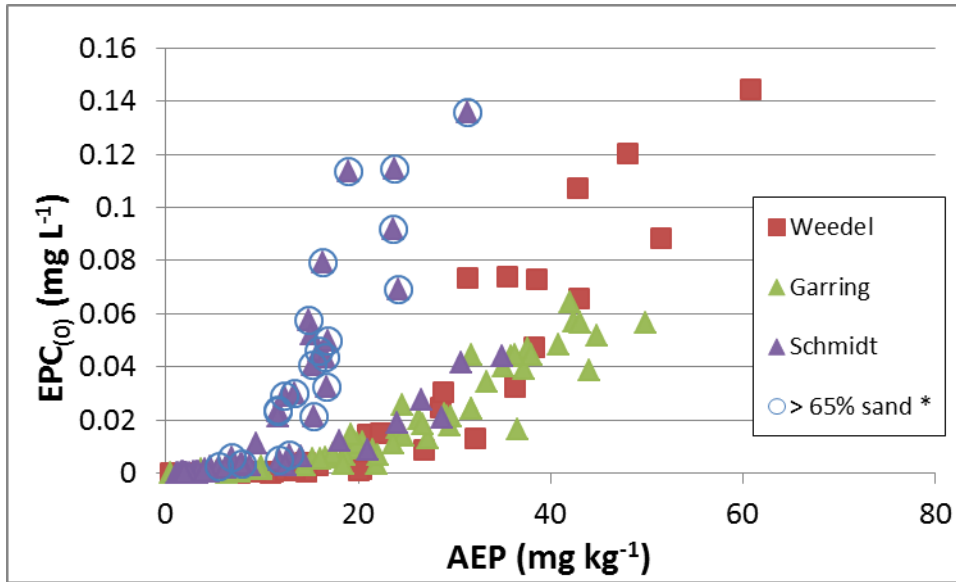


Figure 2.10. The relation between equilibrium phosphorus concentration at zero point sorption (EPC_0) and anion exchange phosphorus (AEP)

* Samples that contain over 65% sand, all of which are from Schmidt field

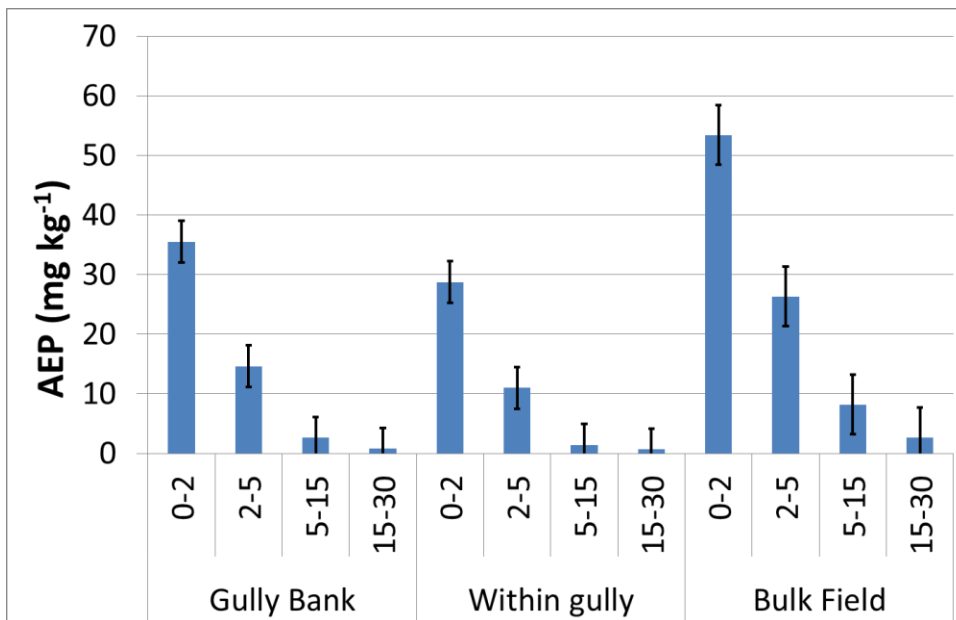


Figure 2.11. Anion exchange phosphorus for Weedel field based upon soil depth and field location

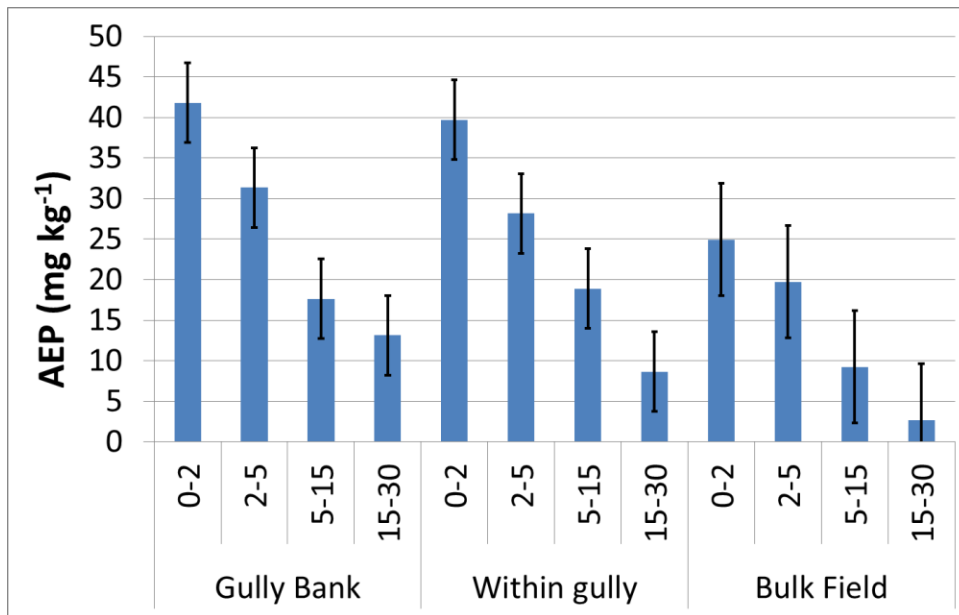


Figure 2.12. Anion exchange phosphorus for Garring field based upon soil depth and field location

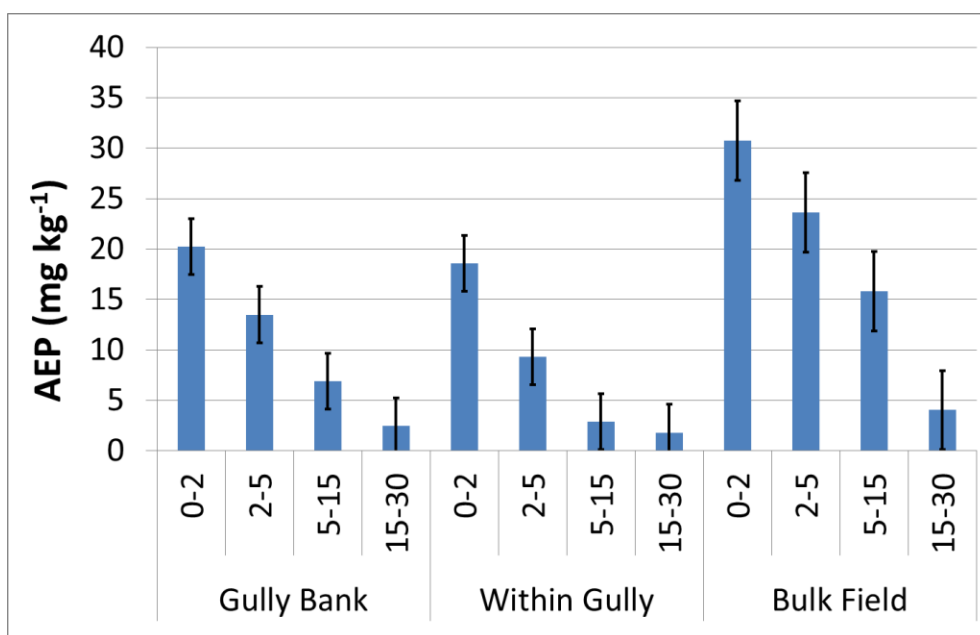


Figure 2.13. Anion exchange phosphorus for Schmidt field based upon soil depth and field location

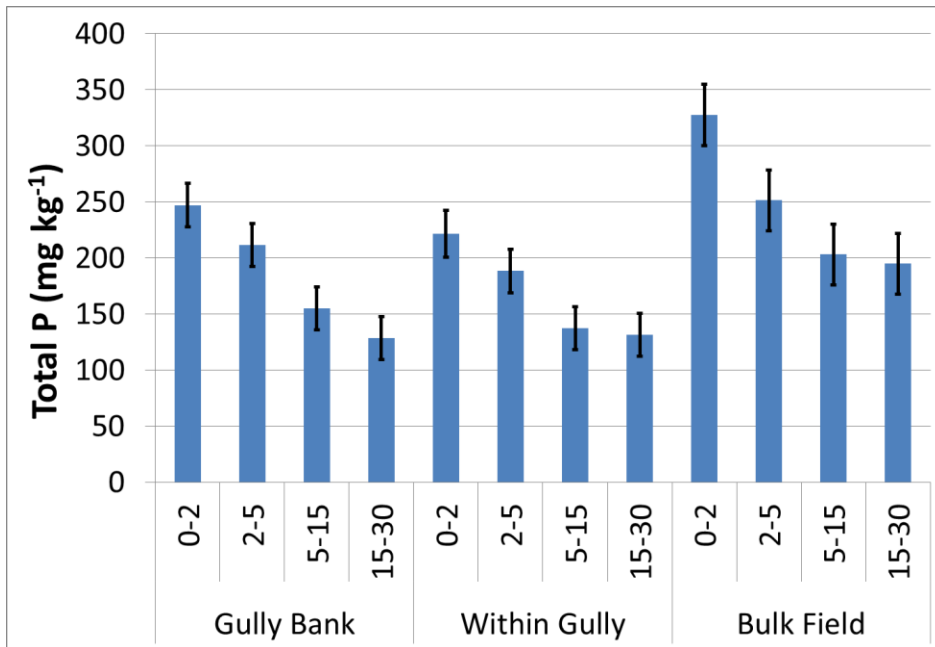


Figure 2.14. Total phosphorus for Weedel field based upon soil depth and landscape position

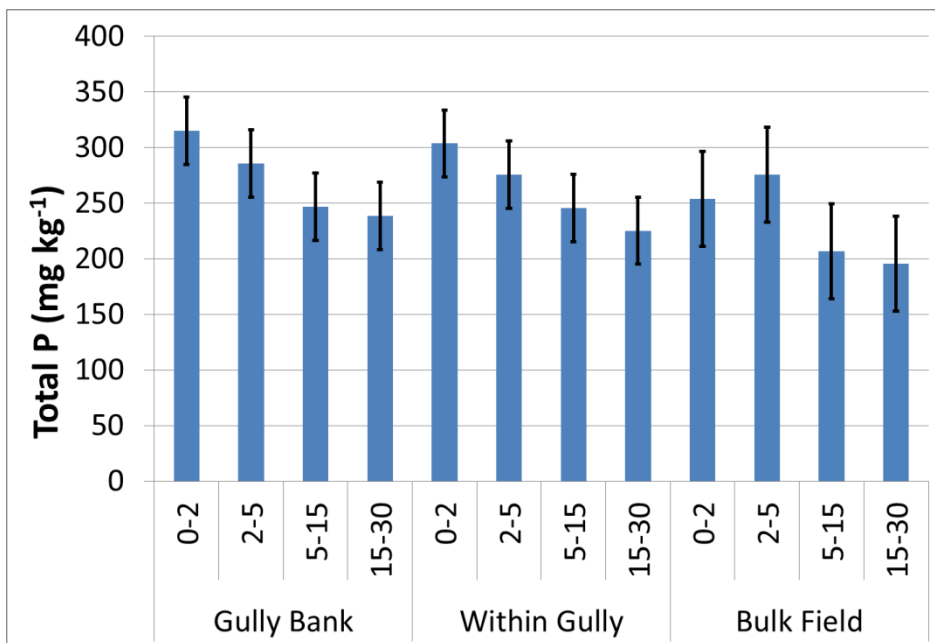


Figure 2.15. Total phosphorus for Garring field based upon soil depth and landscape position

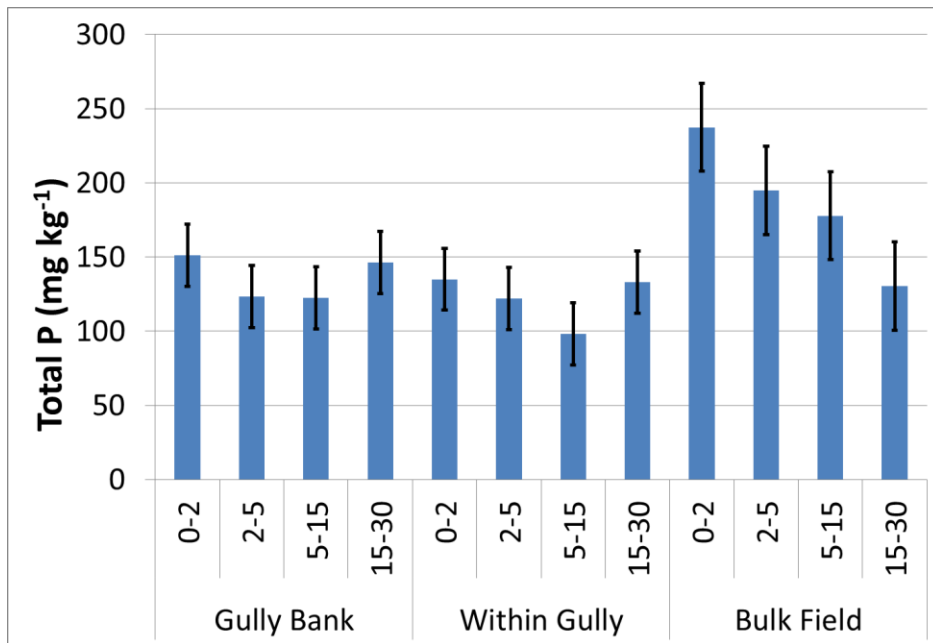


Figure 2.16. Total phosphorus for Schmidt field based upon soil depth and landscape position

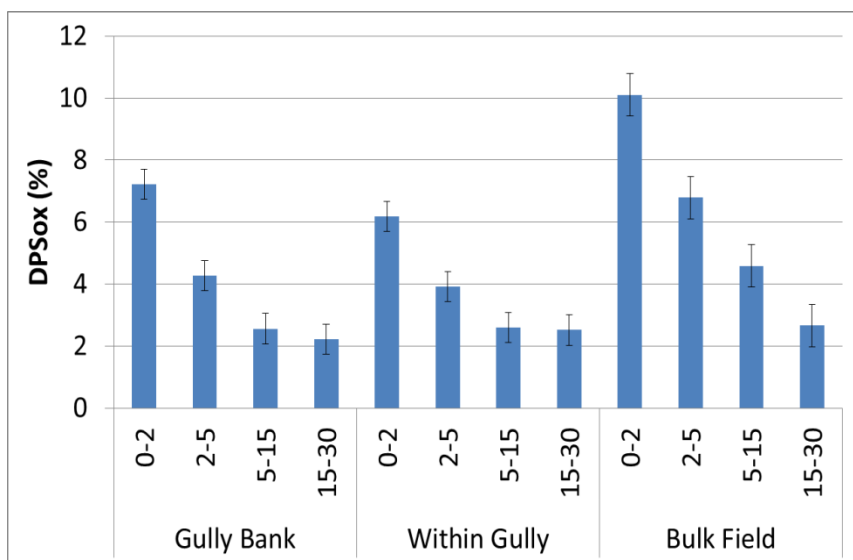


Figure 2.17. Degree of phosphorus saturation index of oxalate extraction (DPS_{ox}) for Weedel field based upon soil depth and field location

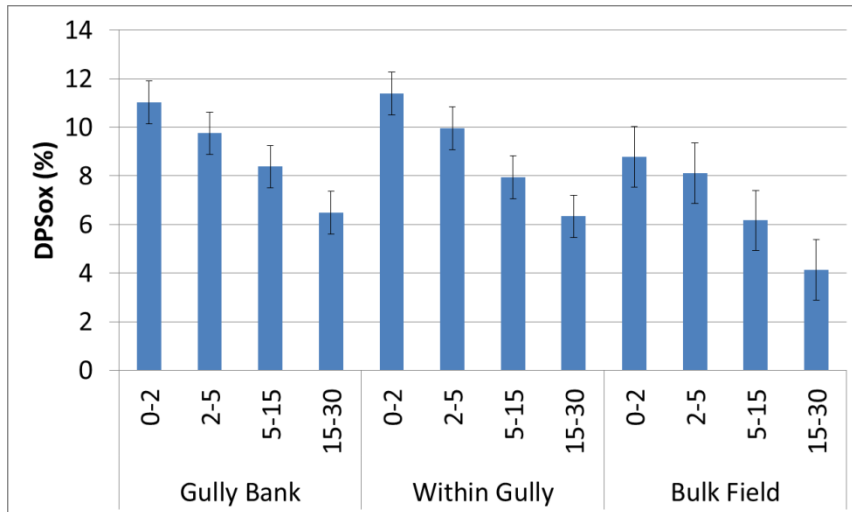


Figure 2.18. Degree of phosphorus saturation index of oxalate extraction (DPS) for Garring field based upon soil depth and field location

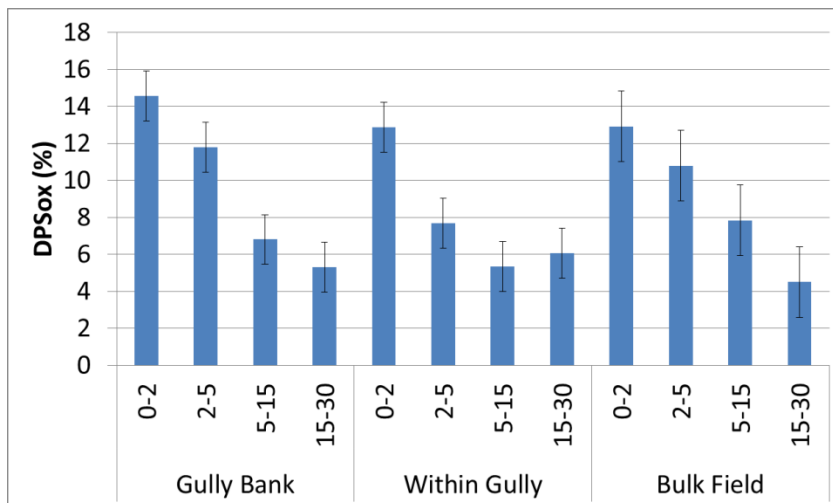


Figure 2.19. Degree of phosphorus saturation index based on ammonium-oxalate extraction (DPS_{ox}) for Schmidt field based upon soil depth and field location

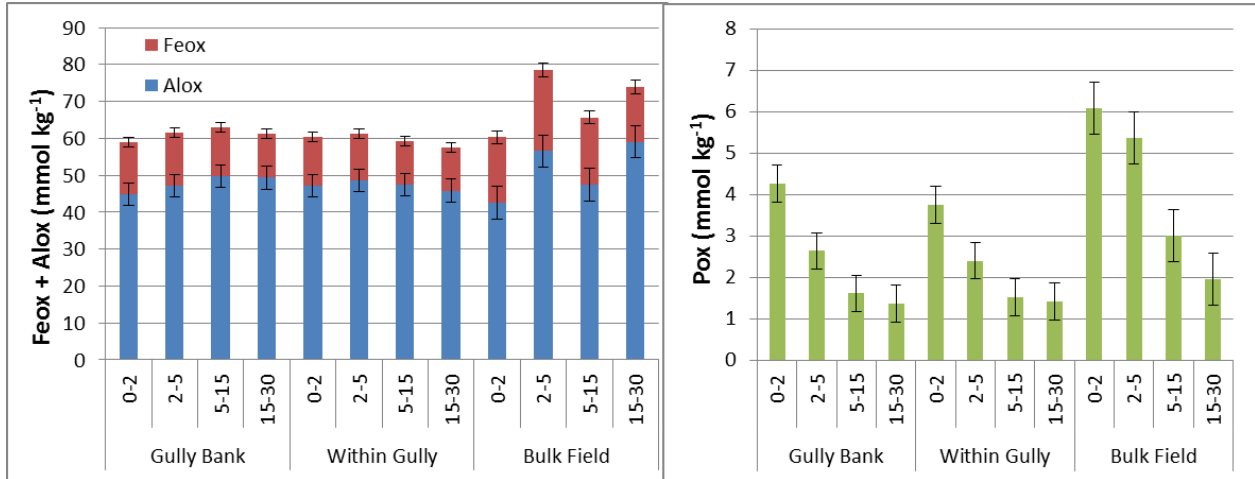


Figure 2.20 Al_{ox} , Fe_{ox} , and P_{ox} for Weedel field based upon soil depth and field location

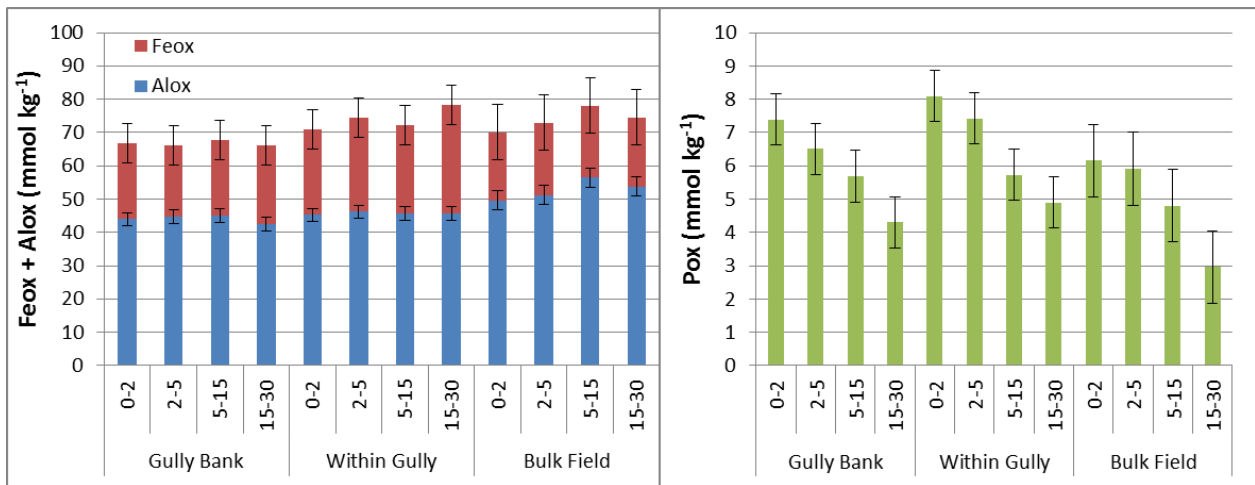


Figure 2.21. Al_{ox} , Fe_{ox} , and P_{ox} for Garring field based upon soil depth and field location

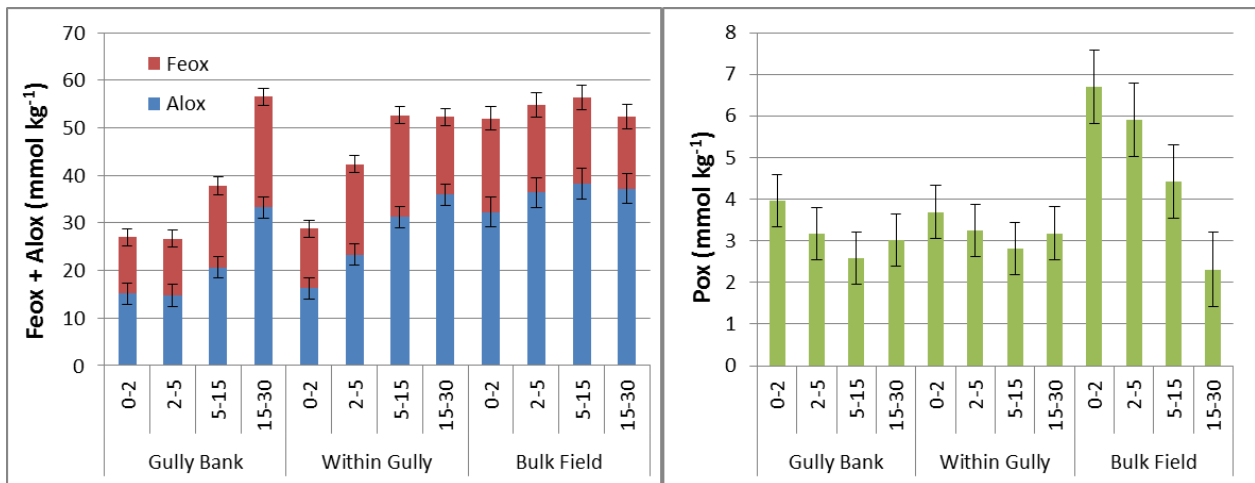


Figure 2.22. Al_{ox} , Fe_{ox} , and P_{ox} for Schmidt field based upon soil depth and field location

Chapter 3:

Mixing of sediments with differing phosphorus buffering capacity

Introduction

During erosional events the loss of sediment from the field is usually considered in one mass quantity rather than the combined masses of separate erosional process. Large erosional events, and at times smaller erosional events, have the ability to mix soils from differing depth fractions throughout the soil profile. While sheet and rill erosion is largely within the 0 to 35 mm depth (Whiting et al., 2001); ephemeral gullies can cause the erosion of much deeper soil depth fractions. Ephemeral gullies can represent a major portion of soil lost from a field (Poesen et al., 2003) and much of this subsoil can have very different soil properties than that of the surface. These soil properties can affect the sorption of phosphorus (P) and control the form P leaving a watershed.

Phosphorus loss from a field is often quantified using broad quantities of inputs and outputs such as the Kansas phosphorus index (Sonmez et al., 2009) and soil samples are often taken randomly and at a set depth around a sampling area. However the P sorption of the surface soil can be very different than that of the subsoil (Hongthant et al., 2011). Because of this P stratification, erosional processes must be examined individually to identify each processes contribution to its effects on soil loss and P loss.

To identify the expectations of P loss in runoff, equilibrium phosphorus concentration at zero net sorption (EPC_0) is a commonly used. EPC_0 describes the expectations of a soil's P release into a water column, as it describes the point of P in solution at which the soil will neither absorb nor desorb phosphorus. Generally EPC_0 is expected to drop quickly with soil depth

(Hongthant et al., 2011) as it did with the tested fields in chapter 2. Peltovuorui, (2002) performed a study that mixed A horizon (approximately 0-20cm) with the B horizon (20-45cm), at different A to B soil fraction percentages and determined the resulting change in EPC_0 . In this study it was found that even a small amount of B subsoil had a dramatic effect on the resulting EPC_0 of the mixture, due to the B horizon subsoil high P buffering capacity. Results from chapter 2 showed that the difference in P sorption is largely due to P saturation of surface soils rather than the differences of P binding capability. Phosphorus sorption can be related to a number of physical factors such as texture and aggregate size. Maguire et al., (2002) demonstrated that aggregate (particle) size can play an important factor in the buffering of P and its influence on dissolved P. It was shown that small aggregates from non-calcareous soils were more likely to have an increased P buffering capacity and that solution that held soil with larger aggregates was likely to have increased dissolved P. When two soils of different aggregate sizes were mixed, the smaller aggregate size soil sorbed P that was desorbed from the larger aggregate soil.

How the EPC_0 of surface soil responds when mixed with subsoil needs to be quantified to determine what the expectations of P sorption/desorption are when different layers of soil depth with differing P buffering capacity are mixed in erosional events. The objectives of this study are to: develop and test a model to predict the EPC_0 when subsoil is mixed with surface soil.

Materials and Methods

Sampled soils used in mixing study

Soils used in the mixing study were chosen from the three fields; Weedel (W), Garring (G), and Schmidt (S) that was described in chapter 2. Preparation of the soil (also described in

chapter 2) involved drying samples at 50 °C for 2 days, ground, then passed through a 2 mm sieve. Select characterizations of the soils used in the mixtures are described in table 3.1. The chosen soils attempted to relate to what sediment would likely be mixed in an erosion event while having some mixtures with similar and different buffering capacities. Anything below the 0 to 2 cm fraction is considered subsoil as the sheet and rill erosion of the three tested fields rarely exceeded a 2 cm. However some of the soils used in this mixing study were both from the 0 to 2 cm fraction. The EPC_0 prediction models that are described were created with intention to be able to predict EPC_0 from any two soils that are mixed, even if their location of origin is illogical for them to be mixed in an erosion event. The chosen mixtures with anion exchange P (AEP), EPC_0 , and buffering capacity are described in table 3.2. In comparison to other studies, all tested EPC_0 would have been considered low in comparison to EPC_0 described in other research (Agudelo et al., 2011; Hongthant et al., 2011; Peltovuori, 2002).

The 1-g soil samples used for determining EPC_0 were created by mixing certain fractions of soil 1 with a certain fraction of soil 2 (table 3.2). All soils were mixed with the following soil percentages; 100% soil 1 + 0% soil 2, 75% soil 1 + 25% soil 2, 50% soil 1 + 50% soil 2, 25% soil 1 + 75% soil 2, and 0% soil 1 + 100% soil 2. Enough soil was weighed out in the proper percentages to test the P sorption isotherm and the AEP into sampling cups, then hand shook well to mix the soils. All mixtures and testing were done in duplicate.

Determining EPC_0 and EPC_0 determined buffering capacity

The initial quantity of labile P adsorbed to the soil was assumed to be equal to the AEP, where AEP was determined using the methods described in chapter 2. A phosphorus sorption isotherm was determined by mixing 1 g of soil with 25 ml of solution containing a background

electrolyte and increasing concentrations of P (KH₂PO₄) (0.00, 0.05, 0.1, 0.2, 0.5, 2, 10 mg P L⁻¹). The background electrolyte was 0.006 M CaCl₂ to simulate the ionic strength of stream water. The soil solutions were mixed on an end to end mixer for 24 hours then centrifuged at 10,000 rpm for 10 min. The supernatant was filtered through a 0.45-mm nylon syringe filter and stored in a 15-ml vial at 4 °C. The final dissolve P concentration in the supernatant (C_f) was determined by analyzing samples for molybdate reactive P with an automated flow-injection analyzer (Lachat Quick Chem method 10-115-01-1-A, Lachat Instruments, 2000). The quantity of P adsorbed to the soil during the experiment (ΔQ) was determined based on the change in the solution P concentration. The final quantity of adsorbed P (Q_f) was computed as the initial quantity of adsorbed P (Q_i, or AEP) plus ΔQ.

The Freundlich equation (Equation 3.1) was fit to a plot of Q_f vs. C_f using SAS proc nlin for parameter determination (SAS code: Appendix B: Figure B.5).

$$Q_f = K_f C_f^b \quad \text{Equation 3.1.}$$

Where Q_f is the concentration of adsorbed P at equilibrium (mg kg⁻¹), K_f is the Freundlich adsorption coefficient, C_f is the equilibrium concentration of P in solution (mg L⁻¹), and b is a fitting variable. The EPC₀ was calculated by solving the Freundlich equation for C_f and replacing Q_f with Q_i, or AEP (Equation 3.2).

$$EPC_0 = 10^{\frac{(\log(\frac{Q_i}{K_f}))}{b}} \quad \text{Equation 3.2}$$

Phosphorus buffering capacity, or the slope of Q vs. C, was determined by taking the first derivative of the Freundlich equation (Equation 3.3),

$$\beta = K_f * b * C^{(b-1)} \quad \text{Equation 3.3}$$

Where β is the buffering capacity ($L \text{ kg}^{-1}$), K_f is the adsorption coefficient, b is a fitting variable, C is the P concentration in solution (mg L^{-1}). Because P buffering capacity is a function of P concentration in solution, the P buffering capacity of the soils as sampled was determined by replacing C in equation 3.3 with the EPC_0 (i.e. buffering at EPC_0). Because of the strong non-linearity of the P adsorption isotherms, P buffering capacity as determined by the Freundlich equation can differ by orders of magnitude.

Linear and FMBP model for determining EPC_0 of mixed sediments

An EPC_0 model formed under the assumption that each soil has the same P buffering capability would form a straight line between the EPC_0 of soil 1 and the EPC_0 of soil 2 following the equation 3.4. For example, in equation 3.4, a mixture where the mass of soil 1 is 50% total mass and the mass of soil 2 is 50% total mass, the EPC_0 would be the 50% the difference between the EPC_0 of soil 1 and soil 2.

$$EPC_{0final} = f_1 * EPC_{01} + f_2 * EPC_{02} \quad \text{Equation 3.4}$$

$$f_1 = \frac{\text{mass of soil 1}}{\text{total mass}}; f_2 = \frac{\text{mass of soil 2}}{\text{total mass}}$$

The quantity of P in a sediment mixture solution can be calculated by the adding the sediment bound P of each soil in the mixture and the dissolved P in solution (Equation 3.5).

$$T_p = C * v + m_1 Q_1 + m_2 Q_2 + \dots + m_n Q_n \quad \text{Equation 3.5}$$

Where T_p is quantity of P (mg), C is concentration of P in solution (mg L^{-1}), v is volume of solution (L), m is mass of soil (kg), Q is concentration of P in soil (mg kg^{-1}) and 1, 2, or n determines the soil fraction included in mixture.

The Freundlich mass-balance of P (FMBP) model uses the quantities of P determined in two conditions to solve for unknown parameters. The first condition (initial condition) used in this model was defined by the sediment sorbed P determined by the AEP and an initial concentration of P in solution (Equation 3.6).

$$T_i = C_i * v + m_1 Q_{i1} + m_2 Q_{i2} + \dots + m_{in} Q_{in} \quad \text{Equation 3.6}$$

Where T_i the total quantity of P in the initial condition (mg), C_i is concentration of P in solution of the initial condition (mg L^{-1}), v is volume of solution (L), m is mass of soil (kg), Q_i is the concentration of P sorbed onto soil determined by AEP (mg kg^{-1}), and 1, 2, or n determines the soil fraction included in mixture.

The second condition (final condition) in the FMBP model uses the Freundlich isotherm to determine the expected quantity of P sorbed at a certain concentration of P in solution (Equation 3.7). When two or more sediments are mixed it is expected that P will desorb from some sediments and sorb onto others. The final condition uses the Freundlich equation $Q=K_f C^n$ (Equation 3.1) to determine Q at certain concentrations of P in solution. The K_f and n terms were previously determined for each sediment to be added into the mixture and are independent to that sediment fraction. The final condition follows the equation 3.7 where T_f is the total quantity of P in the final condition (mg), C_f is concentration of P in solution in the final condition (mg L^{-1}), v is volume of solution (L), m is mass of soil (kg), Q_f is the concentration of P sorbed onto soil determined by the Freundlich equation (mg kg^{-1}), and 1, 2, or n determines the soil fraction included in mixture. Concentration (C in mg L^{-1}) defined in the Freundlich equation for the final condition is C_f and is same as P concentration in solution.

$$T_f = C_f * v + m_1 Q_{f1} + m_2 Q_{f2} + \dots + m_{fn} Q_{fn} \quad \text{Equation 3.7}$$

The total quantity of P in the initial condition must equal the total quantity of P in the final condition or that $T_i=T_f$ (Equation 3.8). In this experiment there are only two terms; soil 1 and soil 2. To solve for EPC_0 , the initial solution concentration (C_i) and the final solution concentration (C_f) are equal, meaning that P in solution is in equilibrium for the two conditions. The point where $T_i=T_f$ is equation 3.8.

$$T_i = T_f \quad C_i * v + m_1 Q_{i1} + m_2 Q_{i2} = C_f * v + m_1 Q_{f1} + m_2 Q_{f2} \quad \text{Equation 3.8}$$

The final condition is unknown but can be solved with only one variable, C_f . Equation 3.8 can be re-written as equation 3.9.

$$C_i * v + m_1 AEP_{i1} + m_2 AEP_{i2} = C_f * v + m_1 K_{f1} C_f^{n1} + m_2 K_{f2} C_f^{n2} \quad \text{Equation 3.9}$$

The initial condition is already known for the two soils and the final condition can be solved with the C_f term. Goal seek in excel (2003) was used to find the concentration where P in solution was in equilibrium for both initial and final conditions which is EPC_0 or that $C_i=C_f$.

Statistical Analysis

Relation fit between the linear model and FMBP model to the observed EPC_0 outcome were tested with R^2 in a linear regression using excel (2003). R^2 values and p-values for mixture figures were found by using LINEST in excel (2003). Data for the error bars at 95% probability was analyzed with SAS version 9.2 using proc MIXED and proc GLM (SAS code- Appendix B: Figure B.5).

Results and Discussion

Mixture 1 (Figure 3.1) had a large difference in EPC_0 of the two mixed sediments with the FMBP model predicting EPC_0 better than the linear model but under estimating the effect of subsoil. Mixture 2 (Figure 3.2) mixed two low EPC_0 soils with small P buffering capacities however both models poorly fit the observed data and neither are statistically significant to the observed data. The observed EPC_0 of mixture 3 (Figure 3.3) quickly dropped below the detectable limit with just a 25% addition of subsoil soil to surface soil and neither model statistically fit the data. Mixture 4 (Figure 3.4) and mixture 5 (Figure 3.5) used soils with low EPC_0 but large P buffering capacity difference between the surface and subsoil and the FMBP model fit well with the observed data. Mixture 6 (Figure 3.6) had two high EPC_0 soils with low P buffering leading to a similar average fitting linear and FMBP model to the observed data.

The ability of the FMBP model to predict the outcome of mixed sediment EPC_0 depended upon the soil characteristics of the two sediments used in the mixture. When two soils with characteristics lead to a high P buffering capacity soil being mixed with a low P buffering capacity soil, the FMBP model tended to under predict the effect of the high P buffering capacity soil. When two soils were mixed with similar P buffering capacity, the FMBP model was less effective at fitting to the observed data.

When EPC_0 values are very small and close to the detectable limit (approximately 0.01 mg L^{-1}) the ability to predict EPC_0 can be more difficult, as seen in mixture 2 (Figure 3.2) where subsoil points 50% and 75% were below the EPC_0 of the 100% subsoil. In most of the mixtures the R^2 was higher for the FMBP model than the linear model; however the FMBP failed to achieve significant in mixture 2 and 3. The amount of error in the observed data is possibility due

to the EPC_0 only being done in duplication and could be improved if done in triplicate. Due to the closeness of some of the data to the near zero detectable limit, and the multiple magnitude of EPC_0 difference between results; the testing errors were often increased.

The linear model was largely incapable of predicting final EPC_0 when sediments of a high and low P buffering capacity were mixed. In nearly every mixture percentage point the observed EPC_0 was lower than the linear model predicted. A similar result occurred in Maguire et al., (2002) when mixing of soils with different P buffering capacity; the dissolved P in solution was consistently lower than what a linear model would predict. The Maguire study also demonstrates that soils with an increased buffering capacity have more relative control over the sorption of P than soil of a lesser P buffering.

Overall the relations between the observed EPC_0 and the FMBP modeled EPC_0 were better than the linear model. Figure 3.7 shows the ability of the FMBP model data to accurately predict the observed data with an R^2 of 0.81 while the linear model obtained an R^2 of 0.45 (both were statically significant at α of 0.05). The observed data trended to be below the predicted values meaning that the effect of subsoil in lowering of EPC_0 was greater than the prediction. Points above the 1:1 line in figure 3.7 demonstrate when EPC_0 was underestimated which constituted a majority of observations. The results show that subsoil is more capable reducing dissolved P in runoff by lowering the EPC_0 of the final eroded sediments. The low EPC_0 soils of the EG play an important role in P sorption even if the quantity of sediment from the EG is less than that of other types of erosion with higher EPC_0 .

Conclusions

The differences of P sorption and buffering capacity were varied across soil depths and EPC_0 values. When subsoil was added to the surface soil, the soils with largest P buffering capacity tended to affect the P sorption to a greater degree. The results in mixture 1 (Figure 3.1), 4 (Figure 3.4), and 5 (Figure 3.5) showed that a small addition in subsoil would have a greater effect on EPC_0 , as in a 50% addition of subsoil has a larger than 50% of the control on the EPC_0 outcome.

The FMBP model is capable of predicting the EPC_0 outcome of two mixed soils although commonly under predicting the P buffering effect of subsoil. The model is likely accurate to predict other unknown variables such as dissolved P concentration after two soils are mixed (the final P concentration in solution). The linear model is only capable to predict EPC_0 when two soils with similar low P buffering capacity are mixed.

Soil erosion from ephemeral gullies can be a substantial portion, 10 to 90% of soil loss from a field can be from an ephemeral gully and much of this is composed of subsoil (Poesen et al., 2003). The high P buffering capacity of this subsoil can have an overwhelming influence on the sorption of P. It is likely that during erosion events exchangeable P desorbed from surface soil is adsorbing onto sediment eroded from subsoil depths. Altering the erosional mix of surface to subsoil could affect the resulting sediment EPC_0 and could increase the likelihood of the sediment's release of dissolved P into runoff. This dissolved P would be more bioavailable and capable of algae uptake than the sediment bound P.

Implementation of best management practices (BMPs) that decrease subsoil loss (i.e., reduce ephemeral gully erosion) may result in increased dissolved P loss even while total P loss would decrease. This highlights the importance of implementing BMPs to reduce P loss (e.g.,

maintain low soil test P, reduce runoff, sub-surface application of P fertilizers) in combination with BMPs directed at reducing ephemeral gully erosion. BMPs need to be combined to fully control P runoff from fields and the effects of BMPs need to be fully researched as not unintentionally create environmental damaging conditions.

References

- Agudelo, S.C., N.O. Nelson, P.L. Barnes, T.D. Keane, and G.M. Pierzynski. 2011. Phosphorus adsorption and desorption potential of stream sediments and field soils in agricultural watersheds. *J. of Enviro. Qual.* 40:144-152.
- Hongthanat, N., J.L. Kovar, and M.L. Thompson. 2011. Sorption indices to estimate risk of soil phosphorus loss in the Rathbun Lake watershed, Iowa. *Soil Sci.* 176:237-244.
- Maguire, R.O., Edwards, A.C., Sims, J.T., Kleinman, P.J.A., and Sharpley, A.N. 2002. Effect of mixing soil aggregates on the phosphorus concentration in surface waters. *J. of Environ. Qual.* 31:1294–1299
- Peltovuorui, T. 2002. Phosphorus extractability in surface soil samples as affected by mixing with subsoil. *Agri. and Food Sci. in Finland.* 11:371-379.
- Poesen, J., J. Nachtergaele, G. Verstraeten, and C. Valentin. 2003. Gully erosion and environmental change: Importance and research needs. *Catena.* 91-133.
- Sonmez, O., G.M. Pierzynski, L. Frees, B. Davis, D. Leikam, D.W. Sweeney, and K.A. Janssen. 2009. A field-based assessment tool for phosphorus losses in runoff in Kansas. *J. Soil Water Conserv.* 64:212-222.
- Whiting, P., E. Bonniwell, and G. Matisoff. 2001. Depth and areal extent of sheet and rill erosion based on radionuclides in soils and suspended sediment. *Geology.* 29:1131-1134.

Table 3.1. Field, soil depth, texture, DPS, and total P of selected soils

Field	Identifier	Soil Depth (cm)	Field Location	Texture		DPS †	Total P mg kg ⁻¹
				Sand %	Clay %		
Weedel	W49	0-2	Bulk field	10	24	10.04	318.29
Weedel	W19	5-15	Lower gully	10	39	3.05	139.48
Weedel	W29	0-2	Upper bank	13	31	7.06	273.70
Weedel	W9	0-2	Lower bank	13	34	6.38	248.48
Garring	G45	0-2	Upper gully	26	23	10.70	288.82
Garring	G56	15-30	Bulk field	23	32	4.07	207.94
Garring	G13	0-2	Lower gully	28	23	12.15	354.43
Garring	G36	15-30	Upper bank	27	26	4.89	201.89
Schmidt	S53	0-2	Bulk field	58	14	13.61	243.13
Schmidt	S8	15-30	Lower gully	42	33	5.91	169.16
Schmidt	S45	0-2	Upper gully	72	10	16.35	181.78
Schmidt	S1	0-2	Lower bank	71	11	12.19	137.56

† Degree of Phosphorus Saturation

Table 3.2. Soil mixtures 1-6 with AEP, original EPC₀, and buffering determination

	Soil 1					Soil 2			
	Identifier	AEP † mg kg ⁻¹	EPC ₀ ‡ mg L ⁻¹	PBC ¶ L kg ⁻¹		Identifier	AEP † mg kg ⁻¹	EPC ₀ ‡ mg L ⁻¹	PBC ¶ L kg ⁻¹
Mixture 1	W49	45.1	0.119	141	+	W19	0.9	#	116618
Mixture 2	W29	27.1	0.030	312	+	W9	26.2	0.020	440
Mixture 3	G45	29.6	0.027	410	+	G56	1.0	#	1172695
Mixture 4	G13	33.7	0.035	353	+	G36	3.1	#	8849
Mixture 5	S53	23.9	0.022	392	+	S8	2.0	#	183702
Mixture 6	S45	19.4	0.095	78	+	S1	13.0	0.037	130

† Anion Exchange Phosphorus (labile P)

¶ Phosphorus Buffering Capacity

‡ Equilibrium Phosphorus Concentration at Zero Net Sorption

Below detectable limit for EPC₀ (0.001 mg/kg)

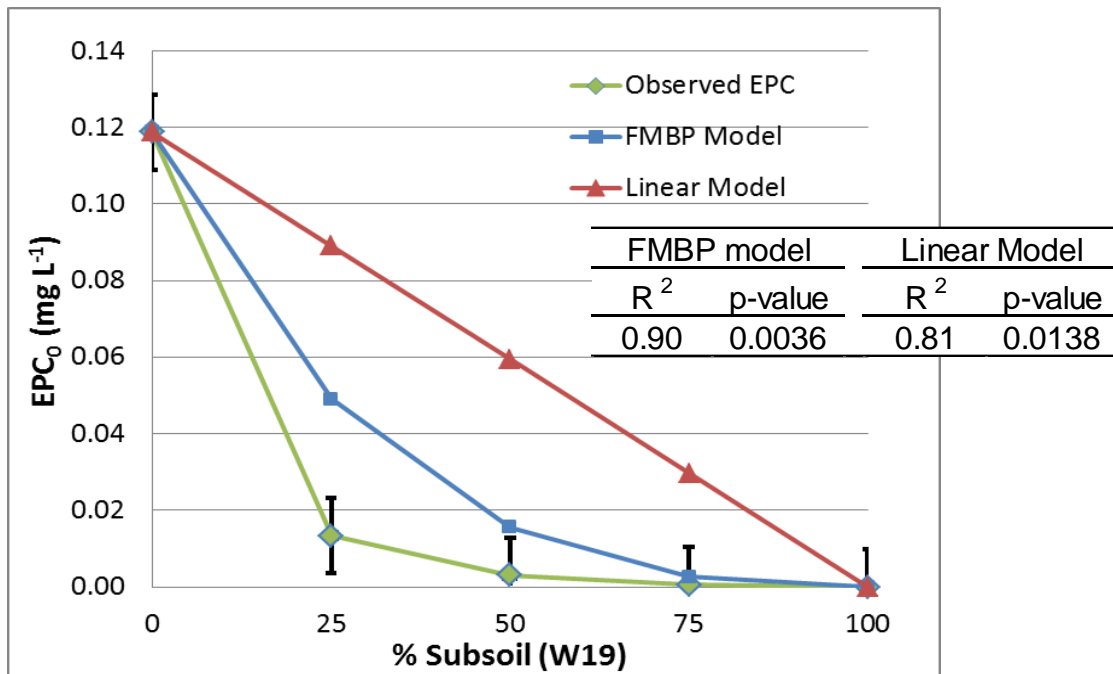


Figure 3.1. Mixture 1 (W49 and W19) - EPC₀ change of surface soil (W49) with percentage of added subsoil (W19)

* Confidence Intervals at 95% probability

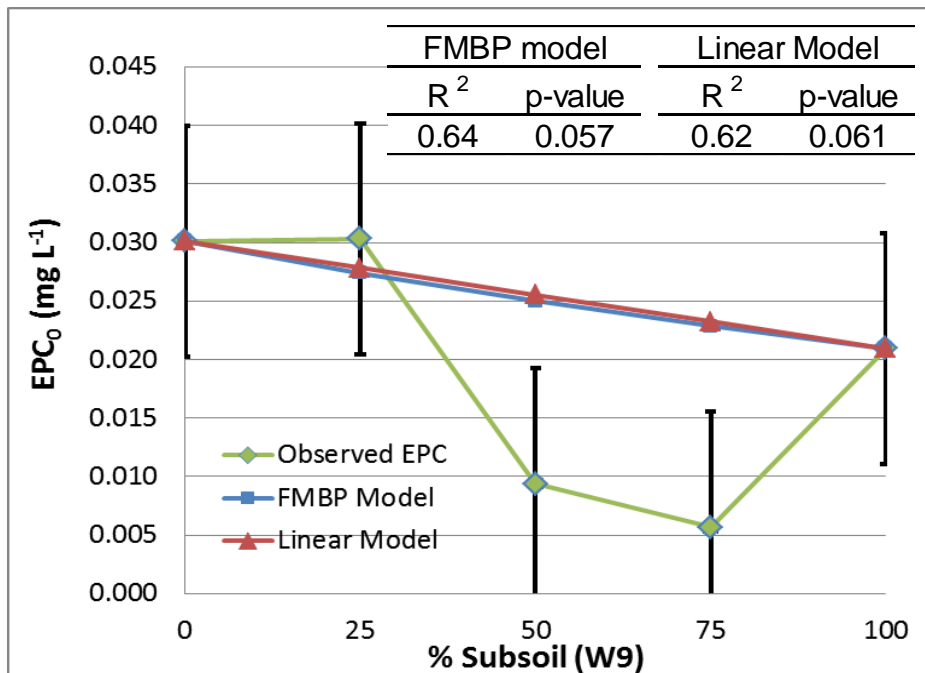


Figure 3.2. Mixture 2 (W29 and W9) - EPC₀ change of surface soil (W29) with percentage of added subsoil (W9)

* Confidence Intervals at 95% probability

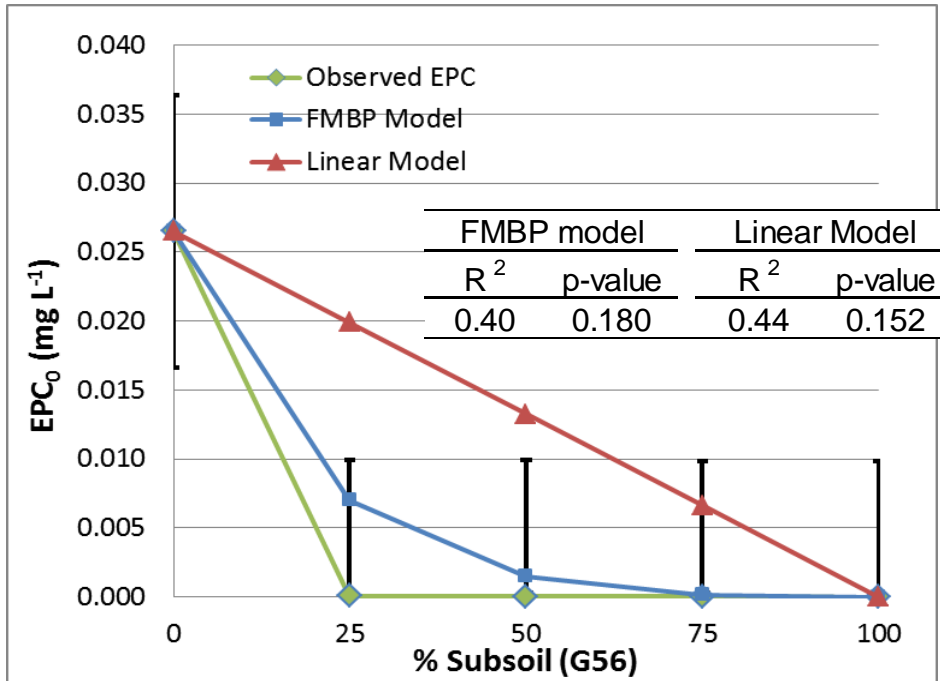


Figure 3.3. Mixture 3 (G45 and G56) - EPC₀ change of surface soil (G45) with percentage of added subsoil (G56)

* Confidence Intervals at 95% probability

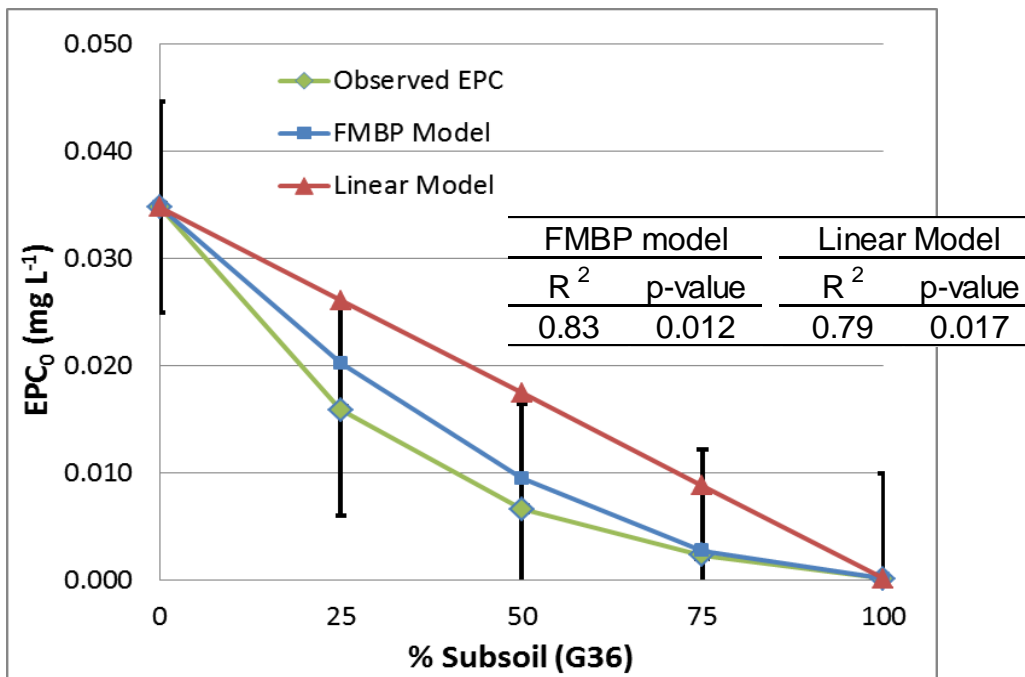


Figure 3.4. Mixture 4 (G13 and G36) - EPC₀ change of surface soil (G13) with percentage of added subsoil (G36)

* Confidence Intervals at 95% probability

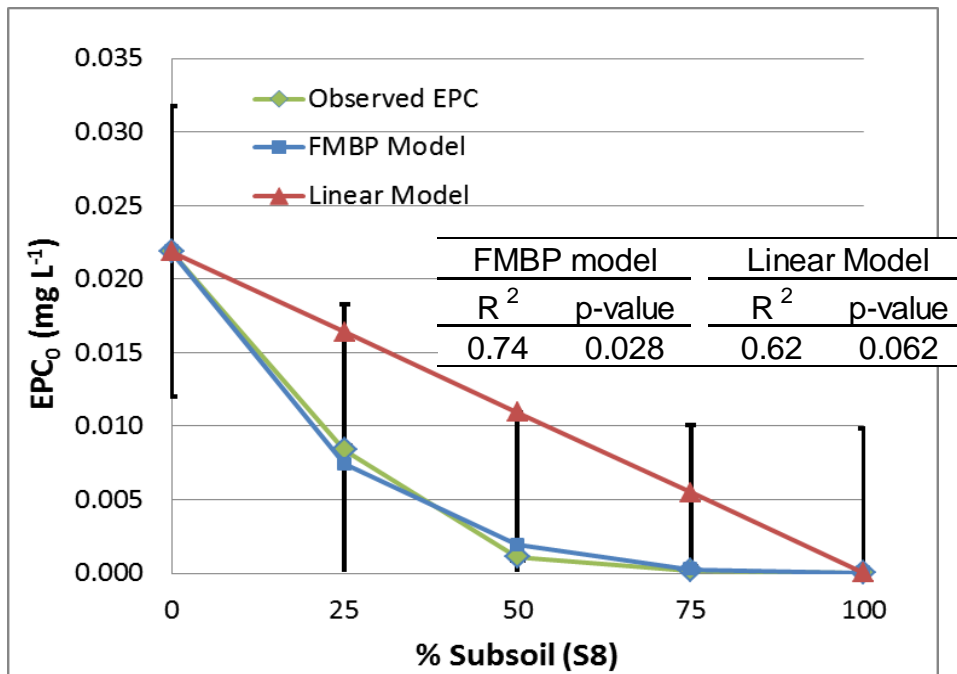


Figure 3.5. Mixture 5 (S53 and S8) - EPC₀ change of surface soil (S53) with percentage of added subsoil (S8)

* Confidence Intervals at 95% probability

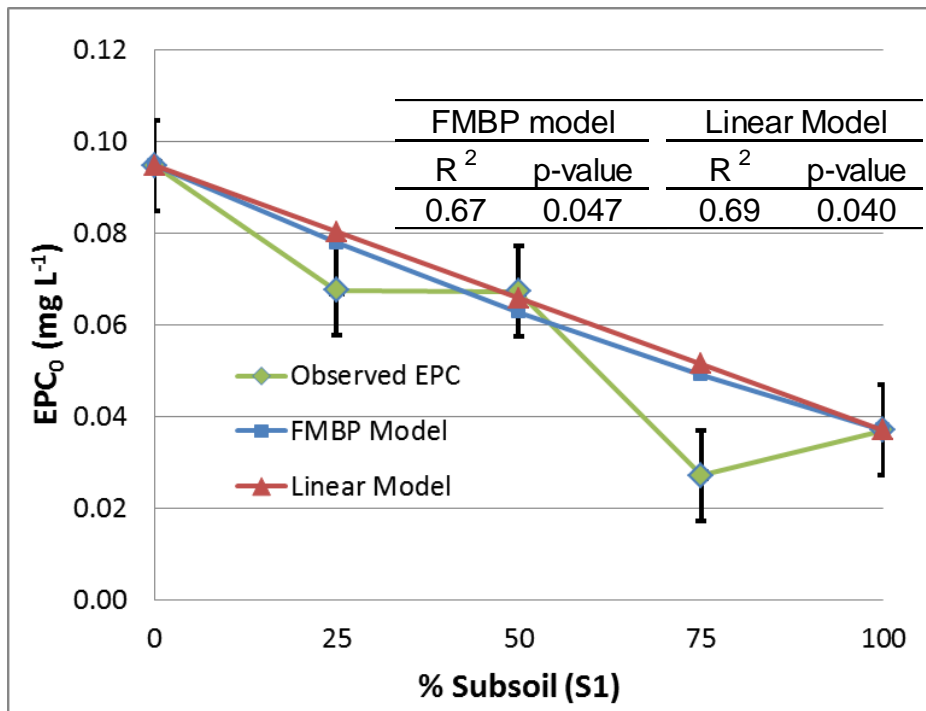


Figure 3.6. Mixture 6 (S45 and S1) - EPC₀ change of surface soil (S45) with percentage of added subsoil (S1)

* Confidence Intervals at 95% probability

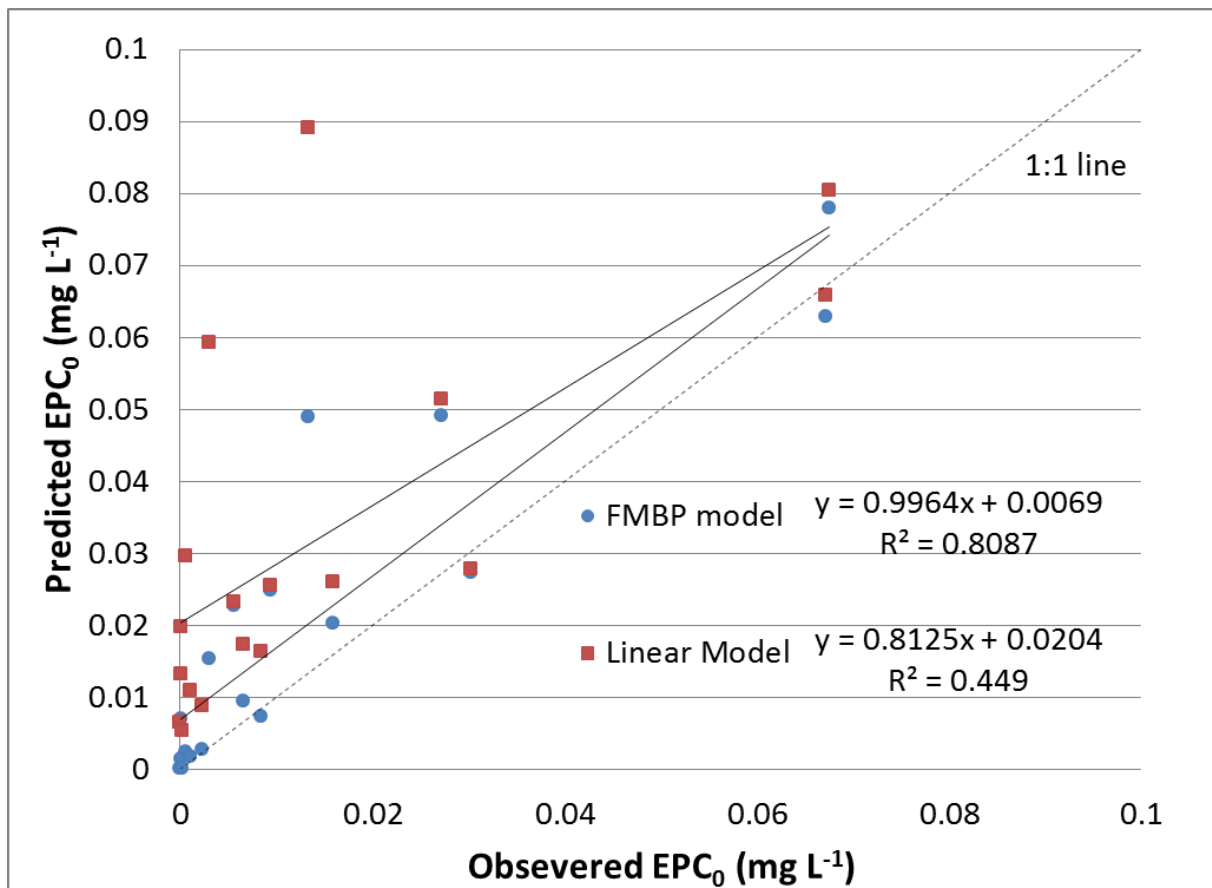


Figure 3.7. Observed EPC₀ vs. Predicted EPC₀ in FMBP and linear model

*Both models had p-value significance at <0.001.

Note: points included from 6 mixtures at points 25%, 50%, and 75% of subsoil to surface soil

Chapter 4:

Phosphorus loss and change in dissolved P caused by ephemeral gullies

Introduction

Phosphorus (P) loss from fields in the U.S. is widespread and causes impairments to freshwater bodies such as eutrophication and algae blooms. This environmental damage is not only costly but also dangerous to the near-by wildlife and people of an impaired water body (Dobbs et al., 2008). The leading source of damaging nutrients comes from non-point sources and agricultural fields (U.S. EPA, 2005). Since P is usually deficient in healthy water body ecosystems, small additions of P can result in large amounts of algae biomass (Carpenter et al., 1998). To be able to effectively control this nutrient we must be able to understand its complex nature and its relation to sediments in agricultural runoff.

Ephemeral gullies (EGs) are much less studied than the sheet and rill erosion from fields, despite the fact that EGs are a large contributor to sediment loss from agricultural fields (Poesen et al., 2003). Ephemeral gullies can contribute from 10% to 94% of sediment loss from a field caused by water erosion (Poesen et al., 2003). Although there is no specific definition for what constitutes an EG, they can be seen as a loss of soil from a deeper depth than from sheet and rill erosion.

Research on P loss from EG erosion is limited. As tested in chapter 2, P tended to decrease quickly with depth so that only the top 5 cm contained a large proportion of P. This stratification makes P loss dependent upon the depth of origination. The ability of the sediments to adsorb P is also dependent on depth of the soil origin, due to differences in P buffering capacity. The capacity of sediment to sorb P is likely to change the dissolved P concentration in

runoff as well. A study done by Zheng et al., (2005) showed that P loss greatly increased with the addition of ephemeral gully erosion as compared to just sheet and rill. Seven years after a deforestation event, the available P reduction in the studied plots with sheet and rill were 45.1% while plots with sheet, rill, and ephemeral gullies were 86.6%. This study also showed that P enrichment in sediment had increased with EG. When sheet and rill erosion was dominate in the first year of the study the P enrichment ratio of eroded sediment was 1.56 and progressed to 2.14 at the end of the 7 year study when EG erosion was added to the sheet and rill erosion. Although this study did not investigate the effects of EG erosion on the ratio of dissolved and sediment-bound P in runoff, it is likely that the ratio of dissolved P to sediment P changes depending on the runoff rates and major erosional processes taking place.

To fully understand the nutrient loss impacts of ephemeral gullies and to better understand the likely impacts of best management practices (BMPs) that are implemented to control them, a case study was done to explore the impact of ephemeral gullies on P loss from agricultural fields. The specific objectives of this case study were to i) determine the relative contribution of ephemeral gullies to the total P loss from agricultural fields and ii) estimate the relative impact of ephemeral gullies on the dissolved P concentration in runoff from agricultural fields.

Materials and Methods

Field surveying- soil loss estimation from ephemeral gully

Two fields in McPherson, KS were chosen to investigate P loss from ephemeral gullies (EGs). The fields surveyed correspond to two of three fields described in chapter 2 (Weedel and

Schmidt). These fields were surveyed by Burke et al. (unpublished data, 2014) who investigated soil loss from EGs. Figure 4.1 and figure 4.2 shows the two fields and the survey lines used to estimate EG soil loss. Due to complications of accuracy in surveying a conventionally-tilled field, the Garring field from chapter 2 was excluded from the soil and P loss described.

The survey data was collected using cross-section lines across points on the EG. These cross sections described the elevation difference relative to a reference point on the gully bank to estimate deepening and widening that occurred between survey dates on that cross-section line. The Weedel field was first surveyed on June 23, 2013 and surveyed again on April 22, 2014. The Schmidt field had two periods of survey, one from June 21, 2012 to March 16, 2013 and another from March 16, 2013 to April 18, 2014. These survey lines were measured on the active eroding EG below the head cut (lower EG) and in the soon be eroded EG above the head cut (upper EG). The volume of soil loss estimated from the survey line was assumed to be the same for the whole segment of the EG (either upper or lower EG). The Weedel field soil loss was estimated differently than the Schmidt field. The Weedel field had one distinct lower gully and one distinct upper gully with two survey lines crossing each (Figure 4.1). The change in cross-sectional area of the two survey lines were averaged together for each gully segment (upper and lower). The Schmidt field had two upper gully segments and two lower gully segments, each with one cross section (Figure 4.2). The change in cross-sectional area was computed for each segment, and then summed for the upper gully and then for the lower gully.

Change in cross-sectional area was calculated between 0 to 2, 2 to 5, 5 to 15, and 15 to 30 cm depths for both the bank and within the gully soils. Figure 4.3 is an example of the survey measurements and how the change in cross-sectional area at each depth was calculated. The volume of the soil loss was computed as the change in cross-sectional area multiplied by the

length of the gully. The mass of soil loss is the volume of soil multiplied by the bulk density. Bulk density was estimated to be 1.37 g cm^{-3} according to Soil Survey Geographic database (SSURGO) for the soil map units present in the two fields. The soil loss from the side of the EG was considered to belong to bank loss and represents the widening of the EG. Soil loss from the bottom of the EG was considered to be within the gully and represents the deepening of the gully. The sampling and analysis of soil from the EG bank (bank) and soil within the gully (gully) is described in chapter 2.

WEPP modeling- soil loss estimation for sheet and rill erosion

The Water Erosion Prediction Project (WEPP) model was used to estimate the sediment loss from the sheet and rill erosion of the bulk field that was leaving the gully catchment. Using the WEPP model can give accurate soil loss estimations based upon specific rain events and locations or total soil loss over long periods. The WEPP model has been shown to be accurate for field size watersheds, can respond over a large variety of environmental and field conditions, and is similar in accuracy to the commonly used Universal Soil Loss Erosion (USLE) (Ghidey and Alberts, 1996; Laflen et al., 2004). The modeling for this project was conducted by Vladimir Karimov (Karimov, personal communication, (2014), who is working on EG model development using data from the same fields used for this study).

The WEPP model is a mechanistic model that uses erosion theory, infiltration theory, soil physics, plant science, soil hydraulics, and rainfall runoff relationships. The WEPP model is based upon the hillslope, channeling, and impoundments within a field watershed to calculate net soil loss and can be extrapolated over a large range of conditions (Ascough II et al., 1997). Some of the inputs into the WEPP model include environment (rainfall and storm intensity), soil

factors (texture, hydraulics, density, and surface roughness), management (crop and implements), field slope, water channeling, and impoundments (such as culverts and filter fences). One of the limitations of the WEPP model is that it does not predict soil loss from ephemeral gullies or stream banks (Ascough II et al., 1997). Therefore in our study we must estimate ephemeral gully erosion with different methods. Nutrient loss is also not a part of the WEPP model however estimates of sediment bound P losses can be made if P concentration of eroded sediment is known (Perez-Bidegain et al., 2010).

The soil data for the WEPP model used in this study was taken from Soil Survey Geographic database (SSURGO). Other soil factors such as K-factors and roughness are calculated from WEPP using soil texture from the SSURGO data. Field slope and size was formed by ArcMap (version 10.1) using topographical data from KDASC, (2013). The WEPP model was run for the Weedel and Schmidt field using the time period average of a 50 year run with environmental data determined from WEPP using simulated weather data based on long-term climate data from the McPherson, KS weather station. Based on visual observations and the low slope of the fields, it was assumed that the majority of the sediment lost from sheet and rill erosion came from the 0 to 2 cm depth fraction of the bulk field. The management inputs for the Weedel and Schmidt fields came from visual observation and farmer inquiry (Text input- Appendix C: Figure C.1 and Figure C.2). A screen shot of the WEPP model display is provided for reference in figures 4.4 and 4.5 and size of field and runoff is in table 4.2. Sediment enrichment is also predicted by the WEPP model and was used in this study for the enrichment of P from the sheet and rill erosion (Perez-Bidegain et al., 2010).

Estimations of total phosphorus and labile phosphorus loss

The loss of total P and labile P was calculated by multiplying the P concentration in the soil with the corresponding sediment loss estimation for each depth and landscape position. As described in chapter 2, total P was determined by salicylic-sulfuric acid digestion and labile P was determined by anion exchange resin P; total P being the complete quantity of P in a soil and labile P being all P which is desorbable into solution. Enrichment ratio from the WEPP model was used for the sheet and rill erosion to determine the increase to P loss expected due to particle preference in erosion. Quantity of P loss in either labile P or total P is described in equation 4.1 where mass of soil is in kg, soil test P is in mg kg^{-1} , and enrichment ratio is unit less.

$$\text{Mass of soil loss} * \text{soil test P (total P or liable P)} * \text{enrichment ratio} = \text{quantity P loss}$$

Equation 4.1

The EG erosion was considered to have complete loss of sediments so no enrichment ratio was used. Data used for calculations are provided in Tables 4.1 and 4.4 of the result section.

Using FMBP model to determine dissolved P in runoff

The determination of the concentration of dissolved P in runoff that is affected by the addition of subsoil of EG erosion was done using the Freundlich mass-balance of phosphorus (FMBP) model described in chapter 3 (Equation 3.9). The FMBP model estimates the expected equilibrium P concentration in solutions containing sediments from multiple soils. For this calculation, the final dissolved P concentration was estimated assuming the initial dissolved P concentration in rainwater was 0 mg L^{-1} .

Estimate of dissolved P in runoff requires the inputs of a large number of soils from a variety of landscape positions, so the FMBP model was expanded to include 14 (Weedel) or 11 (Schmidt) more soils (Equation 4.2).

$$T_i = T_f \quad m_1 Q_{i1} + m_2 Q_{i2} + m_3 Q_{i3} + m_4 Q_{i4} + m_5 Q_{i5} + m_6 Q_{i6} + m_7 Q_{i7} + m_8 Q_{i8} + m_9 Q_{i9} + m_{10} Q_{i10} + m_{11} Q_{i11} + m_{12} Q_{i12} + m_{13} Q_{i13} = C_f v + m_1 K_{f1} C_f^{n1} + m_2 K_{f2} C_f^{n2} + m_3 K_{f3} C_f^{n3} + m_4 K_{f4} C_f^{n4} + m_5 K_{f5} C_f^{n5} + m_6 K_{f6} C_f^{n6} + m_7 K_{f7} C_f^{n7} + m_8 K_{f8} C_f^{n8} + m_9 K_{f9} C_f^{n9} + m_{10} K_{f10} C_f^{n10} + m_{11} K_{f11} C_f^{n11} + m_{12} K_{f12} C_f^{n12} + m_{13} K_{f13} C_f^{n13} \quad \text{Equation 4.2}$$

Where T_i is the total mass of labile P (AEP) contained in eroded sediments, and T_f is the total mass of labile P leaving the ephemeral gully as either adsorbed P on sediment or dissolved P in solution. The volume of water (v in L) is the total amount of runoff leaving the ephemeral gully catchment (Table 4.2). The mass of soil (m in kg) is the computed soil loss from the respective landscape positions and depths. As in chapter 3, Q_i (mg kg^{-1}) was determined from the AEP determined for that soil fraction (labile P sorbed onto sediment). Q_f (mg kg^{-1}) was determined using the Freundlich equation ($Q=K_f C^n$), using the K_f and n of the specified soil fraction and C is the final P concentration in solution (mg L^{-1}). Equation 4.2 was solved for the only unknown, C_f , using the Goal seek function in Microsoft Excel (2010). The K_f and b values (table 4.3 for Weedel and table 4.6 for Schmidt) were determined by fitting the Freundlich equation to P sorption isotherm data using PROC NLIN (SAS v. 9.1).

The equation 4.2 was used to described the result to dissolved P in runoff (C_f) as the EG soils were hypothetically progressively reduced in quantity until only sheet and rill erosion was present. The dissolved P concentration and quantity of total P resulting from hypothetically decreasing EG erosion was estimated by equally reducing the mass of soil lost from each EG

section (upper and lower), source (bank or gully), and depth fraction in equation 4.2 until the only soil left that was lost was from sheet and rill erosion.

Results and Discussion

Weedel field

The Weedel field had extensive soil loss from the EG in comparison to the sheet and rill from the small source watershed (Table 4.1). The average soil loss from sheet and rill erosion calculated by the WEPP model was 0.43 Mg ha^{-1} ($0.192 \text{ tons ac}^{-1}$) over the 11-month time period corresponding to estimates EG erosion (June 23, 2013 to April 22, 2014). The low sheet and rill loss was likely largely due to the field being in no-till and a shallow slope of field. The results from the WEPP model also demonstrated that the erosion from year to year is highly variable with a maximum loss of 2876 kg ha^{-1} and a minimum of only 6 kg ha^{-1} . The gully lost 8.02 m^3 of soil, which is about 5 cm of soil depth if erosion loss was even over the whole EG. The upper gully of the Weedel field lost most of its sediment from the upper depths of 0 to 2 and 2 to 5 while the lower gully lost more sediment from the lower depths 5 to 15 and 15 to 30. This would represent the upper gully is incising down into the soil profile while the lower gully is widening into the bank.

The total P and labile P loss for the Weedel field followed the same trends as the loss of sediment, with the EG responsible for losing the majority of P. Table 4.1 also describes the P loss for each depth and landscape position. The loss of total P came to 1.96 kg ha^{-1} , which is a small quantity from a land manager's perspective. The concentration of total P in runoff would be 4.1 mg L^{-1} which is more than the historical average of 0.8 mg L^{-1} for the Little Ark River

watershed; however P has been placed low as an environmental concern for the watershed (WRAPS, 2011). The enrichment ratio from the WEPP model was low at 1.03, likely due to the consistent heavy texture of soil in the Weedel field.

The estimated dissolved P concentration in runoff as predicted using the FMBP model for the Weedel field is $< 0.005 \text{ mg P L}^{-1}$ (Figure 4.6). The model demonstrated that while total P decreases with reduction in EG erosion, the dissolved P in runoff will increase. The loss of total P is largely tied the loss of sediment and since most of the sediment lost was from the EG, the loss of total P was highly influenced by the reduction of the EG erosion. Total P decreased from 1.954 to 0.141 kg P ha⁻¹ with full reduction in the EG soil loss. The dissolved P increased from 0.0034 to 0.0204 mg L⁻¹, or by 600%, with the full reduction of the soil loss from the EG. Table 4.3 describes the EPC₀ and sediment contribution of each soil fraction involve in erosion. The bulk soil had an EPC₀ higher than any of the EG soil fractions and had a minor contribution to total soil loss. This allowed for the dissolved P in runoff to remain low until the sheet and rill erosion was contributing to the majority or all of the soil loss. Using the FBMP model, figure 4.6 demonstrates the impact of subsoil on the dissolved P concentration leaving a field. Although the EG sediment loss from the Weedel field is high compared to the sheet and rill, so is its control on dissolved P, which has high bioavailability in water bodies.

Schmidt field

The Schmidt field had very different results than the Weedel field; the sediment loss from EG erosion was less and the sediment loss from the sheet and rill erosion was greater. Table 4.4 describes the area of loss for each depth and landscape position and the length of the gully for the first survey time period. The Schmidt field was much larger than the Weedel field (Table 4.2),

which lead to the increased overall quantity of sediment leaving the bulk field through sheet and rill erosion. However the sediment loss per acre was less with sheet and rill, at 0.198 Mg ha^{-1} ($0.088 \text{ ton ac}^{-1}$) over the first period time survey (June 21, 2012 to March 16, 2013) and 0.325 Mg ha^{-1} ($0.145 \text{ ton ac}^{-1}$) over the second time period (March 16, 2013 to April 18, 2014). The volume of sediment lost from the EG in the first time period was 2.27 m^3 and the second time period actually saw a net gain of 7.7 m^3 of sediment. This increase in the second period had to have come from the trapping of sediment lost from the upper field, likely due to thick residue cover and the slowing of water velocity. A net gain of 7.7 m^3 of sediment is approximately 10,549 kg of sediment, which is 8,092 kg more than the 2,457 kg predicted as the long-term average expected erosion from the sheet and rill. This difference is due to the possible inaccuracies in the estimation of sediment gained in the EG or possibly from the second time period eroding more sheet and rill sediment than the average prediction. Table 4.5 describes the sediment volume increase calculations for the second survey period; most of the sediment was trapped by the large lower gully segment.

The loss of total P from the Schmidt field was insignificant from a land manager's point of view at only at $0.0957 \text{ kg P ha}^{-1}$ for the first time period (table 4.4). Of this total P loss, only 10.4% of it was available as labile P. The soil test P wasn't measured again after the second time period's sedimentation, so it would hard to estimate the total P trapped in the EG. Given the assumption that the concentration of total P in the trapped sediment was the same as the sheet and rill in the first time period, that quantity of P trapped would be about $0.33 \text{ kg P ha}^{-1}$.

The FMBP model results for the first period of the Schmidt field are shown in figure 4.7. As with the Weedel field, the Schmidt field FMBP model demonstrated that while total P decreases with reduction in the EG, the dissolved P in runoff would increase. The increase in

dissolved P in the Schmidt field however was only from 0.0126 to 0.0136 mg L⁻¹, or by 7.9%. The small rate of increase was part due to the EPC₀ of the bulk field 0 to 2 (associated with the sheet and rill erosion) was lower than the 0 to 2 fractions than any of the EG soils (Table 4.6) and part due to the high volume of runoff in the Schmidt field (table 4.2). However the EG still eroded enough high P buffering capacity subsoil to still drop the dissolved P in runoff. The Schmidt field also demonstrated that the subsoil in erosion of EG has a strong influence in the dissolved P in runoff events.

There were many assumptions taken in the modeling of the soil loss and P estimations for the W and S fields. These assumptions could be distorting the end results of the models used to predict P loss from the fields. To be more accurate the erosion loss would need to be calculated repeatedly, along with environmental data that fits specifically with that year. Soil sampling and P measurements would also need to be repeated yearly as P status is likely changing with fertilization by the manager and from crop uptake. Runoff sampling would also need to be collected at the end the EGs to calibrate and verify the results. Although this data presents interesting look on the effects of EGs on the form and quantity of P loss of which research is limited, it is important for the reader to know the limitations of this study.

Conclusions

The presence of EG in fields has many resulting effects on the outcome of sediment and nutrient loss. This research has shown the P is dynamic throughout the field and with soil depth. To fully monitor the loss of P and the forms of P in runoff, it is necessary to monitor all the sediment contribution locations and their effect on the final P outcome. The presence of the EGs

in the Weedel field reduced the dissolved P from 0.0204 to 0.0034 mg L⁻¹ while the loss of total P increased from 0.141 to 1.954 kg P ha⁻¹. The Schmidt field EG reduced the dissolved P from 0.0136 to 0.0126 mg L⁻¹ while the loss of total P increased from 0.05 to 0.096 kg P ha⁻¹ (first time period). The subsoil eroded in EGs has an important effect on the sorption on P in runoff, and even a small contribution of highly P sorptive subsoil can have a large outcome in dissolved P concentration.

At times, erosion from EG can be the majority of the sediment lost. Weedel field had 8.02 m³ of sediment lost from the EG from June 23, 2013 to April 22, 2014, which was considerably more than that lost from the sheet and rill erosion. The Schmidt field had 2.27 m³ lost during the first monitored time period (June 21, 2012 to March 16, 2013) and a gain of 7.71 m³ in the second time period (March 16, 2013 to April 18, 2014), showing the dynamic nature that EG are at times capable of.

Phosphorus is a major nutrient that contributes to algae blooms and subsequent eutrophication in water bodies; however its application is necessary for crop production. Best management practices are an important part of limiting sediment loss, and generally P loss which is largely sediment bound. However implementing BMPs can change the landscape's sediment contribution to soil loss. By altering this erosional mix of sediment the P buffering ability of the sediment is changed and possible negative outcomes, such as the increase in dissolved P, can be a result. Best management practices such as contour and conservation tillage, maintaining low soil test P, and subsurface application of nutrients could help counter-act the increase of dissolved P loss when EG erosion is reduced.

References

- Ascough II, J.C., C. Baffaut, M.A. Nearing, and B.Y. Liu. 1997. The WEPP watershed model 1. hydrology and erosion. *Trans. ASAE* 40:921-933.
- Carpenter, S. 2008. Nonpoint pollution of surface waters with phosphorus and nitrogen. *Iss. in Eco.* 3.
- Dodds, W.K., W.W. Bouska, J.L. Eitzmann, T.J. Pilger, K.L. Pitts, A.J. Riley, J.T. Schloesser, and D.J. Thornbrugh. 2009. Eutrophication of US freshwaters: analysis of potential economic damages. *Environ. Sci. Technol.* 43:12-19.
- Ghidey, F., and E.E. Alberts. 1996. Comparison of measured and WEPP predicted runoff and soil loss for Midwest claypan soil. *Trans. ASAE* 39:1395–1402
- KDASC. 2013. Kansas Data Access and Support Center, Topeka, Kan., USA. Available from <http://www.kansasgis.org/>. [cited 2014].
- Lafren, J., D. Flanagan, and B. Engel. 2004. Soil erosion and sediment yield prediction accuracy using WEPP. *J. Am. Water Resour. Assoc.* 40:289-297
- Perez-Bidegain R., M. Helmers, and M. Cruse. 2010. Modeling phosphorus transport in an agricultural watershed using the WEPP model. *J. Environ. Qual.* 39:2121-9.
- Poesen, J., J. Nachtergaele, G. Verstraeten, and C. Valentin. 2003. Gully erosion and environmental change: importance and research needs. *Catena.* 91-133.
- U.S. EPA. 2005. United States Environmental Protection Agency. Bulletin: Protecting Water Quality from Environmental Runoff. EPA 841-F-05-001

WRAPS. 2011. Watershed restoration and protection strategy: Little Arkansas River watershed.
available from www.kcare.ksu.edu/doc4282.ashx

Zheng, F., X. He, X. Gao, C. Zhang, and K. Tang. 2005. Effects of erosion patterns on nutrient loss following deforestation on the loess plateau of China. *Agric. Ecosyst. Environ.* 108:85-97.

Table 4.1. Landscape position and depth of soil and phosphorus loss in the Weedel field from June 23, 2013 to April 22, 2014

Landscape Position	Depth	Surveyed Area of Loss †	Length of gully	Volume of sediment loss	Soil density	Sediment loss mass	Soil total P	Soil AEP ‡	ER ¶	Total P loss	Total AEP loss
	cm	m ²	m	m ³	g cm ⁻³	kg	mg kg ⁻¹	mg kg ⁻¹		g	g
Upper Bank	0 to 2	0.4505	26.2128	1.1822	1.37	1620	242.3	41.5	1	392.4	67.1
Upper Bank	2 to 5	0.03412	26.2128	1.3395	1.37	1835	210.9	15.9	1	387.0	29.1
Upper Bank	5 to 15	0.0235	26.2128	0.6946	1.37	952	150.6	2.9	1	143.3	2.8
Upper Gully	0 to 2	0.0353	26.2128	0.464	1.37	636	232.9	36.7	1	148.0	23.3
Upper Gully	2 to 5	0.0474	26.2128	0.6212	1.37	851	211.4	13.5	1	179.9	11.5
Upper Gully	5 to 15	0.0061	26.2128	0.1599	1.37	219	137.0	1.8	1	30.0	0.4
Lower Bank	0 to 2	0.0056	33.6804	0.1886	1.37	258	251.9	29.6	1	65.1	7.6
Lower Bank	2 to 5	0.0144	33.6804	0.485	1.37	664	212.2	13.4	1	141.0	8.9
Lower Bank	5 to 15	0.0901	33.6804	1.519	1.37	2081	159.7	2.3	1	332.4	4.7
Lower Bank	15 to 30	0.00605	33.6804	0.5187	1.37	711	135.9	0.7	1	96.5	0.5
Lower Gully	0 to 2	0.0089	33.6804	0.2998	1.37	711	213.8	20.8	1	151.9	14.8
Lower Gully	2 to 5	0.0093	33.6804	0.3132	1.37	429	165.3	8.4	1	70.9	3.6
Lower Gully	5 to 15	0.0070	33.6804	0.2358	1.37	323	138.0	1.0	1	44.6	0.3
Total bank and gully				8.02	1.37	11289				2183	174.7
Bulk Field	0 to 2					518	327.4	53.4	1.03	174.7	28.5

† The average area of loss from first survey line and second survey line across the gully from specified depth

‡ AER is anion exchange phosphorus (labile P)

¶ Enrichment ratio (ER) of

Table 4.2. WEPP predicted water runoff and size of field

Field and survey period	WEPP predicted runoff	Size of field	Runoff Quantity
	mm	ha	L
Weedel June 23, 2013 to April 22, 2014	47.58	1.204	572839
Schmidt June 21, 2012 to March 16, 2013	29.31	7.586	3743691
Schmidt March 16, 2013 to April 18, 2014	49.35	7.586	2223456

Table 4.3. Soil landscape and depth with corresponding EPC₀, Freundlich coefficients, and contribution percentage to total soil loss for Weedel field.

Landscape Position	Depth cm	EPC ₀ † mg L ⁻¹	Contribution % to total soil loss %	Freundlich Coefficient K _f	Fitting Coefficient n
Upper Bank	0 to 2	0.000	5%	117.78179	0.391607
Upper Bank	2 to 5	0.082	14%	118.2656	0.324344
Upper Bank	5 to 15	0.003	16%	149.05267	0.291734
Upper Gully	0 to 2	0.000	8%	122.17241	0.379879
Upper Gully	2 to 5	0.051	6%	120.40116	0.303342
Upper Gully	5 to 15	0.001	8%	149.47017	0.335811
Lower Bank	0 to 2	0.000	2%	111.0426	0.377255
Lower Bank	2 to 5	0.043	2%	115.86026	0.313333
Lower Bank	5 to 15	0.001	6%	150.98686	0.409463
Lower Bank	15 to 30	0.000	18%	134.47462	0.439987
Lower Gully	0 to 2	0.000	6%	118.31161	0.382453
Lower Gully	2 to 5	0.013	6%	112.69008	0.287686
Lower Gully	5 to 15	0.000	4%	126.29269	0.438555
Bulk Field	0 to 2	0.118	3%	116.71455	0.342056

† Equilibrium Phosphorus Concentration at Zero Net Sorption

Table 4.4. Landscape position and depth of soil and phosphorus loss in the Schmidt field from June 21, 2012 to March 16, 2013.

Landscape Position	Depth	Survey Area of Loss 1 †	Gully Length 1 †	Survey Area of Loss 2 ‡	Gully Length 2 ‡	Volume sediment loss ¶	Soil density	Sediment loss mass	Soil test total P	Soil test AER §	ER #	Total P loss	Total AER loss
	cm	m ²	m	m ²	m	m ³	g cm ⁻³	kg	mg kg ⁻¹	mg kg ⁻¹		g	g
Upper Bank	0 to 2	0.0037	5.94	0.0009	6.48	0.02809	1.37	38.48	174.0	23.87	1	6.7	0.9
Upper Bank	2 to 5	0.0009	5.94	0.0028	6.48	0.0236	1.37	32.33	132.4	15.14	1	4.3	0.5
Upper Bank	5 to 15	0.0177	5.94	0.0058	6.48	0.1409	1.37	193.03	139.6	8.15	1	27.0	1.6
Upper Bank	15 to 30	0.01858	5.94	0.0	6.48	0.1104	1.37	151.25	146.2	3.28	1	22.1	0.5
Lower Bank	0 to 2	0.0074	53.5	0.0018	11.1	0.418	1.37	572.66	128.6	16.55	1	73.6	9.5
Lower Bank	2 to 5	0.0074	53.5	0.0074	11.1	0.481	1.37	658.97	114.3	11.84	1	75.3	7.8
Lower Bank	5 to 15	0.0009	53.5	0.03159	11.1	0.4013	1.37	549.78	105.2	5.68	1	57.8	3.1
Lower Bank	15 to 30	0.0	53.5	0.00650	11.1	0.072	1.37	98.64	151.6	1.65	1	15.0	0.2
Lower Gully	0 to 2	0.00557	53.5	0.0	11.1	0.2979	1.37	98.64	119.1	16.01	1	11.7	1.6
Lower Gully	2 to 5	0.00557	53.5	0.0	11.1	0.2979	1.37	408.12	129.6	9.22	1	52.9	3.8
Total bank and gully						2.27		2801.9	118.1	2.88		346.4	29.4
Bulk Field	0 to 2							1494.5	237.4	53.4	1.07	379.6	46.0

† Area of loss and length for first segment of the upper or lower gully.

‡ Area of loss and length for the second segment of the upper or lower gully

¶ The volume of loss is the added first and second segments.

Enrichment ratio (ER) of P

Table 4.5. Sediment gained from Schmidt field from March 16, 2013 to April 18, 2014

Landscape Position	Surveyed area of gain m ²	Length of gully m	Volume of sediment gained m ³
Lower Gully Section 1	0.11055	53.49	5.9133
Lower Gully Section 2	0.09848	5.49	0.5406
Upper Gully Section 1	0.07897	11.13	0.8789
Upper Gully Section 2	0.05760	6.477	0.3731

Table 4.6. Soil landscape and depth with corresponding EPC₀, Freundlich coefficients, and contribution percentage to total soil loss for Schmidt field

Landscape Position	Depth cm	EPC ₀ ‡ mg L ⁻¹	Contribution % to total soil loss %	Freundlich Coefficient K _f	Fitting Coefficient n
Upper Bank	0 to 2	0.0919	1%	59.476966	0.404929
Upper Bank	2 to 5	0.0401	1%	54.01953	0.392965
Upper Bank	5 to 15	0.0033	4%	73.866702	0.383196
Upper Bank	15 to 30	0.0002	4%	97.253513	0.325651
Lower Bank	0 to 2	0.0724	13%	46.227387	0.383304
Lower Bank	2 to 5	0.0253	15%	49.861105	0.389863
Lower Bank	5 to 15	0.0034	13%	63.402509	0.419293
Lower Bank	15 to 30	0.0001	2%	102.35114	0.412233
Lower Gully	0 to 2	0.0583	2%	48.836247	0.384586
Lower Gully	2 to 5	0.0119	9%	66.028217	0.422025
Bulk Field	0 to 2	0.0376	35%	103.11941	0.367754

‡ Equilibrium Phosphorus Concentration at Zero Net Sorption

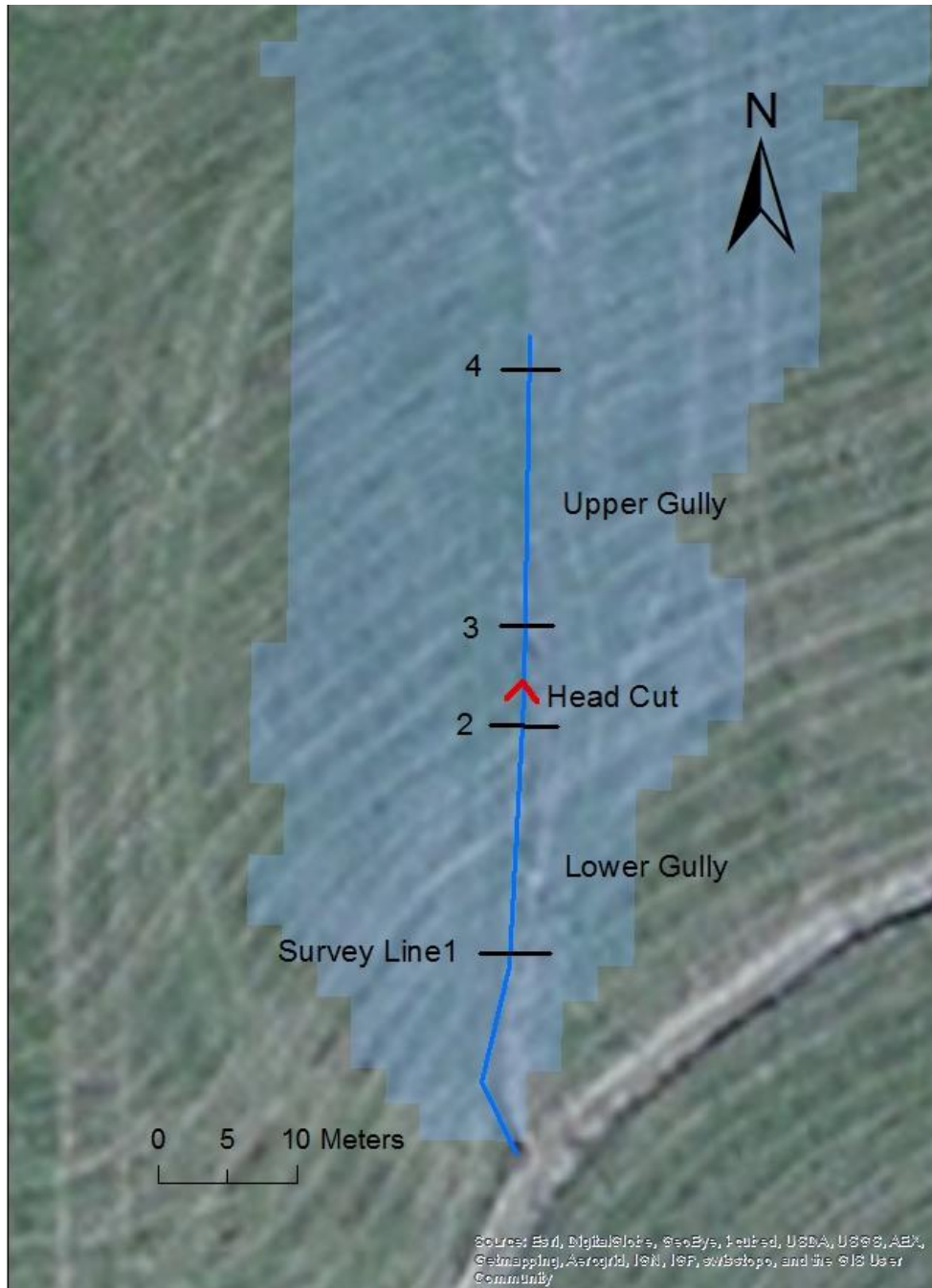


Figure 4.1. Weedel field ephemeral gully with survey lines of cross sectional loss

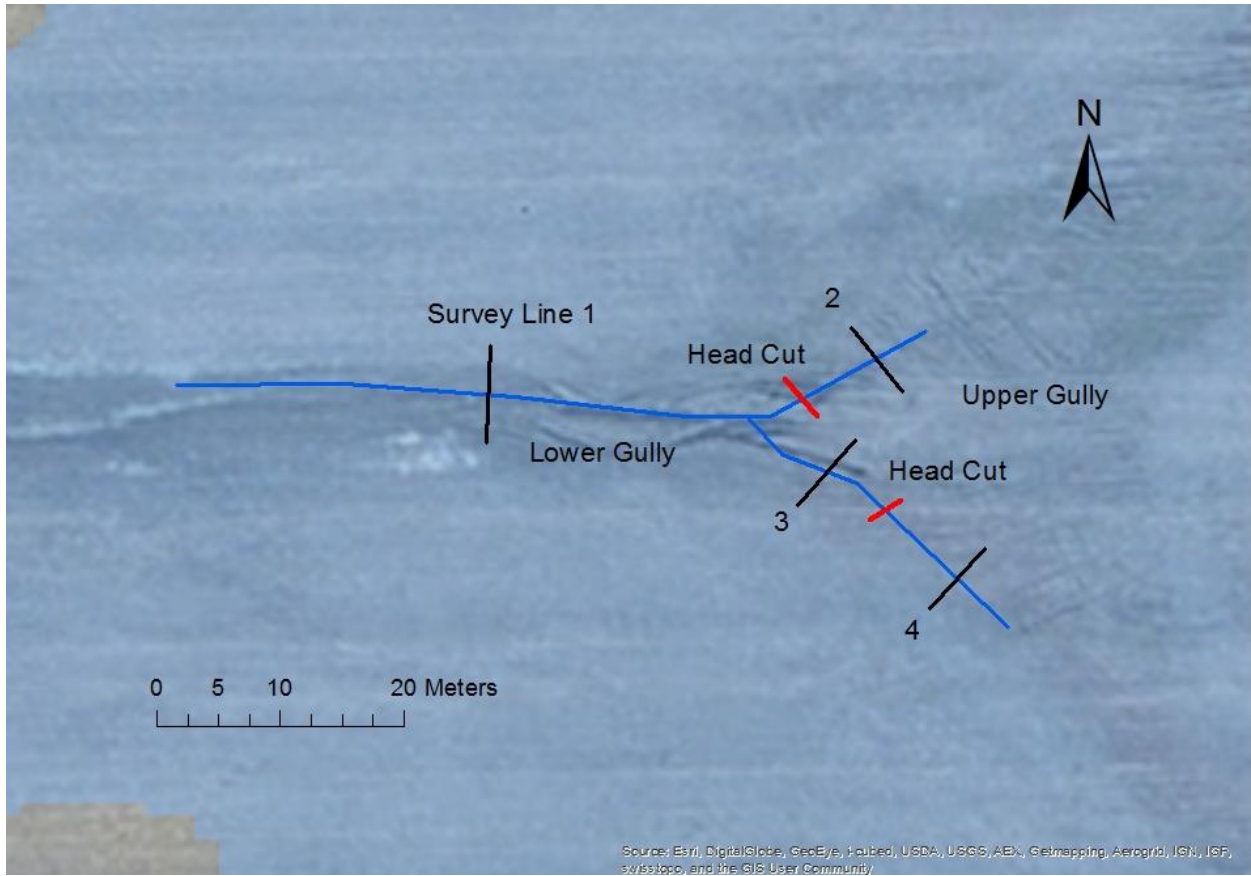


Figure 4.2. Schmidt field ephemeral gully with survey lines of cross sectional loss

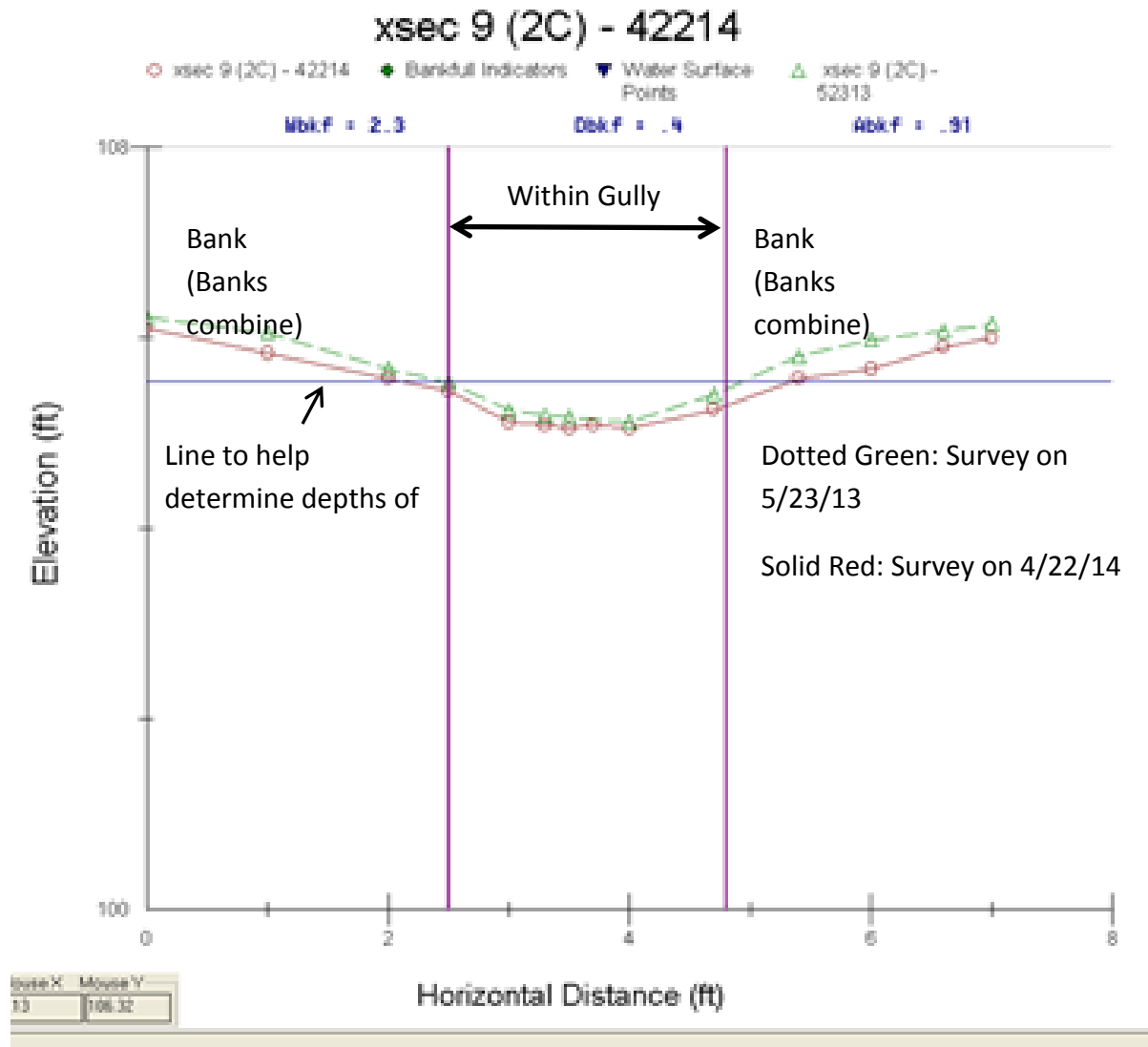


Figure 4.3. River Morph (version 5.1) example of lower gully survey line in Weedel field

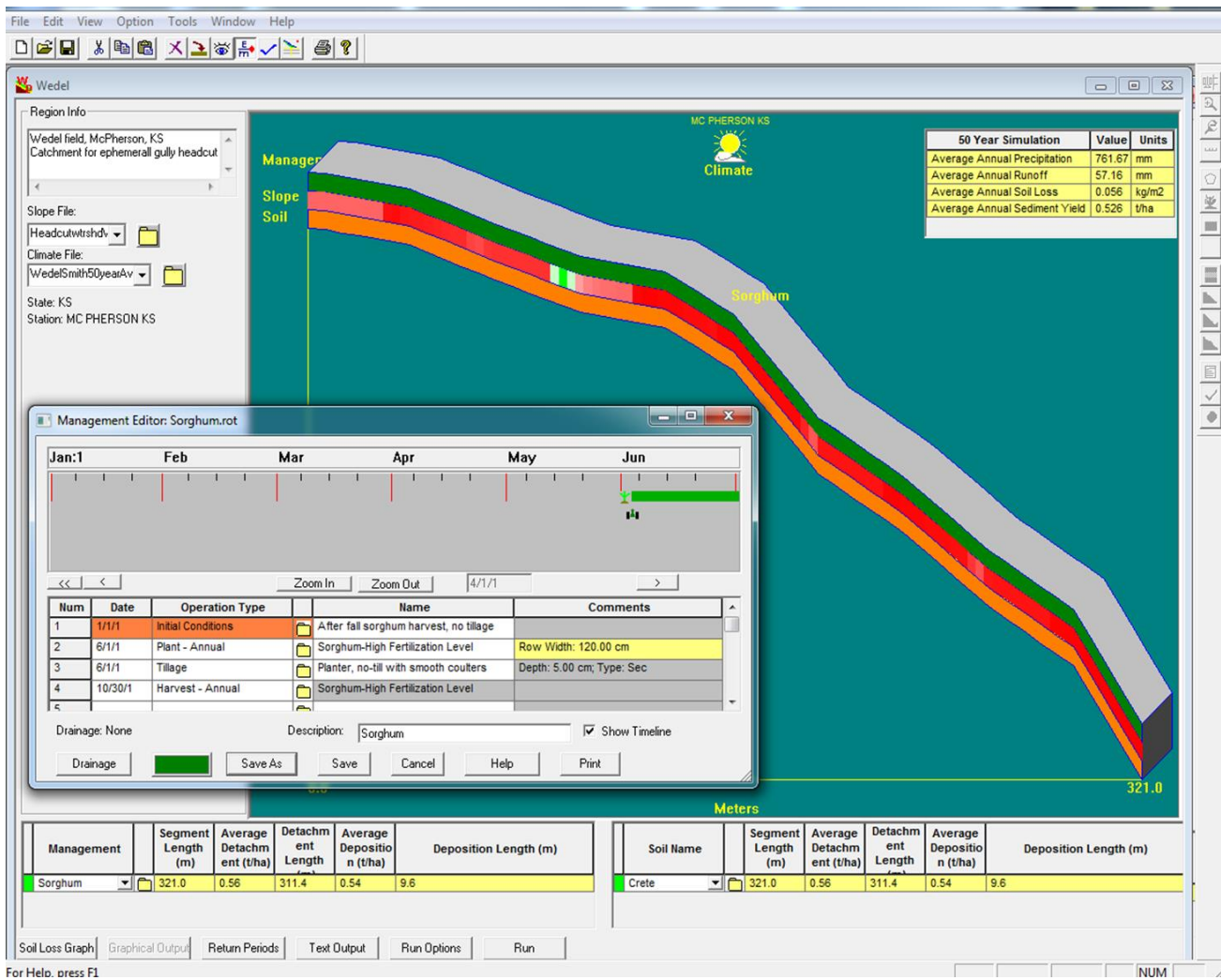


Figure 4.4. WEPP model display of Weedel field showing field slope, manager inputs, and prediction values.

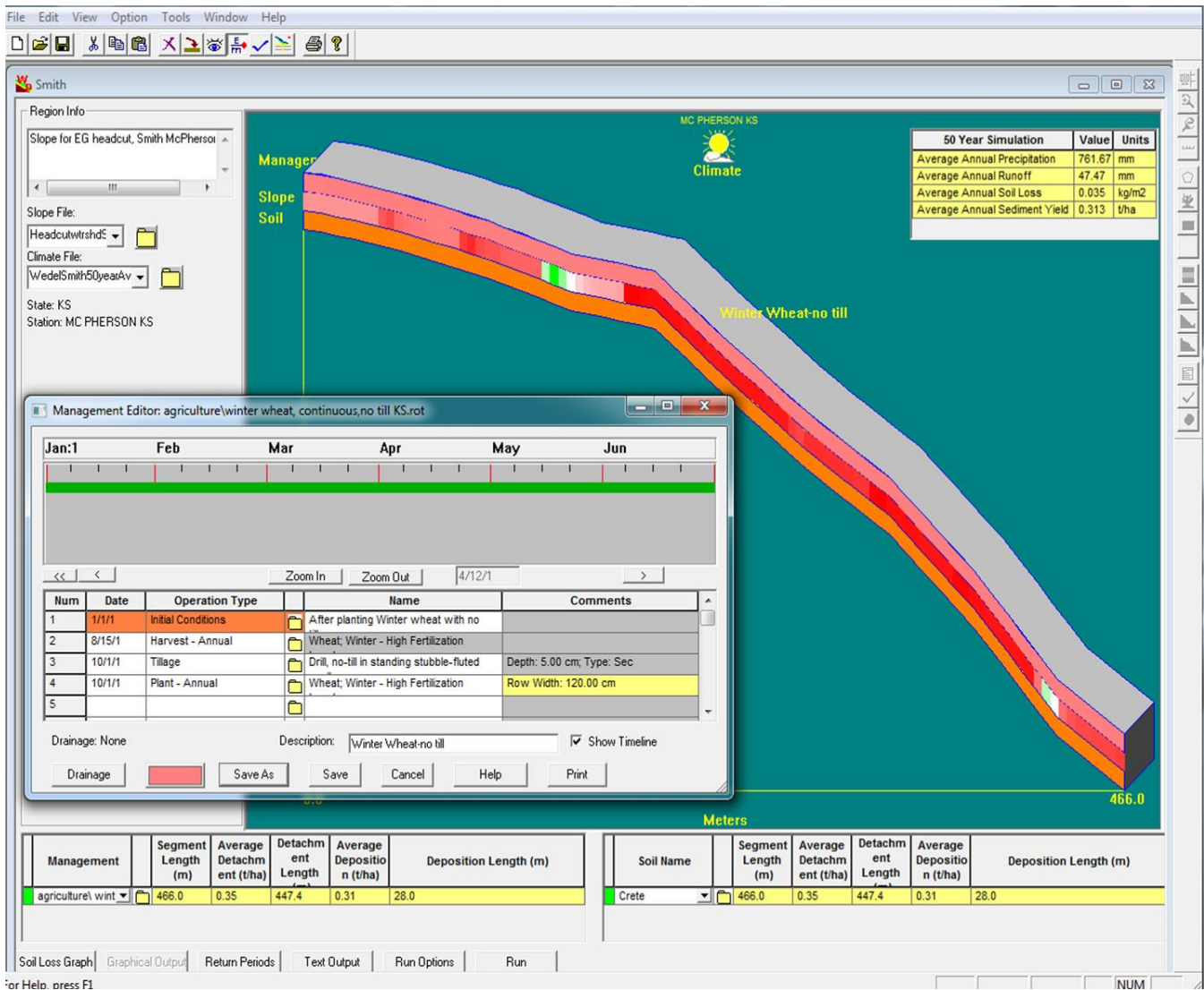


Figure 4.5. WEPP model display of Schmidt field showing field slop, manager inputs, and prediction values.

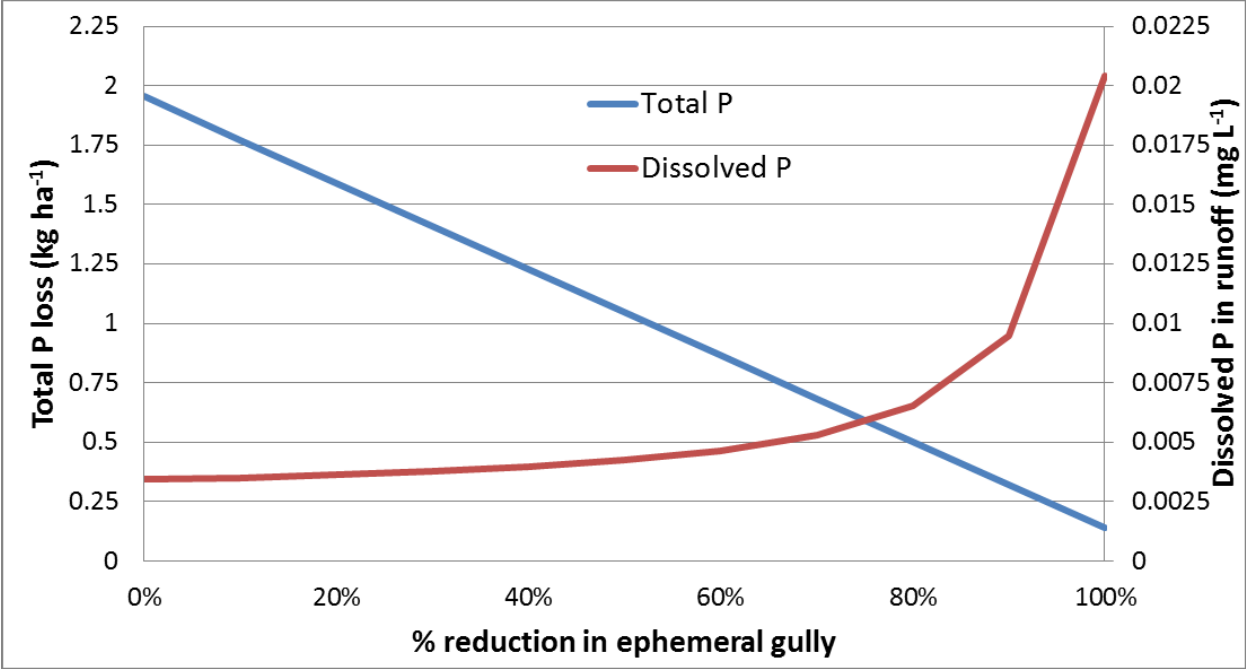


Figure 4.6. Changes in total P loss and dissolved P due to reductions in ephemeral gully erosion in the Weedel field

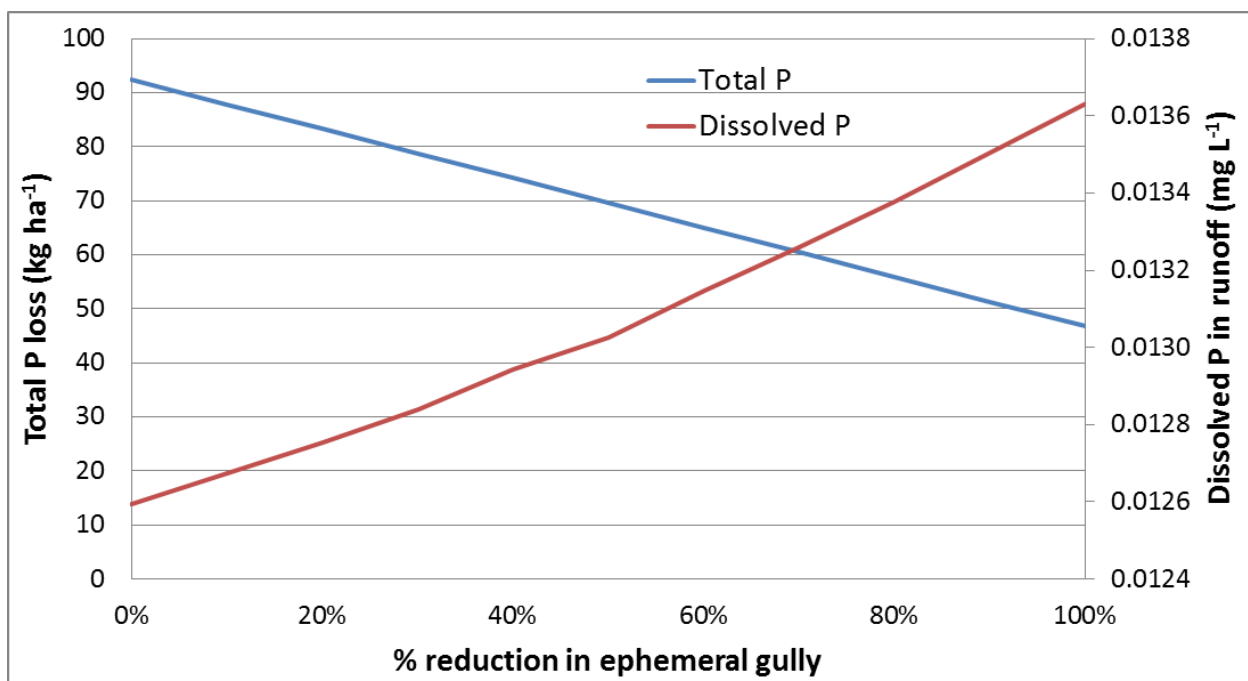


Figure 4.7. Changes in total P loss and dissolved P due to reductions in ephemeral gully erosion for the Schmidt field in the first time period

Chapter 5:

Conclusion and Recommendations

Ephemeral gullies (EG) were shown in this study to have a substantial ability to control the forms of phosphorus (P) leaving a field in runoff. Subsoil erosion that is possible with EG erosion has a high P buffering capacity and usually a lower concentration of soil test P. Therefore, sediment eroded from EGs can adsorb dissolved P that has been desorbed from sheet and rill sediment. The capability of sediment to adsorb P is dependent on the soil properties that influence P sorption (e.g., concentrations of semi-crystalline Al and Fe) and the concentration of labile P. A small quantity of high P sorptive subsoil in an erosional mix with surface soil can have a large effect on the ability of eroded sediments to adsorb dissolved P. The erosion from EGs can at times be the major contributor of sediment eroded from a field, leading to a larger loss of total P, which is mostly sediment bound. However, this loss of EG soil can also have the effect of reducing the dissolved P in runoff. The dissolved form of P is considered to be the form that is bioavailable and capable to contribute to algae blooms and eutrophication in freshwater. Therefore, to fully control P, it is important to consider how different erosional processes affect the final quantity and forms of P leaving a field. Best management practices that limit EG erosion could have the unintended consequence of increasing dissolved P in runoff although reducing overall total P and sediment loss. Best management practices need to be combined, such as grass waterways to control EG erosion with conservation and contour tillage, terraces, or subsurface P application to control P loss from sheet and rill erosion.

Appendix A: Extra Explanatory Figures for Chapter 2

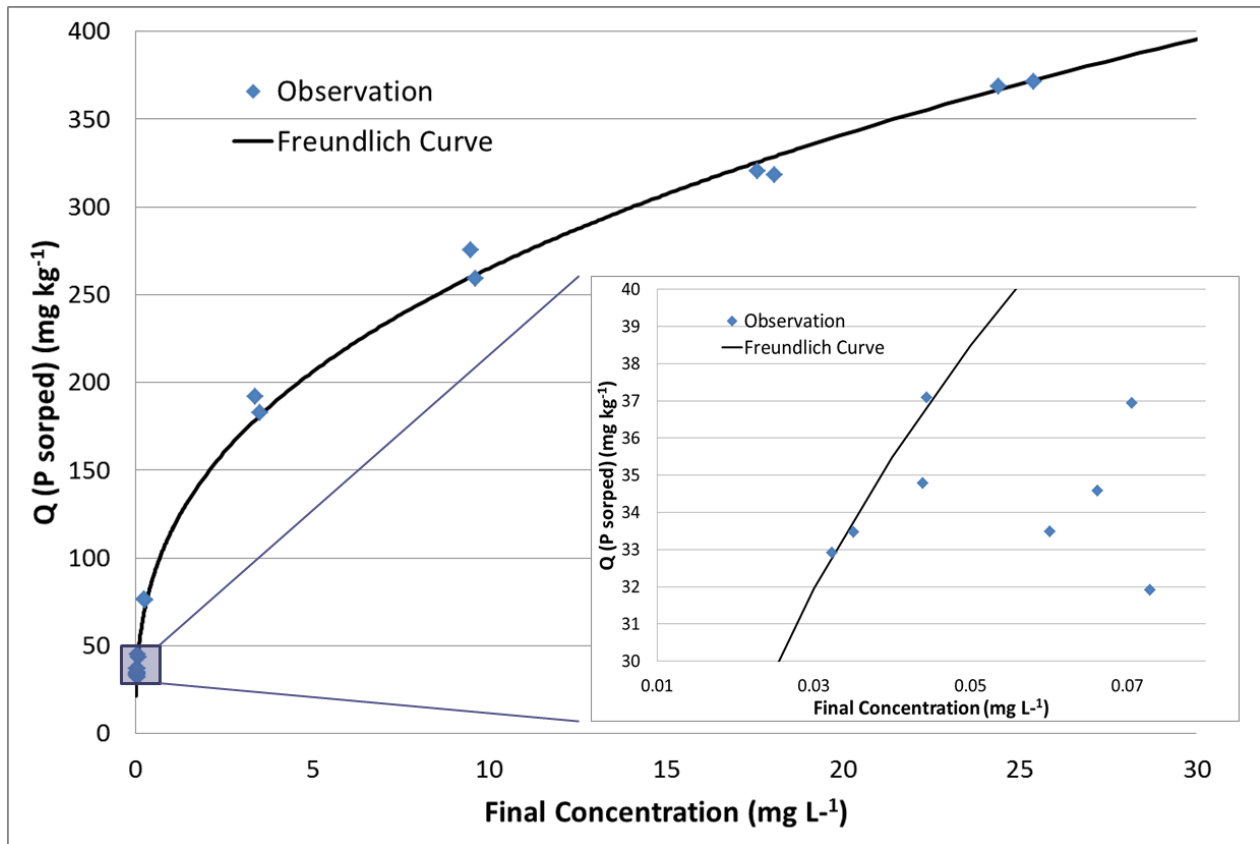


Figure A.1. Phosphorus Sorption Isotherm and fitted Freundlich equation curve

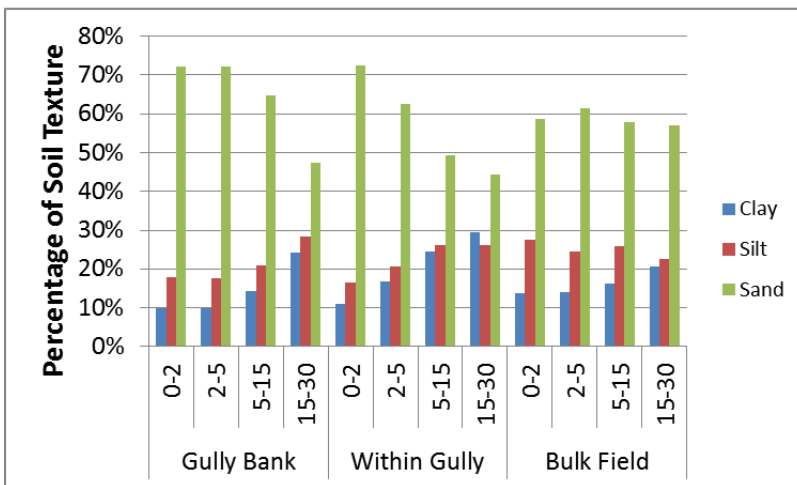
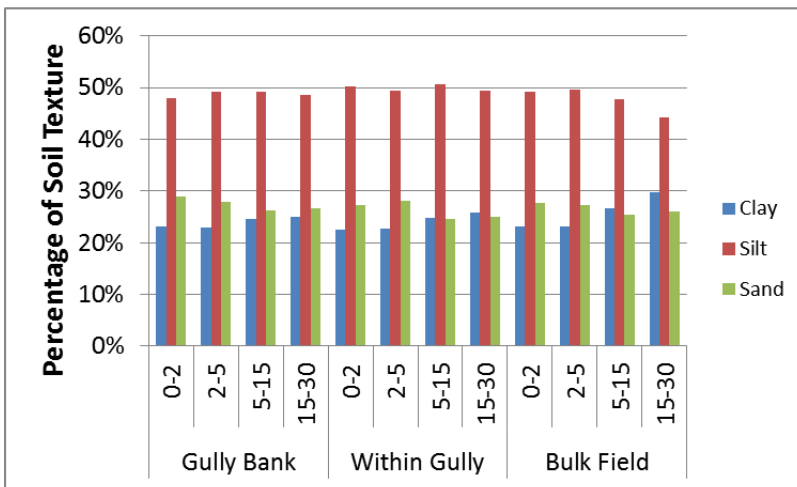
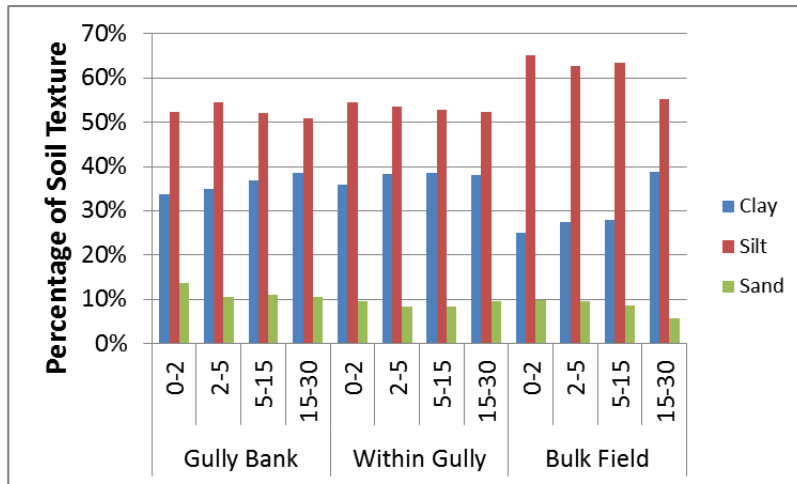


Figure A.2. Texture analysis for Weedel (top), Garring (middle), and Schmidt (bottom) by depth and landscape

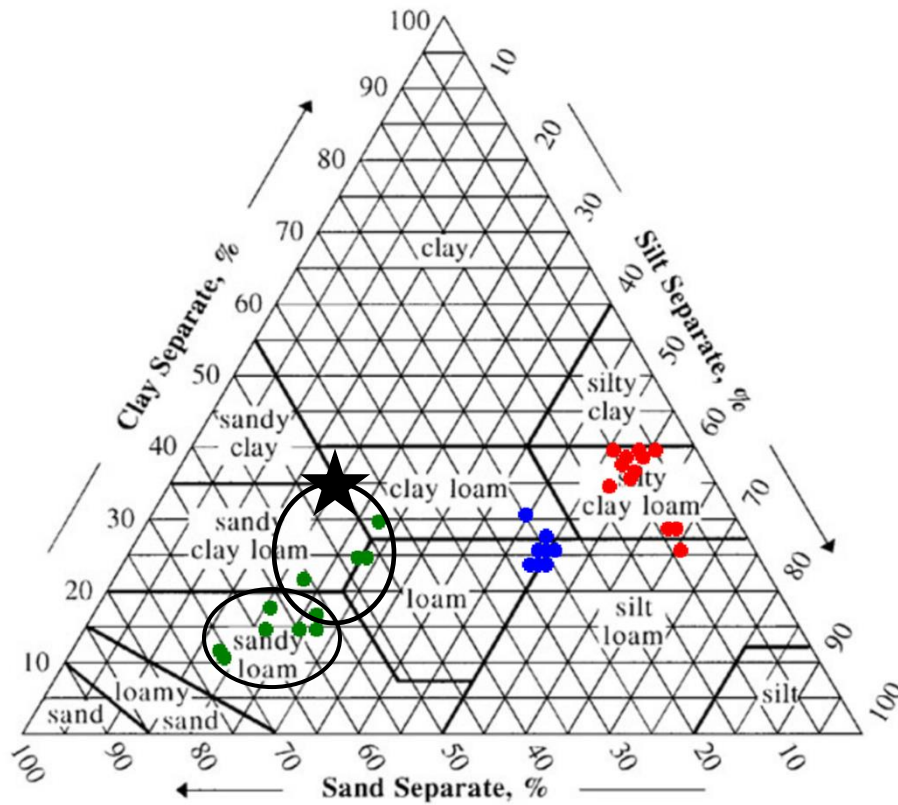


Figure A.3. Textural triangle of tested texture of the three fields.

Note: Red is Weedel, Blue is Garring, Green is Schmidt, starred circle is Schmidt field subsoil of 5-15 and 15-30 cm, and other green dot circle is surface soil of 0-2 and 2-5cm *Template sourced from NRCS, 2013*

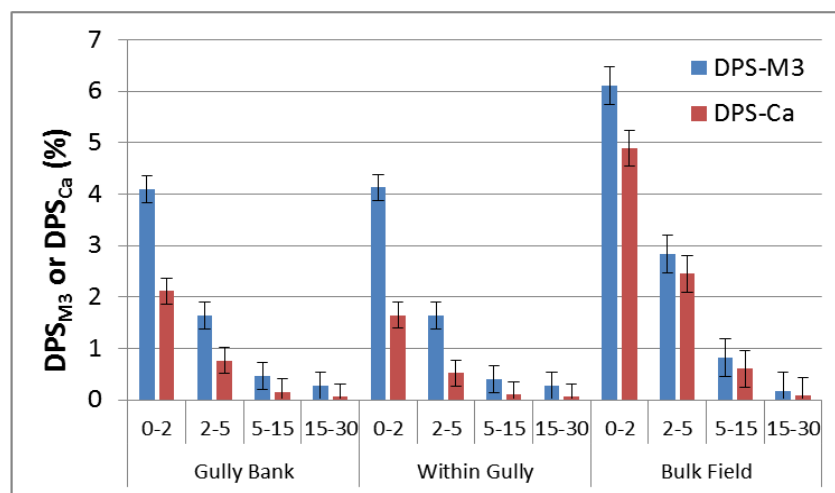
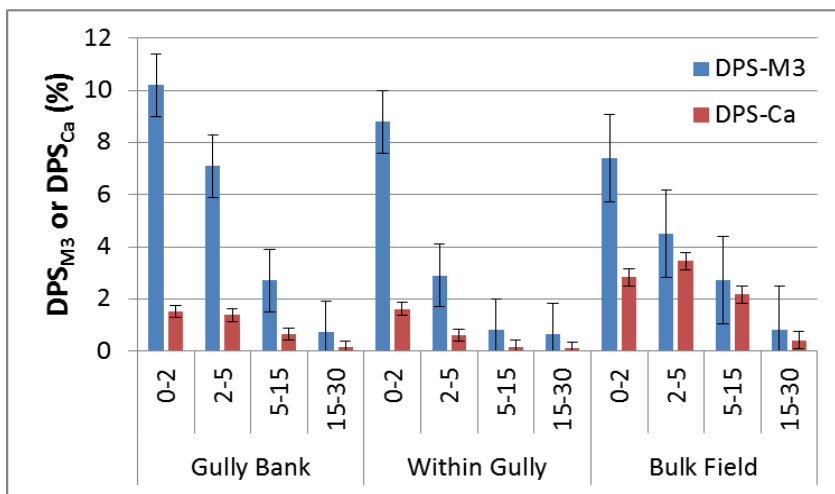
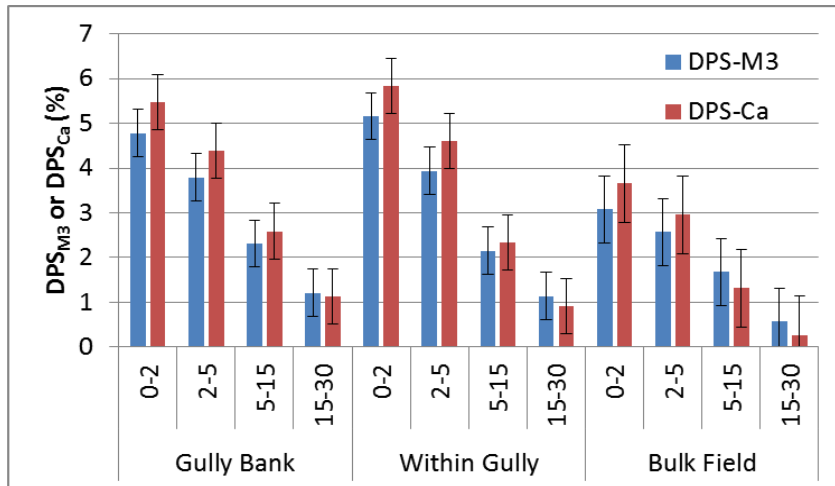


Figure A.4. Degree of Phosphorus Saturation for Mehlich extracted Fe & Al (M3) and Ca (Ca) for Weedel (top), Garring (middle), and Schmidt (lower) by depth and landscape

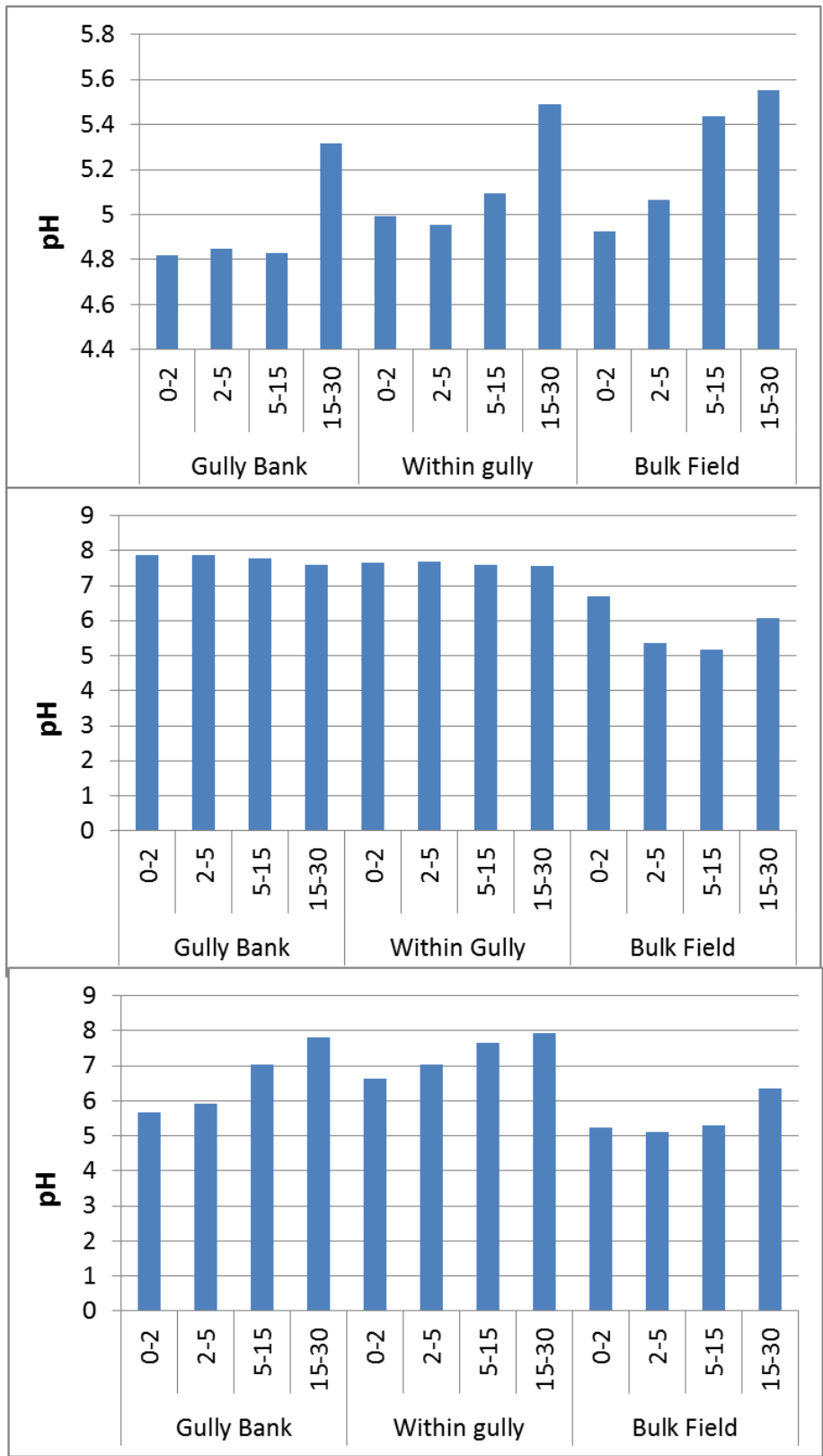


Figure A.5. 1:1 soil to water pH analysis by depth and landscape position for Weedel (top), Garring (middle), and Schmidt (lower)

Appendix B: SAS code

```
proc sort data=aaa; by loc rep set;
proc nlin data=aaa; by loc rep;
  parms Qm=300 Kl=0.05;
  model Q = Qm*(Kl*Cf)/(1+Kl*Cf);
  ods output ParameterEstimates=LangParms2;
  title 'Langmuir on Q';
proc nlin data=aaa; by loc rep;
  parms Kf=100 n=.3;
  model Q=Kf*Cf**n;
  ods output ParameterEstimates=FreuParms2;
  title 'Freundlich on Q';
**/;
data L_kl; set LangParms2 (where=(parameter='Kl')); Kl=estimate;
data L_Qm; set LangParms2 (where=(parameter='Qm')); Qm=estimate;
data F_Kf; set FreuParms2 (where=(parameter='Kf')); Kf=estimate;
data F_n; set FreuParms2 (where=(parameter='n')); n=estimate;
data mmm; merge L_kl L_Qm F_Kf F_n; by loc rep; keep loc rep Kl Qm Kf n;
proc export data = WORK.LangParms2 DBMS=EXCEL2000
  outfile = "H:\combine1.xls" replace; sheet=Lang2;
proc export data = WORK.FreuParms2 DBMS=EXCEL2000
  outfile = "H:\combine1.xls" replace; sheet=Freu2;
proc export data = WORK.mmm DBMS=EXCEL2000
  outfile = "H:\combine1.xls" replace; sheet=parms;
proc export data = WORK.aaa DBMS=EXCEL2000
  outfile = "H:\combine1.xls" replace; sheet=data;
**/;
run;
quit;
```

Figure B.1. SAS code for Langmuir and Freundlich curve parameters

```

proc sort data=aaa; by field LP loc;

proc mixed data=aaa; by field;
class loc depth;
model sand = loc depth loc*depth/ddfm=satterth;
lsmeans loc depth loc*depth/CL pdiff;
ods output LSMeans=mydata;
ods output tests3=ANOVA;
proc mixed data=aaa; by field;
class LP depth;
model sand = LP depth LP*depth/ddfm=satterth;
lsmeans LP depth LP*depth/CL pdiff;
ods output LSMeans=mydata2;
ods output tests3=ANOVA2;
proc print data=aaa;

proc export data = WORK.mydata DBMS=EXCEL2000
  outfile = "H:\sandAnova.xls" replace;
  sheet=CL;
proc export data = WORK.mydata2 DBMS=EXCEL2000
  outfile = "H:\sandAnova.xls" replace;
  sheet=CL2;
proc export data = WORK.ANOVA DBMS=EXCEL2000
  outfile = "H:\sandAnova.xls" replace;
  sheet=CLA;
proc export data = WORK.ANOVA2 DBMS=EXCEL2000
  outfile = "H:\sandAnova.xls" replace;
  sheet=CLA2;
run;
quit;

```

Figure B.2. SAS code for ANOVA and error bars

```

data bbb;
set aaa;

D2FEPC= 1/(log (FEPC));

proc corr data=bbb;
var D2FEPC FEPC AEP Feox Pox Alox DPSox TP PM3 FeM3 AlM3 CaM3 DPSM3 DPSCa
DPSall AlFe Sand Silt Clay pH;
run;
quit;

```

Figure B.3. SAS code for Pearson Correlation table

```

data bbb;
set aaa;
D2FEPC= 1/(log(FEPC));
run;
proc sort data=bbb; by field;
proc reg data=bbb; by field;
model D2FEPC = DPSox /selection=
stepwise slentry=0.05 slstay=0.05;
run;
QUIT;

```

Figure B.4. SAS code for EPC₀ stepwise comparisons

```

proc glm data = aaa;
class call frac;
model EPC = call frac call*frac;
means call frac call*frac /CLM lsd lines;
ods output CLMeans=mydata;
run;
proc mixed data=aaa;
class call frac;
model EPC = call frac call*frac/ddfm=satterth;
lsmeans call frac call*frac/CL pdiff;
ods output LSMeans=mydata2;
/**;
proc export data = WORK.mydata DBMS=EXCEL2000
  outfile = "I:/MixCISAS.xls" replace;
  sheet=CL;
  proc export data = WORK.mydata2 DBMS=EXCEL2000
  outfile = "I:/MixCISAS.xls" replace;
  sheet=CL2;
run;
quit;

```

Figure B.5. SAS for EPC₀ in mixed sediments

Appendix C: WEPP model inputs

Figure C.2. Abbreviated Weedel INPUT.txt

```

CLIMATE
4.30
1 0 0
Station: MC PHERSON KS                CLIGEN VERSION 4.3
Latitude Longitude Elevation (m) Obs. Years Beginning year Years simulated
38.37 -97.67 454 93 1 50
Observed monthly ave max temperature (C)
4.7 7.9 14.1 20.2 24.8 30.7 34.2 33.6 28.6 22.1 13.1 6.3
Observed monthly ave min temperature (C)
-6.4 -4.6 0.1 6.2 11.6 17.2 20.0 19.4 14.6 8.1 0.6 -4.7
Observed monthly ave solar radiation (Langleys/day)
240.0 304.0 401.0 506.0 558.0 627.0 616.0 576.0 473.0 359.0 271.0 216.0
Observed monthly ave precipitation (mm)
17.7 26.6 47.2 67.5 107.6 111.1 79.3 82.1 80.9 58.8 35.1 22.7
***Generated Climate Data removed for brevity***
MANAGEMENT
98.4
1 # number of OFE's
50 # (total) years in simulation
#####
# Plant Section #
#####
1 # Number of plant scenarios
sorghum1
Abbreviated Weedel INPUT.txt
`Sorghum-High Fertilization Level'
(from WEPP distribution database)
1 #landuse
WeppWillSet
3.60000 3.00000 25.00000 10.00000 2.90000 60.00000 0.00000 0.60900 0.90000 0.03200
0.85000 0.90000 0.60000 0.99000 0.00000 1450.00000 0.50000 1.01000
2 # mfo - <non fragile>
0.00740 0.00740 27.50000 0.00000 0.13000 1.50000 0.25000 0.00000 40 0.00000
0.00000 5.00000 0.00000
#####
# Operation Section #
#####
1 # Number of operation scenarios
PLNTSC

```

```

`Planter, no-till with smooth coulters'
(from WEPP distribution database)
1 #landuse
0.1000 0.0500 0
4 # pcode - other
0.0250 0.7500 0.1000 0.0500 0.0120 0.1500 0.0000
#####
# Initial Conditions Section #
#####
1 # Number of initial scenarios
Aft_0243
After fall harvest of sorghum, no till
John Laflen
(null)
1 #landuse
1.10000 0.00000 200 115 0.00000 0.90000
1 # iresd <sorghum1>
3 # mang fallow
500.00000 0.02000 0.90000 0.02000 0.00000
1 # rtyp - temporary
0.00000 0.00000 0.10000 0.20000 0.00000
0.00000 0.00000
#####
# Surface Effects Section #
#####
1 # Number of Surface Effects Scenarios
# Surface Effects Scenario 1 of 1
Year 1
From WEPP database
1 # landuse - cropland
1 # ntill - number of operations
152 # mdate --- 6 / 1
1 # op --- PLNTSC
Abbreviated Weedel INPUT.txt
0.050 # depth
2 # type
#####
# Contouring Section #
#####
0 # Number of contour scenarios
#####
# Drainage Section #
#####
0 # Number of drainage scenarios

```

```

#####
# Yearly Section  #
#####
1 # looper; number of Yearly Scenarios
# Yearly scenario 1 of 1
Year 1
1 # landuse <cropland>
1 # plant growth scenario
1 # surface effect scenario
0 # contour scenario
0 # drainage scenario
1 # management <annual>
  303 # harvest date --- 10 / 30
  152 # planting date --- 6 /1
  1.2000 # row width
  6 # residue man - <none>
#####
# Management Section #
#####
Manage
description 1
description 2
description 3
1 # number of OFE's
  1 # initial condition index
50 # rotation repeats
1 # years in rotation
***Annual rotation listing removed for brevity***
SOIL
97.5
comments: soil file
1 1
'Crete' 'CLAY' 3 0.230000 0.700000 0.000000 0.000000 0.000000 0.000000
  240 8.0 27.0 3.000 18.0 0.0
  730 4.0 45.0 1.000 15.8 0.0
  1062 4.0 32.0 1.000 12.3 0.0
SLOPE
Abbreviated Weedel INPUT.txt
97.5
# from slope
1
0.000 37.500
21 321.000000
0.000000, 0.000800 0.010000, 0.001600 0.090000, 0.001600 0.110000, 0.003700 0.190000,

```

0.003700 0.210000, 0.003400 0.290000, 0.003400 0.310000, 0.001600 0.390000, 0.001600
0.410000, 0.005600 0.490000, 0.005600 0.510000, 0.010900 0.590000, 0.010900 0.610000,
0.006200 0.690000, 0.006200 0.710000, 0.007800 0.790000, 0.007800 0.810000, 0.006200
0.890000, 0.006200 0.910000, 0.015000 1.000000, 0.015000

Figure C.1. Abbreviated Schmidt INPUT.txt

CLIMATE

4.30

1 0 0

Station: MC PHERSON KS

CLIGEN VERSION 4.3

Latitude Longitude Elevation (m) Obs. Years Beginning year Years simulated

38.37 -97.67 454 93 1 50

Observed monthly ave max temperature (C)

4.7 7.9 14.1 20.2 24.8 30.7 34.2 33.6 28.6 22.1 13.1 6.3

Observed monthly ave min temperature (C)

-6.4 -4.6 0.1 6.2 11.6 17.2 20.0 19.4 14.6 8.1 0.6 -4.7

Observed monthly ave solar radiation (Langleys/day)

240.0 304.0 401.0 506.0 558.0 627.0 616.0 576.0 473.0 359.0 271.0 216.0

Observed monthly ave precipitation (mm)

17.7 26.6 47.2 67.5 107.6 111.1 79.3 82.1 80.9 58.8 35.1 22.7

Generated Climate Data removed for brevity

MANAGEMENT

98.4

1 # number of OFE's

50 # (total) years in simulation

#####

Plant Section

#####

2 # Number of plant scenarios

Whe_27068

`Wheat; Winter - for State of Washington

JML, 3-28-01

(null)

1 #landuse

WeppWillSet

5.20000 3.00000 35.00196 3.00000 5.40026 60.00000 0.00000 0.15200 1.00000 0.00640

0.80000 1.00000 0.65000 0.99000 3.00000 1700.00000 0.40000 1.00001

2 # mfo - <non fragile>

0.00850 0.00850 15.00000 0.25000 0.00500 1.49989 0.25000 0.00000 14 0.00000

0.00000 5.00000 0.00000

WHEAT

`Wheat; Winter - High Fertilization Level'

(from WEPP distribution database)

1 #landuse
WeppWillSet
5.20000 3.00000 25.00000 4.00000 5.40000 60.00000 0.00000 0.15200 1.00000 0.00640
0.80000 1.00000 0.65000 0.99000 3.00000 1700.00000 0.40000 0.91000

2 # mfo - <non fragile>
0.00850 0.00850 15.00000 0.25000 0.00500 1.50000 0.25000 0.00000 14 0.00000
0.00000 5.00000 0.00000

#####

Operation Section

#####

1 # Number of operation scenarios

DRNTRFC

`Drill, no-till in standing stubble-fluted coulters'

(from WEPP distribution database)

1 #landuse

0.3000 0.2000 0

4 # pcode - other

0.0250 0.2000 0.3000 0.2000 0.0120 0.6000 0.0000

#####

Initial Conditions Section

#####

1 # Number of initial scenarios

Aft_31305

For continuous winter wheat, no till. Wheat was planted Oct 1

90 residue cover

175 mm of rain since last tillage in fall prior

1 #landuse

1.10000 0.20000 90 150 0.00000 0.90000

1 # iresd <Whe_27068>

1 # mang annual

175.00600 0.02000 0.90000 0.01000 0.00000

1 # rtyp - temporary

0.00000 0.00000 0.10000 0.20000 0.00000

0.40005 0.10000

#####

Surface Effects Section

#####

1 # Number of Surface Effects Scenarios

Surface Effects Scenario 1 of 1

Year 1

Annual rotation listing removed for brevity

From WEPP database

Your name, phone

```
1 # landuse - cropland
1 # ntill - number of operations
  274 # mdate --- 10 / 1
1 # op --- DRNTRFC
  0.050 # depth
  2 # type
#####
# Contouring Section #
#####
0 # Number of contour scenarios
#####
# Drainage Section #
#####
0 # Number of drainage scenarios
#####
# Yearly Section #
#####
1 # looper; number of Yearly Scenarios
# Yearly scenario 1 of 1
Year 1
1 # landuse <cropland>
2 # plant growth scenario
1 # surface effect scenario
0 # contour scenario
0 # drainage scenario
1 # management <annual>
  227 # harvest date --- 8 / 15
  274 # planting date --- 10 / 1
  1.2000 # row width
  6 # residue man - <none>
#####
# Management Section #
#####
-Manage
description 1
description 2
description 3
1 # number of OFE's
  1 # initial condition index
50 # rotation repeats
1 # years in rotation
-SOIL
```

97.5

comments: soil file

1 1

'Crete' 'CLAY' 3 0.230000 0.700000 0.000000 0.000000 0.000000 0.000000

240 8.0 27.0 3.000 18.0 0.0

730 4.0 45.0 1.000 15.8 0.0

1062 4.0 32.0 1.000 12.3 0.

-SLOPE

97.5

from slope

1

45.000 162.800

21 466.000000

0.000000, 0.000850 0.010000, 0.001700 0.090000, 0.001700 0.110000, 0.002200 0.190000,

0.002200 0.210000, 0.002800 0.290000, 0.002800 0.310000, 0.001500 0.390000, 0.001500

0.410000, 0.006900 0.490000, 0.006900 0.510000, 0.006400 0.590000, 0.006400 0.610000,

0.005600 0.690000, 0.005600 0.710000, 0.007900 0.790000, 0.007900 0.810000, 0.009200

0.890000, 0.009200 0.910000, 0.005800 1.000000, 0.005800
